NTNU

Norwegian University of
Science and Technology

Pipeline damage assessment after trawling impact

Sondre Lydvo Ellingsen

Marine Technology
Submission date: June 2018
Supervisor: Sigmund Kyrre Ås, IMT

Norwegian University of Science and Technology
Department of Marine Technology

Preface

This thesis is the conclusion to my master at NTNU-IMT. During this final semester a lot of things have gone wrong, a lot has been learned and a lot has been achieved .

Sondre Lydvo Ellingsen

Trondheim, 2018-06-18

Acknowledgment

The person most deserving of my sincere gratitude is professor Sigmund Kyrre Ås, my supervisor during this project, who's shown great interest in this thesis and has always been available for consulting. Special thanks is given to Kristian Aamot and Emil Bratlie, who has been working day and night with the test-rig and corresponding equipment while also being available whenever I was need of assistance or help.

0.1 Abstract

Denting of subsea pipelines due collision with trawling equipment may have a significant impact on the remaining fatigue-life of the pipe. The criteria used to determine if a pipeline is safe after denting have a lot of conservatism built into them to account for uncertainties. Repair of subsea pipelines is not cheap, therefor it exits a desire for more knowledge with regards to pipe-denting such that conservatism can be reduced. This thesis have been concerned with attempts at predicting the remaining fatigue-life of the dented pipelines by creating a 3D-model using photos of dented pipes with two different geometries and then performing a fatigue-analysis of the dented geometry.

Static impact between an indenter and a pressurized pipe have been conducted in both laboratory and finite-element (FE) software to simulate pipe/trawler impact. Knowledge of residual stress from impact have been obtained by the means of X-ray diffraction and simulation in FEM-software.

Estimates of remaining fatigue-life and stress/strain state were obtained by subjecting pipes, which were dented in laboratory, to fatigue-tests. Dented pipe has been filled with oil and subjected to cyclic, internal pressure with constant-amplitude. Stresses were obtained by mounting strain-gauges on surface where cracks were likely to occur. 3D- models of the dented pipes have been created by the use of photogrametry and imported to FE-software for analysis. The imported geometry is free of any residual stress. However, FE-simulation containing the simulated dent is not. Both models are subjected to internal pressure corresponding to internal pressure from laboratory fatigue-tests. Stresses at critical locations from laboratory tests, and FE-simulations have been used as input for the Matlab extension 'Quick Fatigue Tool', which employs multiaxial-fatigue theory to determine fatigue life.

Sammendrag

Bulking av subsea-rørledning på grunn av kollisjon med trålere kan ha en betydelig effekt på den gjenverende utmattings-levetiden til røret. Kriterie som benyttes til å avgjøre om et rør et sikkert etter bulking har innebyg en betydelig andel konservatisme for å ta hensyn til usikkerheter. Reparasjon av subsea-rørledningeer er ikke billig, derfor eksisterer det ønske om mer kunnskap slik at konservatismen kan bli redusert. Denne avhandlingen har sett på muligheten for å estimere levetiden til et bulket rør ved å ved å; fotografere det bulkede røret, importere bilder til en passende programvare, som gjenskaper en 3D-modell av det bulkede røret, for deretter å utføre utmattings-analyse av den gjenskapte geometrien. Statisk sammenstøt mellom en indenter og en trykkstatt rør har blitt utført både i laboratorie og programvare, hvilket benytter elementmetoden, for å etterlinkne kollisjon mellom rørledning og tråler. Kjennskap til restspenninger fra sammenstøt har blitt funnet ved hjelp røngtendiffraksjon og simulering i numerisk programvare. Estimat for gjenverende levetid og spenningstilstand har blitt funnet ved å utføre utmattings-tester i laboratorie. Utmattingstestene ble utført ved å utsette røret for syklisk indre trykk, med konstant amplitude, hvor olje ble brukt som fluid. Spenninger ble funnet ved å feste strekk-lapper på kritiske lokasjoner.

Resultater viser at det bulkede området har en veldig komplisert spenningstilstand, med store restspenningsgradienter. Sprekkene som oppstår i utmattingstestene ser ut til å oppstå i områdende hvor restspenningen er realtivt lave. Analyser tyder på at det er gode muligheter for å kunne estimere levetiden på bulkede rørledninger ved bruk av importert geometry, men mange antakelser og begrenset med data tyder på store usikkerheter.

Contents

List of Figures

List of Tables

Chapter 1

Introduction

1.1 Background

Suppose you are the owner of a subsea-pipeline, transporting oil gas along the continental shelf. Now, the last thing that you want to happen is for the pipeline to rupture and cause another environmental disaster. While leakage is not a primary concern while the pipeline is in its intact condition, it is a grave issue once the pipe is damaged by heavy trawling equipment in the form of dents or scratches. This is because dents and scratches cause stress concentrations in the pipe, which has been found to severely impact the design fatigue-life. Procedures that serve to determine if a dented pipeline needs repair exits. They do however, have a great deal of conservatism built into them, which suggests there is room for improvement. Repairing subsea pipelines is an operation that is neither easy, nor cheap. It is therefor in the owner's best interest to increase the pool of knowledge related to the fatigue-life of damaged subsea-pipelines.

Literature Survey

A summary of earlier master-thesis projects carried out at NTNU IMT has been reviewed as part of the master thesis.

1.1.1 Review of 'Assessment of Pipeline Integrity after Trawling Impact by Investigating Dent with Gouge'

To expand the understanding of stress concentrations in dented pipes containing a gouge Eliassen (2016) conducted laboratory tests of dented pipes with gouge and numerical simulations using Abaqus. In addition, a review of different pipeline acceptance criteria was conducted. The results can be found in Fig:1.1. It was found that none of these Standards allow gouges in the pipe and the maximum dent depth cannot exceed more than 7% of the diameter at most.

	Plain Dents		Dents with
	Constrained	Unconstrained	cracks or gouges
API 1156 (1997)	Upto 6 % of D, > 2 % requires fatigue assessment		Not allowed
ASME B31.8 (2014)	Upto 6 % of D or not exceed 6 % strain		Not allowed
ASME B31.4 (1992)	Upto 6 % of D or strain level upto 6 % for OD > 4"		Not allowed
	Up to 6 mm in pipes with D < 4"		
DNV (2010)	3.5 % of D with low impact frequency		Not allowed
EPRG (2000)	≤ 7 % of D at a hoop stress of 72 % SMYS		Not allowed
CSA - Z662 (1999)	Upto 6 mm for ≤ 101.6 mm D or		Not allowed
	< 6 % of D for > 101.6 mm		

Figure 1.1: Overview of different pipeline dent/gouge damage criteria.

A gouge was created in the bottom of a dented pipe. The dented/gouged pipe was filled with oil and subjected to cyclically increasing internal pressure. The strains on the dent were measured using standard equipment and converted to stresses for further analysis. Eliassen (2016) assumed a linear-elastic material model. Von-Mises yield criterion is valid in the elastic domain and was used to determine the SCF in areas that were assumed to provide the highest SCF.

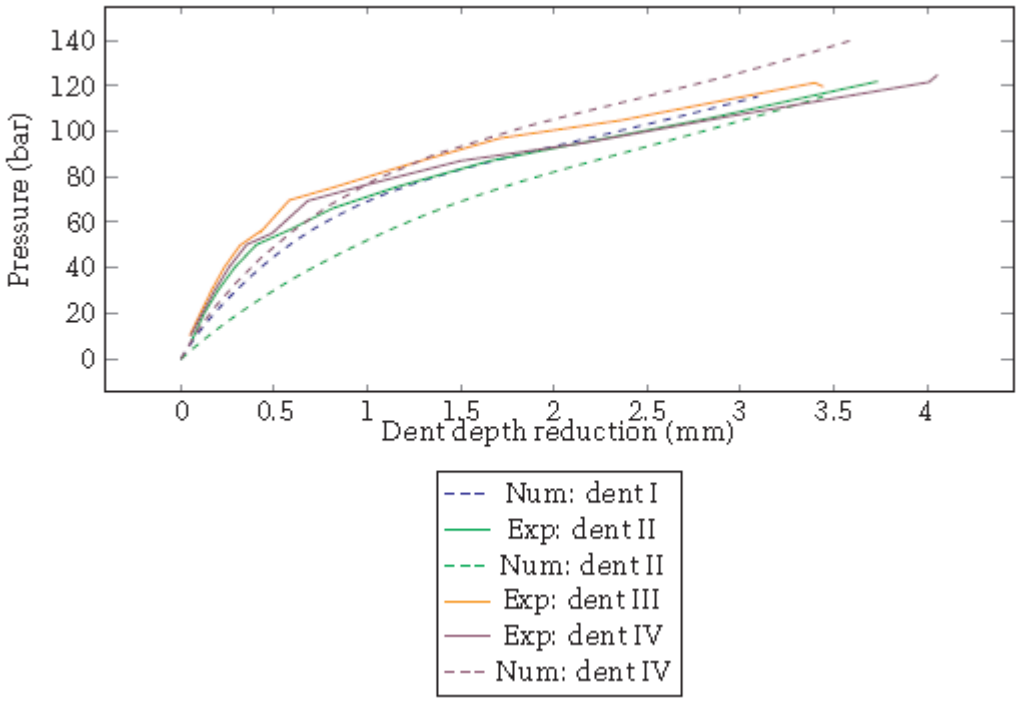

Figure 1.2: Internal Pipe Pressure VS Reduction of pipe dent-depth Eliassen (2016)

Abaqus was used to simulate the physical experiment and a set of numerical stress-concentrations were obtained. The pipe was modelled using solid elements, while the indenter was modelled using shell elements. The gauge which existed in the lab-experiment was not modelled. Knowledge about residual stresses in the pipe was not determined, but instead assumed to be 0. Results from Abaqus showed reasonably good compliance with lab-experiments when it came to dent re-rounding, but a satisfactory level of compliance between numerical SCF and SCF's obtained from lab-experiments was not present. Comparison between numerical and experimental results are found in Fig:1.2 and Fig:1.3

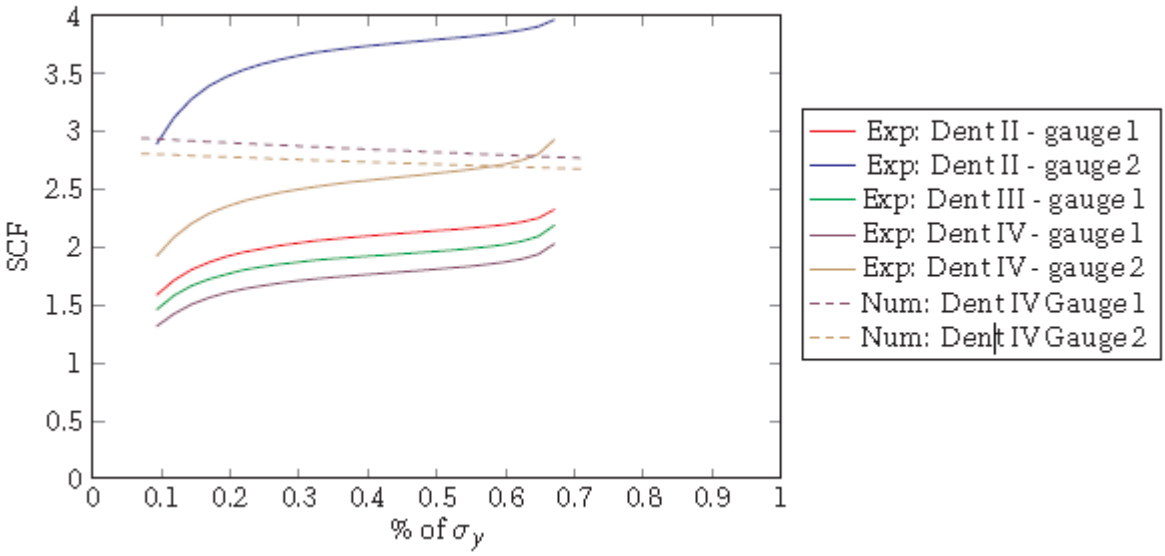

Figure 1.3: Comparison of SCF obtained from lab-experiments and Abaqus Eliassen (2016)

1.1.2 Review of 'Pipeline Integrity Assessment of Dent with Gouge after Trawling Impact'

Aadal (2016) investigated the effect of dents, and dents containing gouge, on the fatigue life of pipes subjected to cyclic loading. Fatigue tests of 10 pipes subjected to varying internal pressure were conducted, similar to Eliassen (2016). The pipes contained either a dent or a combination of dent and gouge. All dents had roughly the same initial depth. Failure was said to occur when a crack was detected in the pipes. The fatigue-test results can be found in Table 1.1. This table contains fatigue-strength as well as crack-location and crack-growth direction.

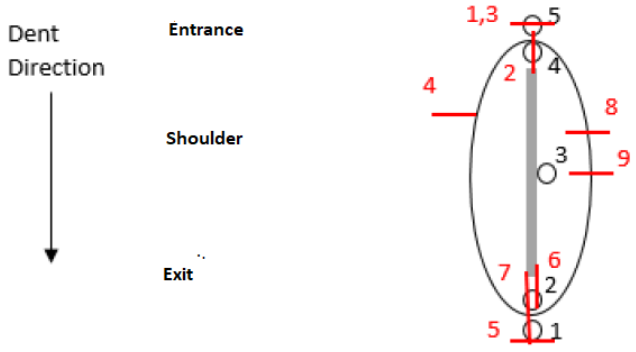

Figure 1.4: Indicates the direction of indentation in addition to crack location and test number corresponding to the crack.Aadal (2016)

Test Nr.	Max. Internal Pressure [Bar]	R-ratio	Contains gouge?	Nr. of cycles to failure	Crack Location	Crack Growth Direction
1	100	0.1	No	18.8k	Entrance	Axial
2	100	0.1	Yes	19.9k	Entrance	Hoop
3	100	0.1	No	16.8k	Entrance	Axial
4	70	0.1	No	112.1k	Shoulder	Axial
5	80	0.1	Yes	42.5k	Exit	Axial
6	70	0.1	Yes	95.5k	Exit	Hoop
7	60	0.1	Yes	111k	Exit	Hoop
8	60	0.1	No	205k	Shoulder	Axial
9	50	0.1	Yes	274.9k	Shoulder	Axial
10	105/60	0.1	No	No.lim	No crack	

Table 1.1: Results from fatigue test of dented and dented+gouged pipes. Explanation of crack location can be found in 1.4

The effect of re-rounding was examined in test nr.10 (Table1.1). The dented pipe was first pressurized to 105 bar before the fatigue tests were conducted with a max. internal pressure at 60 bar. No cracks were observed in pipe nr. 10 after around 600k cycles. When compared to test nr.6, which has no gouge and same pressure, it can be seen that the effect of re-rounding can have a dramatic effect on fatigue-life. It was concluded that re-rounding causes a reduction in SCF and therefore an increased fatigue-life.

An SN-curve was fitted to the obtained data 1.5. It was concluded that a dent with gouge reduced the fatigue-strength by 18.4% as compared to a dent without gouge. Cosham and Hopkins (2004) reported that a gouge could represent a fatigue-life corresponding to one-hundredth of the initial life. None of the fatigue-tests were in proximity to this level of fatigue-life reduction.

The numerical model, which simulates pipe indentation, created by Eliassen (2016) was used to compare measurements from fatigue-test to a numerical approach. The simulation is illustrated in 1.6. The material properties used in Abaqus and those obtained from real tests were different, which inevitably influenced the results. Comparison between real and numerical measurements 1.7 showed that they exhibited the same the same behaviour, but direct comparison was difficult due to material and geometrical differences.

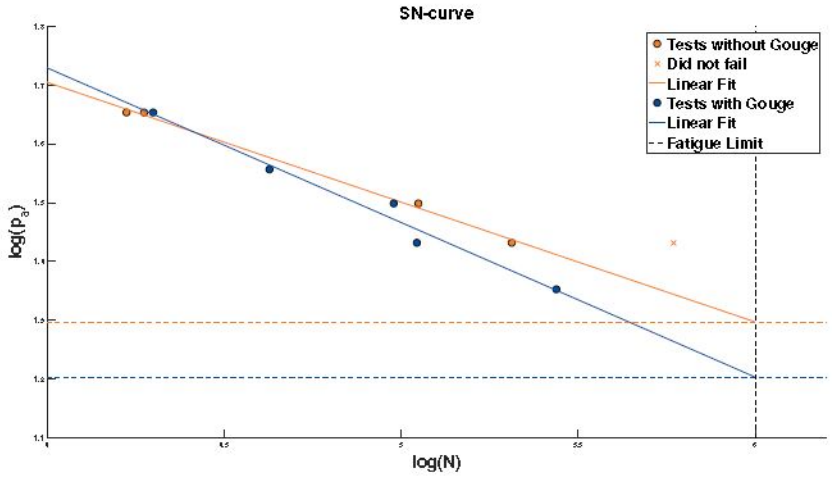

Figure 1.5: SN-curve obtained from fatigue-test of 10 dented/gouged pipes.Aadal (2016)

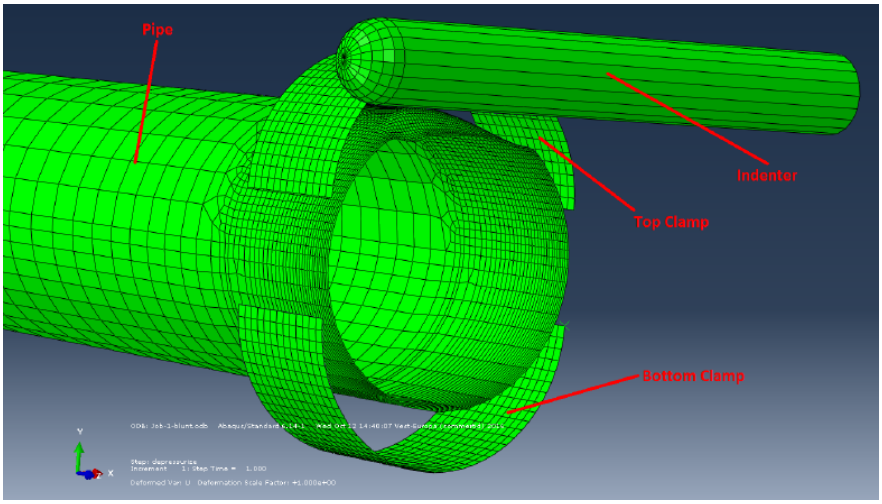

Figure 1.6: Simulation of pipe indentation Aadal (2016)

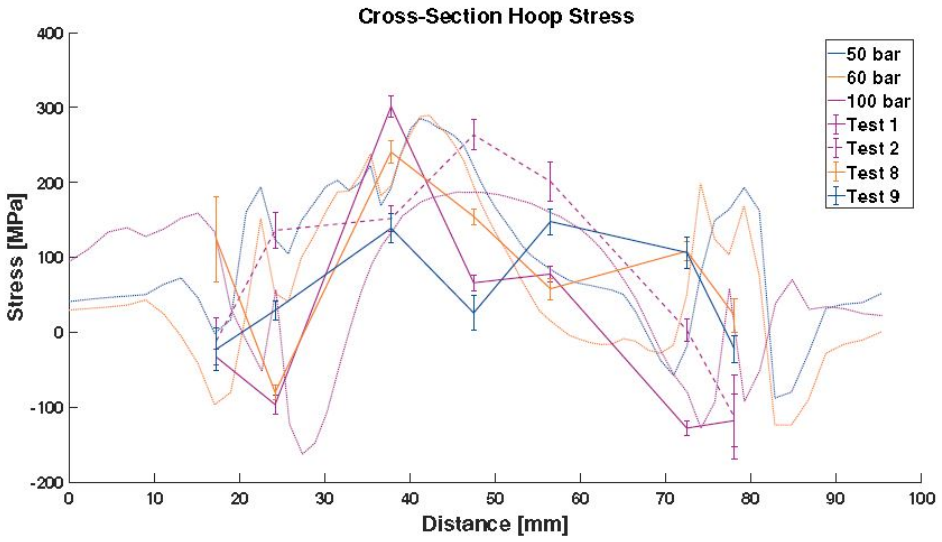

Figure 1.7: Shows variation in Hoop-stress from lab-tests and numerical model. Line=Abaqus, Spike=Lab measurement Aadal (2016)

1.2 Objectives

Before one can assess whether a dented pipe needs repair or is safe, one must first be aware that the damage is present. Inspection of the pipeline can be carried out by ROV's, which carries a camera, making it possible be to take photos of the dented pipeline. This enables the option of re-creating a 3D-model of the dented-pipeline using photogrammetry (converting multiple photos to a 3D geometry). The 3D-model can then be imported to a FE-software for analysis. Based on the stress-state from FE-analysis one can use multiaxial fatigue-theory to predict the fatigue life. This thesis aims to predict the fatigue-life of a dented pipe (simplified subsea pipe) based on a geometry created from photogrammetry. Laboratory experiments and numerical simulations will be used as reference. Challenges, and inaccuracies related to this type of procedure will be identified.

1.3 Limitations

Experiments are limited to thin-walled pipes with diameter of 102mm and thickness 1.8mm. A subsea pipeline is typically much larger and thicker.

Experiments only includes static effects. Denting of pipes are considered purely as a static event, meaning dynamic effects are neglected.

Pipelines may displace several meters along the sea-floor due to impact with trawling equipment. This effect is not included in experiments.

3D models are imported to a free version of 3D Zephyr. This version does not allow models to be created from more than 50 images.

Chapter 2

Theory

2.1 Load-Ratio (R-Ratio)

R-ratio can be expressed as the relation between minimum and maximum cyclic stress:

$$R = \frac{\sigma_{min}}{\sigma_{max}} \tag{2.1}$$

It is an important parameter for the fatigue-life because it has a considerable effect on the crack-growth rate Huang and Moan (2007). A Load ratio of -1 corresponds to testing with stress with same amplitude in compression and tension. It it is common to use a load ratio of 0.1 when performing fatigue tests where it is not possible and/or desired to create compression. This value is selected due to practical reason, where one may run into issues with the equipment for lower values.

2.2 Constant Amplitude Loading

Components subjected to repeated loading are susceptible to fatigue. Methods have been developed to estimate the fatigue performance of components afflicted by loads of constant amplitude. Three common methods are stress-life, strain-life and crack-growth analysis eFatigue (2017a). Stress-life analysis is used when the stresses are purely elastic. When plastic deformation occurs, strain-life analysis is a method which may be employed. This method can

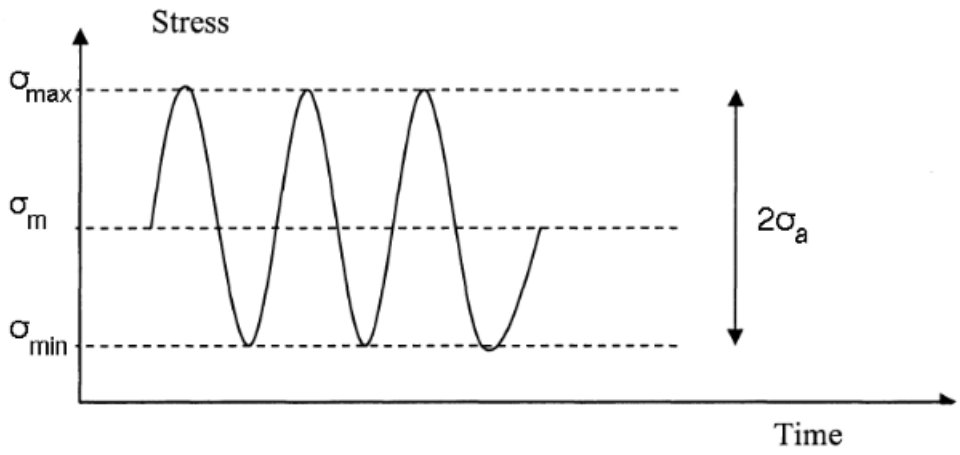

Figure 2.1: Shows max. and min. values of cyclic stress Berge (2016)

be well suited for areas with large stress-concentrations. Crack-growth analysis is used to determine how long it will take for a crack to grow to failure. Refereces: eFatigue (2017a),eFatigue (2017b),Berge (2016)

2.3 Proportional and Non-proportional loading

For components subjected so cyclic loading, one often refer to two types of loading conditions; proportional and non- proportional.
The definition of proportional loading is: "Any state of time varying stress where the orientation of the principal stress axes remained fixed with respect to the axes of the component." Physically, this means that the loads are in-phase. The magnitude of the loads may vary with time, but the plane of which the maximum normal-stress occurs will not change. The definition of non-proportional loading is: "Any state of time varying stress where the orientation of the principal stress axes remained fixed with respect to the axes of the component." Opposite of proportional loading, the loads are now out of phase implying that the orientation of the principal planes will change with time since the plane of which maximum normal stress is located also changes with time. The effect of non-proportional loading will not be discussed in detail, however it is reported by Skibicki (2014) to have an increasingly negative effect on the fatigue life of metals for increasing phase-angles.

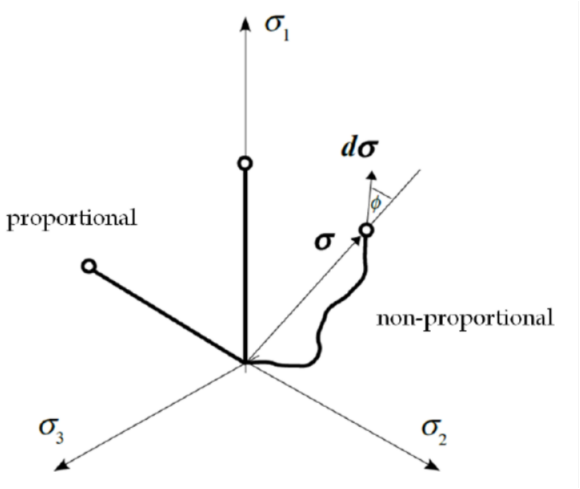

Figure 2.2: Illustration of proportional vs non-proportional loading Socie (2017)

2.4 Fatigue Damage Mechanisms

Fatigue-crack growth can be divided into three separate stages; nucleation, coalescence followed by stable growth. Slip bands are directions of which material-grains can translate and are formed once the material is subjected to a cyclic loading and the local shear stress reaches the critical value. Dislocations will start to move due to repeated cyclic deformation, which forms slip planes. The local shear stress will vary depending on the orientation of the dislocation. Thus, only the dislocations with the most favorable orientations will form slip bands when the applied stress is low. Once enough slip planes have been formed, they will coalesce into a crack. Materials with smaller grains experiences a higher fatigue strength. This is because small grains prevent the motion of dislocations, therefor preventing slip bands from forming, which corresponds to increased fatigue strength.

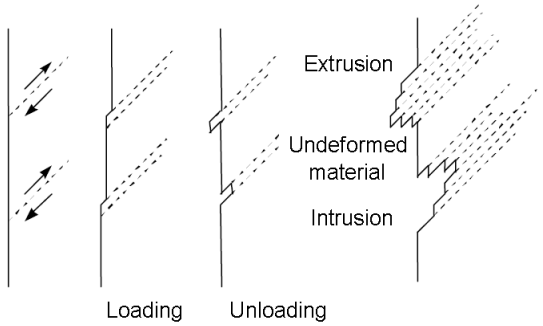

Figure 2.3: Nucleation of cracks due to coalescence of slip-bandsSocie (2001)

2.4.1 Crack Nucleation and Early Growth

Mode I, Mode II and Mode III crack-growth

Mode I loading opens the crack by tensile forces pulling the crack faces apart. Mode II and mode III opens crack by in-plane and out-of-plane shear respectively. Mode II causes the crack to grow along the surface while mode III is found at the crack tip, causing the crack to extend further into the material. Everywhere else round the crack-tip is a combination of mode I, II and III.

Stage I and Stage II growth

Stage I crack growth is dominated by shear-stress and is characterized by crack growth in one direction across the grains before it changes direction on the intersecting grain. Stage II crack growth follows once the crack length has reached an order of magnitude of several grain-lengths. The direction of growth is in stage II is governed by the maximum, applied cyclic stress.

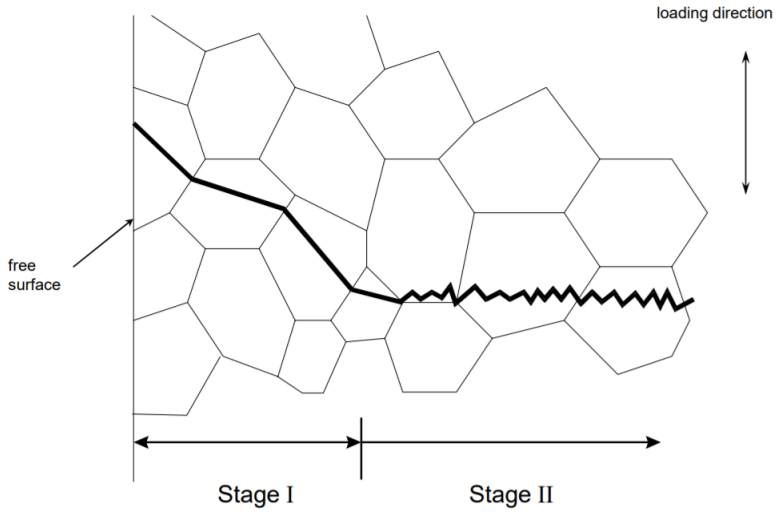

Figure 2.4: Illustrates crack-growth stage I and stage II Socie (2001)

Case A and Case B growth

Shear cracks grow either into the surface of the material due to in-plane shear, or grow into the surface of the material due to out-of-plane shear. These two patterns are referred to as case A

and B crack-growth. Where case A cracks are shallow while case B cracks have large aspect ratios.

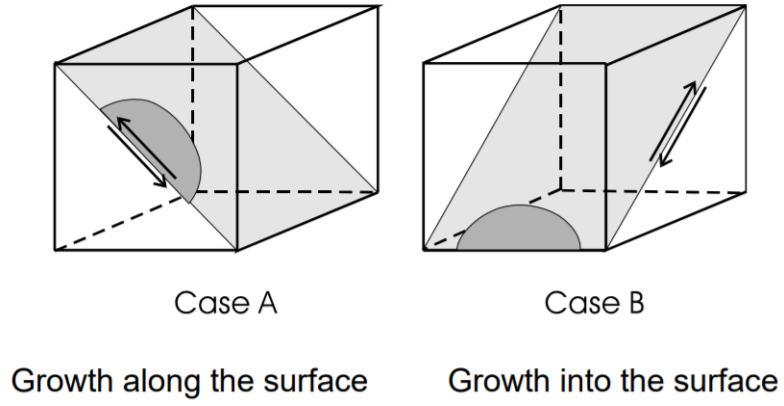

Figure 2.5: Visualizes case A and case B cracksSocie (2001)

2.4.2 Tensile Mechanisms-Mode I Growth

Crack Closure

Upon unloading of tensile stresses, the plastic region at the crack tip reduces and the surrounding elastic material causes residual, compressive stresses that must be overcome before the crack can open. The net effect of crack-close is a reduction on crack growth-rate. Reference: Socie and Marquis (2000)

Chapter 3

Approach

The conceptual approach is to:

Simulate pipe-denting in laboratory and in Comsol Multiphysics.

Dent pipes in laboratory.

The dented surface from laboratory is imported to Comsol using photogrammetry. Imported geometry contains no residual stress.

Fatigue-tests of dented laboratory pipes are conducted to obtain estimates of fatigue-life at different levels of internal pressure.

Pressurize imported geometry and pipe that was dented in Comsol. Same pressure as in fatigue-tests. Two different stress-states are obtained.

Use information about stress-state in real dent, imported dent and simulated dent to calculate fatigue-life of the dents using multiaxial fatigue-theory.

3.1 Laboratory denting and fatigue-tests

3.1.1 Laboratory denting

Stainless steel pipes with diameter 102mm and thickness 1.8mm were filled with oil and subject to a static pressure of 50 [Bar]. Custom-made end-caps were mounted on the pipe

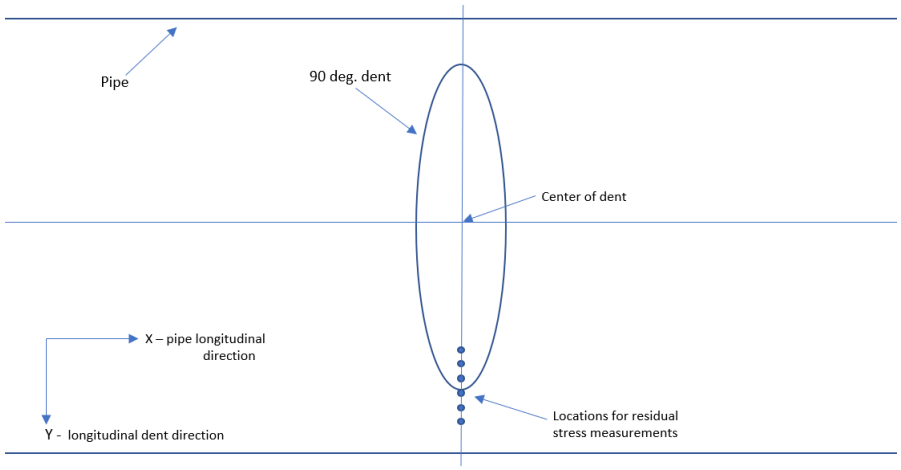

Figure 3.1: Shows a birds-eye view of a pipe containing a dent that is perpendicular to the pipe longitudinal direction, a 90 degree dent.

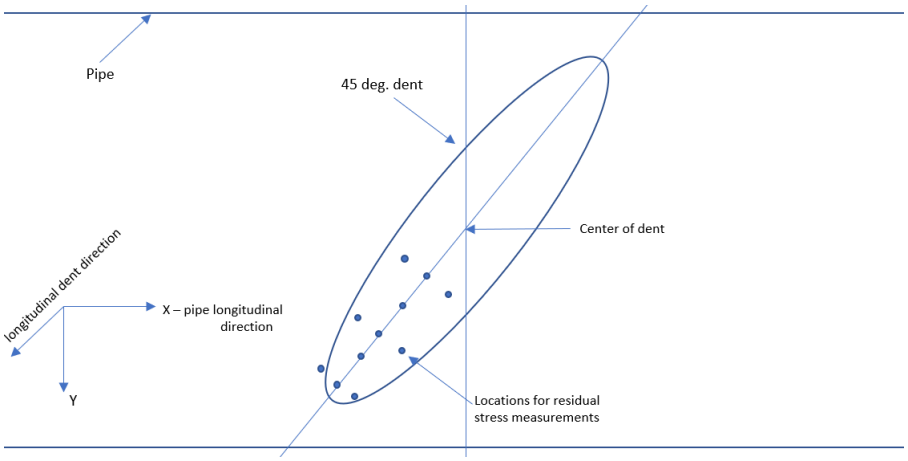

Figure 3.2: Shows a birds-eye view of a pipe containing a dent that is perpendicular to the pipe longitudinal direction, a 45 degree dent.

which not only served the purpose of containing fluid inside the pipe, but also introduced axial forces. The pressurized pipe was dented statically to a depth of 16% of diameter by forcing a solid cylinder with diameter of 30mm into the pipe. The induced dent would re-round from 16mm to around 6-8mm depending on dent-type due to the internal pressure of 50 [Bar].

Dent geometry and description

3.1.2 Fatigue tests

Fatigue-tests of the dented pipe were carried out by subjecting the pipe to cyclic internal pressure with constant-amplitude and R-ratio 0.1. The the pipe-endcap was connected to a piston-cylinder, which regulated the pressure inside the pipe via a computer and associated software. Strain-gauges were mounted on locations were cracks were assumed to nucleate. These locations initially corresponded to an area near the location where the dent-edge meets the longitudinal dent-axis fig:3.1, fig:3.2. Only 2 strain-gauges were used per fatigue-test due to having a limited supply. A linear variable differential transformer (LVDT) were mounted at dent-center to track maximum dent-displacement during fatigue-tests(ref appendix). The fatigue-tests were aborted once a crack had formed in the pipe.

Measurement of strains calculation of stress

The strain-gauges used in the fatigue-tests were of a rectangular, stacked type. By aligning the strain-gauges such that the rectangles aligns with the longitudinal and radial direction of the pipe, the equations for obtaining axial, radial and shear-strains from measured strains simplifies to of Technology (2000):

$$\epsilon_x = \epsilon_a \tag{3.1}$$

$$\epsilon_y = \epsilon_c \tag{3.2}$$

$$\gamma_{xy} = 2\epsilon_b - \epsilon_a - \epsilon_c \tag{3.3}$$

Where ϵ_x, ϵ_y and γ_{xy} is the axial, radial and shear strain on the surface. While, ϵ_a, ϵ_b and ϵ_c is the strains obtained from each rosette in fig:3.3
Plane stress assumption was used to compute the corresponding stresses. Following this assumption, the axial, radial and shear stress is given by:

$$\sigma_x = \frac{E}{(1-\nu^2)}(\epsilon_x + \nu\epsilon_y) \tag{3.4}$$

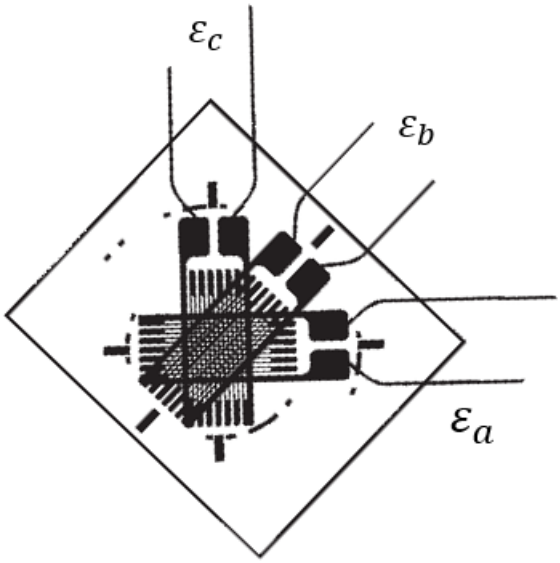

Figure 3.3: Sketch of a rectangular, stacked strain-gauge. Shows strain-component that corresponds to each rectangle.

$$\sigma_y = \frac{E}{(1-\nu^2)}(\epsilon_y + \nu\epsilon_x) \tag{3.5}$$

$$\tau_{xy} = \frac{E}{2(1+\nu)}\gamma_{xy} \tag{3.6}$$

3.1.3 Measurement of residual stress

Measurements of residual stress were conducted at locations indicated by fig:3.1 fig:3.2 using an X-ray diffraction device. This device measures the strain within the crystal lattice of the material and converts the measurements to stress Fitzpatrick et al. (2005). However, the technique which the x-ray diffraction device employs is limited to the surface of the material, thus no inside/subsurface measurements have been conducted. In addition, measurements were limited to measurement of axial- and shear-residual stress. This was due to practical complications related to positional restrictions of equipment relative to pipe. Not every dented pipe had its axial-residual stress measured because the idea of measuring residual stress was not contemplated until a few tests had been conducted. Also, the locations for residual-stress measurements varied slightly from test to test due to relatively inaccurate measuring tools.

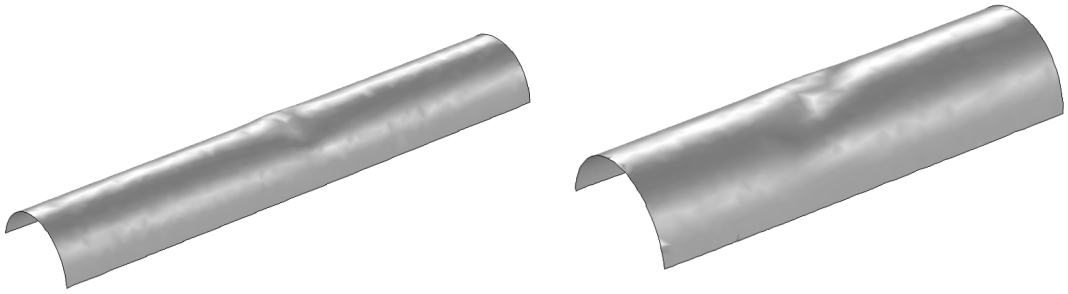

Figure 3.4: Shows geometry resulting from photogrammetry of pipes with 90 and 45 degree dent.

3.1.4 Building 3D-model from photogrammetry

The dented pipe-surface was re-created on the computer using photogrammetry. This technique involves taking photos of the object before importing the pictures to an appropriate software which converts them into a 3D-model. The software 3D Zephyr was put to good use for this purpose. The free version used in this thesis version allowed for up to 50 pictures to be used in creation of the dented pipe-surface. To ensure that the re-created surface had the same size as the real pipe, a 1x1cm paper-square was glued to the real pipe. The size of paper-square could be measured in 3D Zephyr and deviations in size could be accounted for at a later stage by simply scaling the model up or down. The software would frequently include details that were not a relevant part of the pipe-surface. These details were removed before the model was exported in .STL format and imported to the software Comsol Multiphysics for FEM analysis. Additional post-processing of the imported model was carried out in Comsol. The edges of the model were very irregular as a result of post-processing in Zephyr. The solution was to merge irregular edges with adjacent straight edges such that the model-boundary became relatively smooth. Without this process the automatic mesher or solver in Comsol would frequently run into issues.
The imported surface was meshed using quadratic triangular shell elements of size 1-3mm. Significantly smaller elements resulted in errors when Comsol attempted to solve the problem.

3.1.5 Simulated denting

The 45- and 90-degree pipe denting was simulated in Comsol Multiphysics. The simulated pipe proceeded to be pressurized to the same levels used in the laboratory fatigue-tests. This was

Figure 3.5: Shows the meshed imported geometry.

done, firstly because it was intended to be used as a reference model when performing fatigue-analysis through the Comsol fatigue-module, secondly it was a great way of improving the knowledge with regards to the consequences of denting. The custom end-caps were simplified to regular end-caps with thickness 10mm, made of the same material as the pipe. The edge at the bottom of the pipe were fixed against rotation and displacement as to mimic the support in the rig used during laboratory denting. As Comsol only supports contact through solid-mechanics, solid-elements had to be used to when meshing the geometry. Elements used were of type 'quadratic serendipity'. The 90-degree dent simulation used quadrilateral elements with 3 elements over the thickness in the region most affected by contact and tetrahedral elements used elsewhere. The 45-degree dent simulation used tetrahedral elements over the whole model, but a more refined mesh of 2 elements over the thickness in the contact region. The 'Augmented Lagrangian' method was used as the contact pressure method.

3.1.6 Fatigue Analysis

Fatigue-analysis of the imported geometry and simulated contact denting was initially planned to be carried out in Comsol Multiphysics. This plan had to be scrapped due issues with software licence. As a backup solution Quick Fatigue Tool, a Matlab extension, came in handy. Stress-range, residual stress, surface roughness and material-properties was the most important parameters submitted for analysis. Due to lacking an SN-curve for the pipe-material a material, SAE-1022, which had built-in SN-curve (σ_f b) and the same carbon content as the pipe-material, was used for analysis, with a few edited parameters; Young's modulus, proof

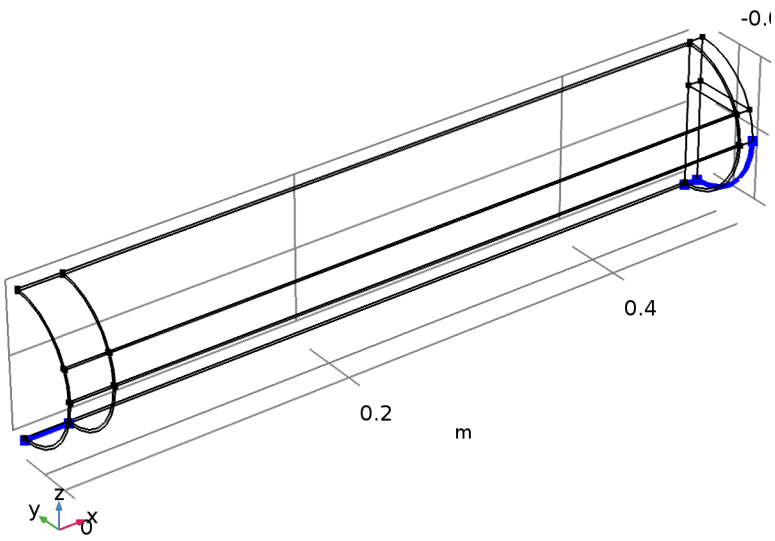

Figure 3.6: Shows edges that were fixed against displacement and rotation during contact-simulation.

Aberration: Findley= F, Brown-Miller=BM, NS=Normal Stress		
Material Property	Symbol	Algorithm
Tensile fatigue strength coefficient	σ'_f	NS, F, BM
Tensile fatigue strength coefficient	b	NS, F, BM
Young's Modulus	E	BM
Normal Stress Sensitivity Constant	k	F

Table 3.1: Shows which material parameters that are required to be specified by the user of Quick Fatigue Tool to run an analysis with corresponding algorithm.

stress, Poisson's ratio and tensile strength. It was therefor assumed SAE-1022's corresponding SN-curve would be the best choice out of materials contained in the software. Quick Fatigue Tool had 3 algorithms that was suitable for this problem; Normal Stress, Stress-Based Brown Miller and Findley's Method. Common for these algorithms is that they are multiaxial fatigue-criteria. Stress obtained from strain-gauges in laboratory, stress from

Fatigue-Life Estimation

The early attempts at trying to predict the fatigue-limit considered reversed bending-,reversed torsion-, static bending- and static torsion-stresses as variables. Moving forward until today, stress-based models are still widely used for predicting high-cycle fatigue while strain-based models are more common for low-cycle fatigue Socie and Marquis (2000).

Figure 3.7: Top figure shows default material parameters of material SAE-1022. Bottom figure shows edited version of SAE-1022, used in fatigue-analysis.

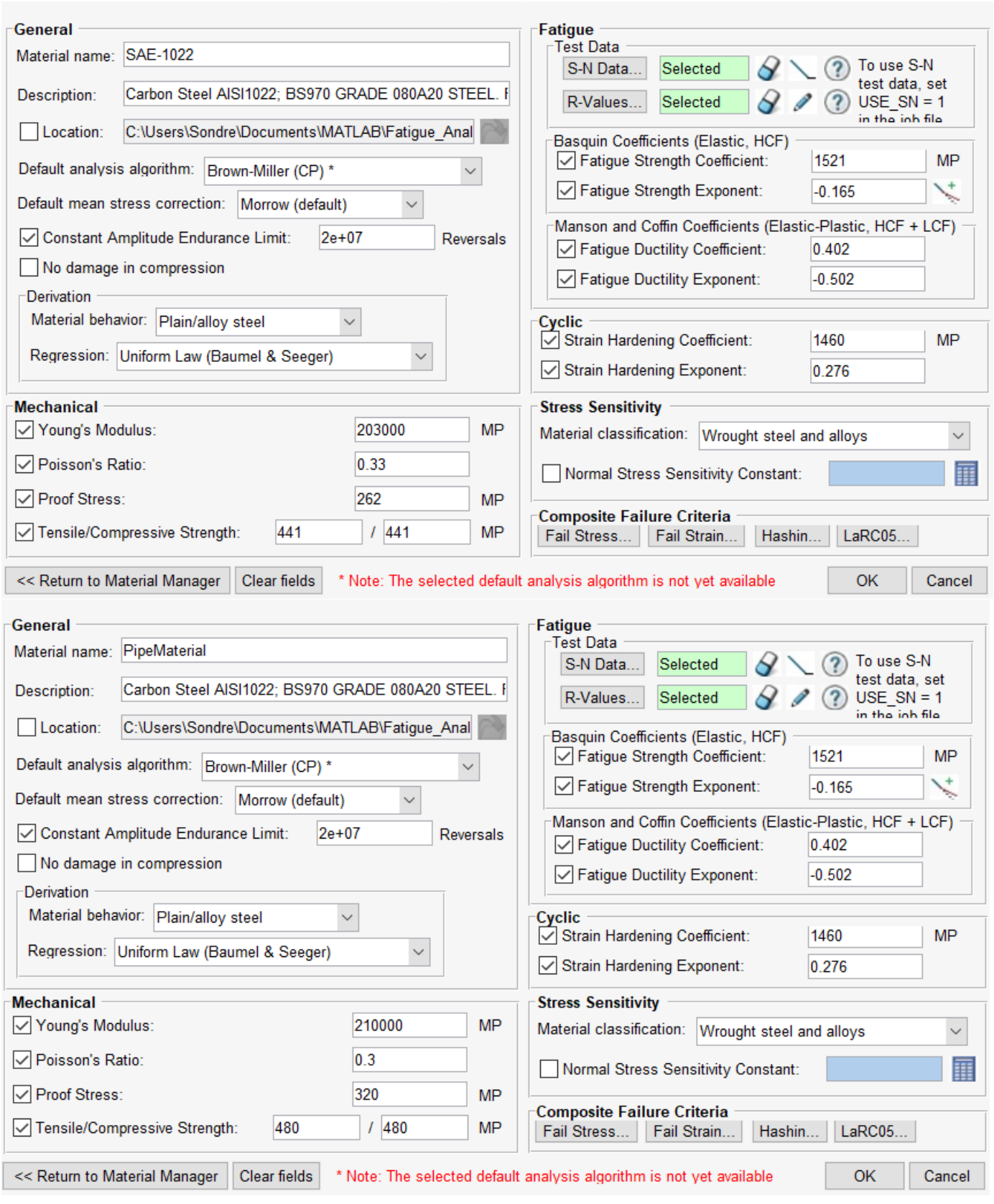

Stress-Based Brown Miller

The stress-based Brown Miller algorithm assumes that the fatigue damage is governed by the combination of shear and normal stress Vallace (2018):

$$\frac{\Delta\tau_{max}}{2} + \frac{\Delta\sigma_N}{2} = E(1.65\frac{\sigma'_f}{E}(2N_f)^b + 1.75\epsilon'_f(2N_f)^c) \tag{3.7}$$

Here the $\frac{\Delta\tau_{max}}{2}$ is the maximum shear-stress amplitude, $\frac{\Delta\sigma_N}{2}$ is the normal-stress while ϵ'_f and c is the fatigue-ductility coefficient and exponent found in fig:3.7

Normal Stress

The Normal Stress algorithm uses the normal stress amplitude as the damage parameter in stress-life equation Vallace (2018):

$$\frac{\Delta\sigma_N}{2} = \sigma'_f(2N_f)^b \tag{3.8}$$

Where the left-hand term is the max normal-stress amplitude, N_f is the number of cycles to failure and the remaining symbols are defined in 3.1.

Findley's Method

This method attempts to predict fatigue-life due to a combination of shear-stress amplitude and normal stress.

$$\frac{\Delta\tau}{2} + k\sigma_n|_{max} = \tau^*_f {N_f}^b \tag{3.9}$$

$$\tau'_f = 0.75\sigma'_f \tag{3.10}$$

$\frac{\Delta\tau}{2}$ is the shear-strain amplitude on the critical plane while σ_n is the normal stress and τ'_f is the shear-strength coefficient. Vallace (2018) Findley's method requires a normal-stress sensitivity constant, k, for the specific material. No value for this parameter was estimated, instead the default value of 0.2857 was used. Typical values for this parameter varies between 0.2 and 0.3 for ductile materials Socie and Marquis (2000).

	Mean Stress Correction						
Algorithm	Morrow	Goodman	Soderberg	Walker	SWT*	Gerber	None
Stress-based Brown-Miller	Yes	Yes	Yes	No	No	Yes	No
Normal Stress	Yes	Yes	No	Yes	Yes	Yes	No
Findley's Method	No	No	No	No	No	No	Yes

Table 3.2: Shows possible combinations of mean-stress corrections and critical-plane algorithms available in Quick-Fatigue Tool. SWT*=Smith-Watson-Topper

Residual Stress in Quick Fatigue Tool

Defining residual stress in Quick Fatigue Tool is limited to an in-plane residual stress. The software applies the defined residual stress value to the mean stress during each load cycle and is applied in all directions. Vallace (2018).

Mean Stress Corrections

Fatigue material data is often based on data in which the mean-stress is 0, meaning a R-ratio of -1. As is often the case, the mean stress in a load-cycle is not 0, thus there is a need for methods that can correct for the presence of a non-zero mean stress. A few mean-stress corrections are compatible with the critical-plane fatigue algorithms in Quick Fatigue Tool. An overview is posted in table:3.2. Explanation of theory and implementation in Quick Fatigue Tool can be found in Vallace (2018).

Chapter 4

Results

4.1 Results from laboratory tests

4.1.1 Result from denting

The force-displacements curves caused by vertical 90- and 45-degree denting of pipes can be found in fig:4.1 and fig:4.2. Although the area that has to be displaced is around 41% larger in the case of a 45 degree dent relative to 90 degree dent, the change in maximum contact force is only around 4kN.

4.1.2 Result from fatigue/pressure test

Most pipes had their dent-depth measured denting at dent-center. As described earlier, the pipes were dented to a depth of 16mm. Due to the internal pressure of 50 bar the dent would re-round as the indenter exited the dent. The measured dent-depth can be found in table:4.1. From this table one can see that 45-degree dents would typically re-round around 1mm more than 90-degree dents, which is mostly due to the 45-degree dent having a 41% longer dented region, which caused higher displacements at dent-center.

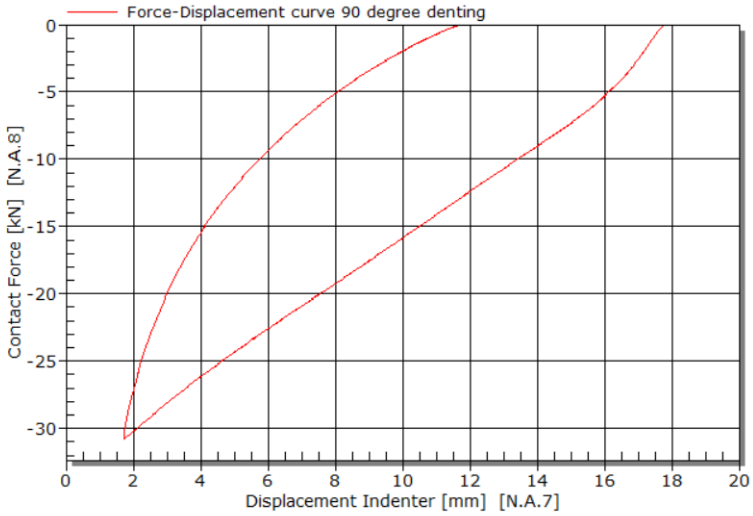

Figure 4.1: Top plot shows measured contact force vs time. Bottom plot shows force-displacement curve. Dent angle is 90 deg.

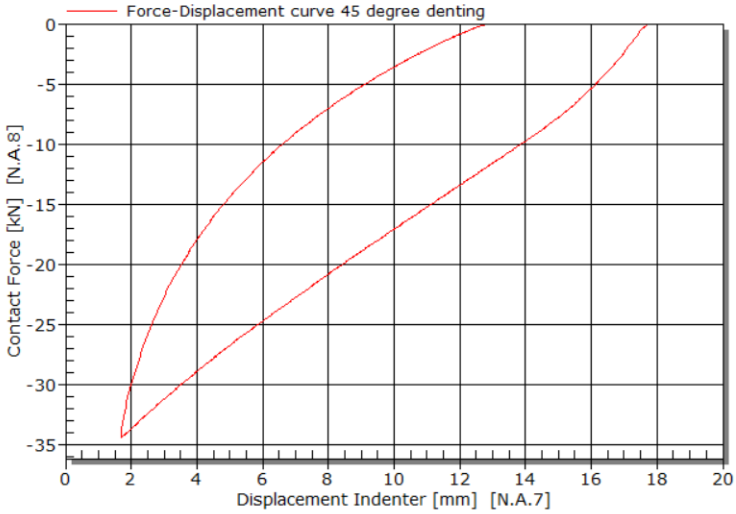

Figure 4.2: Top plot shows measured contact force vs time. Bottom plot shows force-displacement curve. Dent angle is 45 deg.

	Measured Dent Depth [mm]			
90 Degree Dent	7.26	7.51	7.86	7.74
45 Degree Dent	6.46	6.42	6.29	-

Table 4.1: Shows measured dent depth after denting and re-rounding due to internal pressure of 50[Bar]. Location of measurement is center of dent.

	Cycles to failure	
Pressure Range [Bar]	90 Deg Dent	45 Deg Dent
6-60	31.1k	-
5-50	67.5k	-
4-40	215k	68.5k
3.7-37	345k	-
3.2-32	1.4mill	184k
2.5-25	-	2mill

Table 4.2: Overview of fatigue-tests of dented pipes. Shows number of cycles til failure for a given pressure range and dent-angle. Blank field means that no test was conducted.

Results from fatigue-tests

The fatigue-life of each dented pipe and its corresponding pressure-range is shown in fig:4.2. These results are further visualized in fig:4.3. What can be seen is that the pipes containing a 45-degree dent has a lot shorter fatigue-life than the corresponding 90-degree dent. In addition, both the 45- and 90-degree dents, created by vertical displacement of the indenter into the pipe, has a very severe impact on the fatigue-life of the pipe when compared to a 90-degree dent created by horizontal displacement of the indenter in Aadal (2016). The dent depth of the dents created in Aadal (2016) was around 7.5-7.75mm, which is very similar to measured 90-degree dent depth in table:4.1. Although there are only a few tests conducted at various pressure levels the trend is clear. Major differences that can explain the difference in fatigue-life can be traced back to the methods of indentation. The pipes subject to denting in Aadal (2016) were heavily constrained in all directions due to the clamps used at both the top and bottom of the pipe. This limited the deformation due to denting to a small area. The pipes in this thesis only had lateral and vertical support at the bottom of the pipe during denting, allowing a much larger region of the pipe to deform as the indenter was displaced into the pipe.

Crack Locations in Dent

Figure4.4-4.10 shows the location of all cracks that appeared in fatigue-tests. All, but one crack, appeared to grow in the dent-longitudinal direction. The one crack that deviated from the rest is shown in fig:4.7, which grew in the longitudinal pipe-direction. In the case of a 90-degree dent, longitudinal cracks would form in a region corresponding to around 17mm to to to 35mm

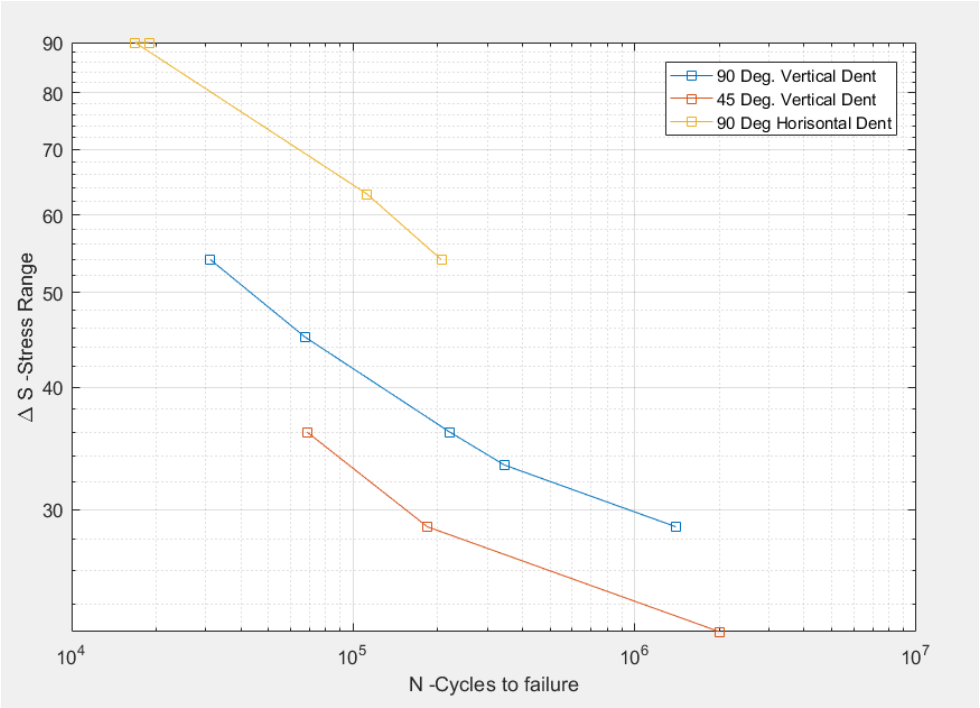

Figure 4.3: Shows fatigue life of 3 different dents. Two types of dents caused by vertical displacement of indenter, one 90- the other 45 degrees. One type of dent caused by horizontal displacement of indenter.

away from the dent-center. Cracks would form in the lower part of this band in the case of high internal pressure (50 60 Bar), while cracks formed in the upper part of this band in the case of lower internal pressure. Pipes cotaining a 45-degree dent had cracks form on the dent-shoulder, near the exit of the dent, growing inwards towrads the dent-center (4-1.5mm from dent-center).

Measured Stress-Range in Dent

The relative change in strains in the surface of the dent were measured at locations where cracks were assumed to nucleate using strain-gauges. Locations varied sligthly between each test due to human error related to glueing strain-gauges. The locations are visualized in figure:4.11 The strains were converted to stress and the calculated stress-values can be found in table:4.4 to 4.10. Direct comparison between stresses in different fatigue-tests are difficult because of the large gradients contained in the dent, causing a slight misplaced of one strain-gauge relative to another test to be of large importance. Nevertheless, a quick review

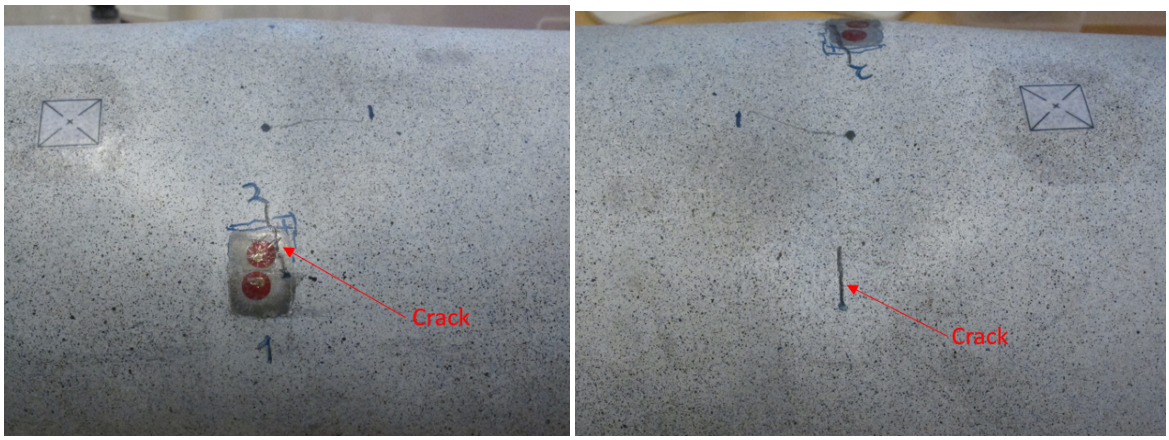

Figure 4.4: Shows location of two cracks on the same pipe in 90 deg dent. Pipe was exposed to a cyclic pressure of 5-50 [Bar] with fatigue life of 68k cycles.

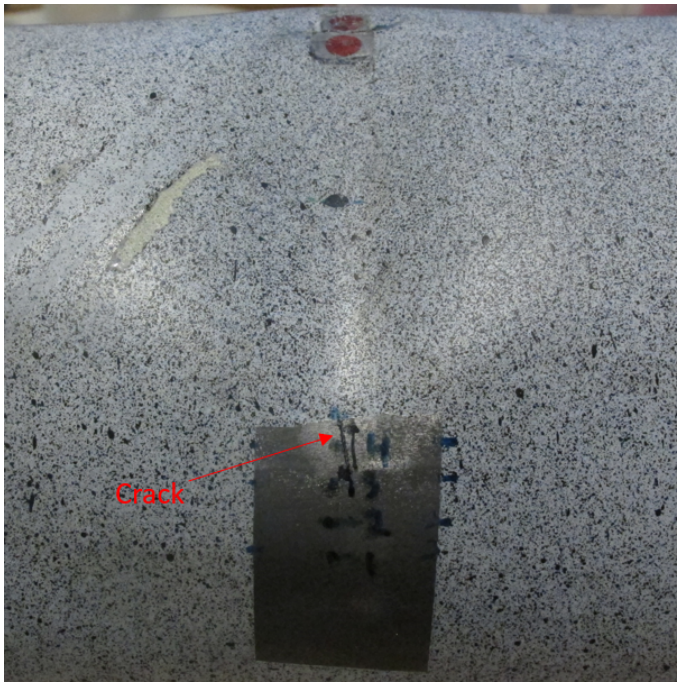

Figure 4.5: Shows location of crack in 90 deg dent. Pipe was exposed to a cyclic pressure of 4-40 [Bar] with fatigue life of 215k cycles.

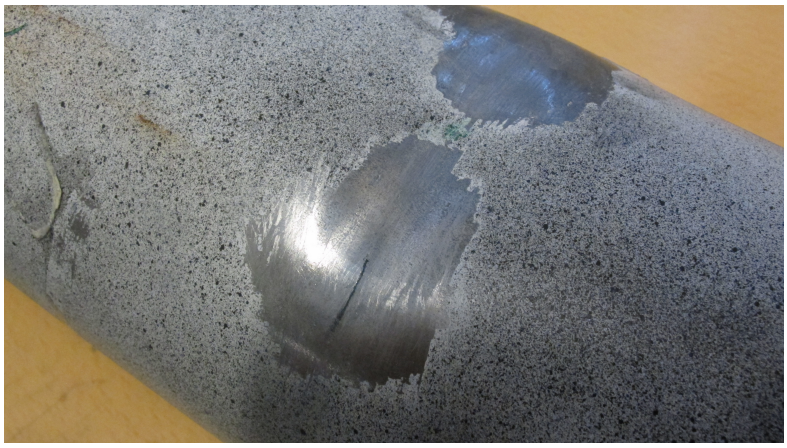

Figure 4.6: Shows location of crack in 90 deg dent. Pipe was exposed to a cyclic pressure of 3.7-37[Bar] with fatigue life of 345k cycles.

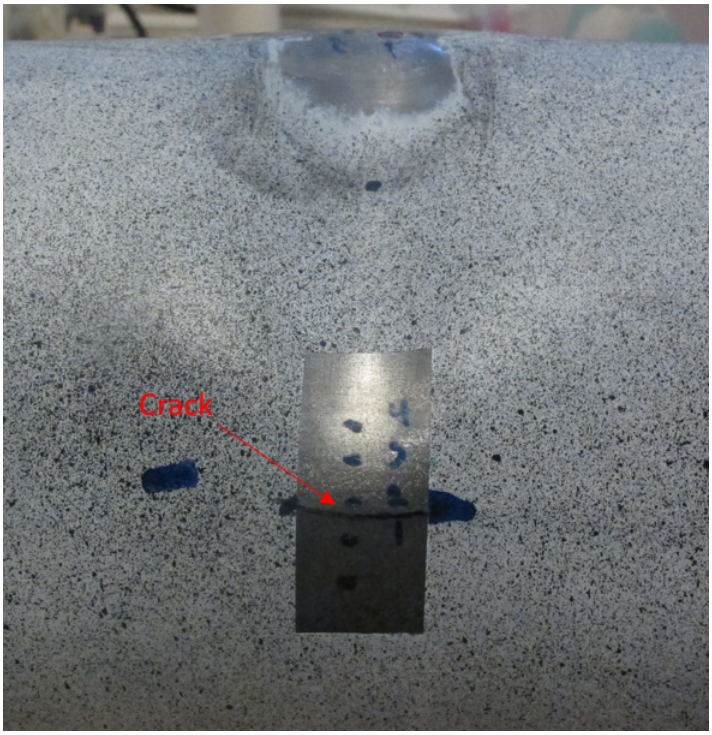

Figure 4.7: Shows location of crack in 90 deg. dent. Pipe was exposed to a cyclic pressure of 3.2-32[Bar] with fatigue life of 1.4mill cycles.

Figure 4.8: Shows location of crack in 45 deg. dent. Pipe was exposed to a cyclic pressure of 4-40[Bar]with fatigue life of 69k cycles.

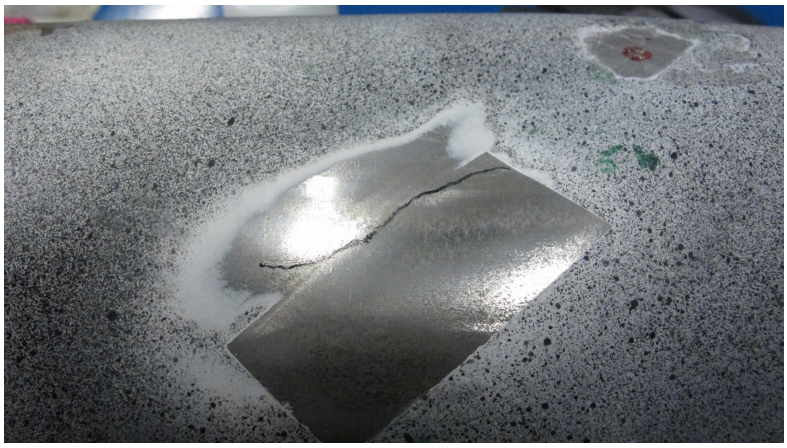

Figure 4.9: Shows location of crack in 45 deg. dent. Pipe was exposed to a cyclic pressure of 3.2-32[Bar] with fatigue life of 184k cycles.

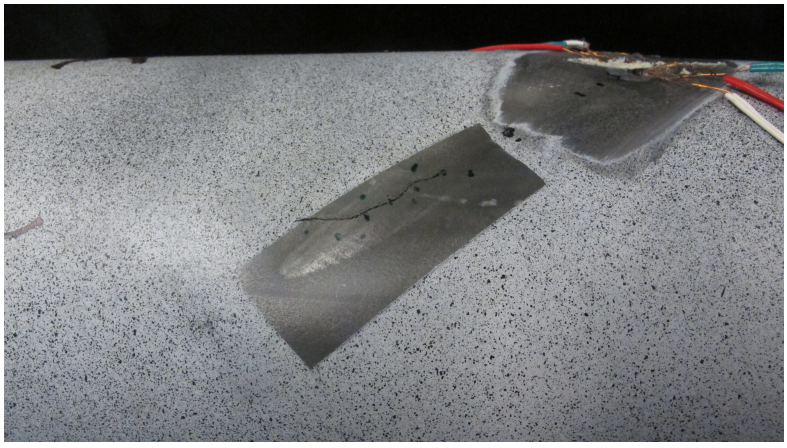

Figure 4.10: Shows location of crack in 45 deg. dent. Pipe was exposed to a cyclic pressure of 2.5-25[Bar] with fatigue life of 2mill cycles.

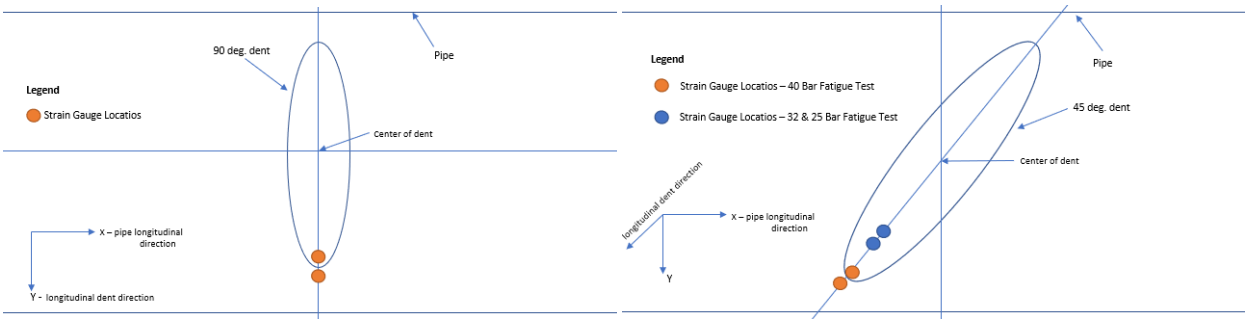

Figure 4.11: Shows a sketch indicating locations of strain-gauges in the various fatigue-tests.

Strain-gauge 1 location		
Pressure Range	90-degree dent	45-degree dent
5-50	3	-
4-40	2.95	4.7
3.7-37	2.1	-
3.2-32	2.95	2.45
2.5-25	-	3.75
Strain-gauge 2 location		
Pressure Range	90-degree dent	45-degree dent
5-50	2.6	-
4-40	2.35	4.25
3.7-37	1.85	-
3.2-32	2.65	2.05
2.5-25	-	3.25

Table 4.3: Shows the location of each strain-gauge. Values on columns 2 and 3 is distance from dent-center in mm. Note that strain-gauge 2 is always closest to the center.

reveals the following: The stress-range in the vicinity of the area where cracks form in 90-degree dents are dominated by large, tensile axial stresses while the shear-stress may be either tensile or compressive, depending on location. The stresses from table4.9 4.10 dents shows that the largest stress component is radial stress, while axial stresses are still of relatively large magnitude. They are also of much more severe magnitude as compared to table4.8, which is solely because of the difference in the position of these strain-gauges. When compared to stress-range from 90-degree dents one should notice that the radial stress is significantly larger. This shift is due to the dent-angle now being 45-degrees causing the stress in the local dent-coordinate system to also have a component in the global x- and y-direction. It should also be noted that the stress-range is in general larger at strain-gauge number two than number one, indicating that the stress-range increased the closer one gets to the center of the dent.

Strain Gauge 1	Axial Stress [MPa]	Radial Stress [MPa]	Shear Stress (XY) [MPa]
At 40 Bar Pressure	736	376	-529
At 4 Bar Pressure	129	72	-86
Stress Range	607	304	-444
Strain Gauge 2	Axial Stress [MPa]	Radial Stress [MPa]	Shear Stress (XY) [MPa]
At 40 Bar Pressure	1042	678	-437
At 4 Bar Pressure	161	108	-64
Stress Range	881	571	-373

Table 4.4: Shows stress obtained from strain-gauges mounted on a pipe containing a 90 degree dent, subject to cyclic internal pressure of 5.0-50 [Bar]

Strain Gauge 1	Axial Stress [MPa]	Radial Stress [MPa]	Shear Stress (XY) [MPa]
At 40 Bar Pressure	561	5.9	-33.5
At 4 Bar Pressure	75.36	-14	-12.4
Stress Range	485	20	-21
Strain Gauge 2	Axial Stress [MPa]	Radial Stress [MPa]	Shear Stress (XY) [MPa]
At 40 Bar Pressure	820	386	-31
At 4 Bar Pressure	112	55	-3.7
Stress Range	708	331	-27

Table 4.5: Shows stress obtained from strain-gauges mounted on a pipe containing a 90 degree dent, subject to cyclic internal pressure of 4.0-40 [Bar]

Strain Gauge 1	Axial Stress [MPa]	Radial Stress [MPa]	Shear Stress (XY) [MPa]
At 40 Bar Pressure	515	47	130
At 4 Bar Pressure	69	14	17
Stress Range	446	33	113
Strain Gauge 2	Axial Stress [MPa]	Radial Stress [MPa]	Shear Stress (XY) [MPa]
At 40 Bar Pressure	561	222	-17
At 4 Bar Pressure	-94	-26	12
Stress Range	655	248	-28

Table 4.6: Shows stress obtained from strain-gauges mounted on a pipe containing a 90 degree dent, subject to cyclic internal pressure of 3.7-37 [Bar]

Strain Gauge 1	Axial Stress [MPa]	Radial Stress [MPa]	Shear Stress (XY) [MPa]
At 40 Bar Pressure	475	222	-327
At 4 Bar Pressure	51	22	-31
Stress Range	424	200	-296
Strain Gauge 2	Axial Stress [MPa]	Radial Stress [MPa]	Shear Stress (XY) [MPa]
At 40 Bar Pressure	699	575	-287
At 4 Bar Pressure	72	60	-31
Stress Range	627	515	-256

Table 4.7: Shows stress obtained from strain-gauges mounted on a pipe containing a 90 degree dent, subject to cyclic internal pressure of 3.2-32 [Bar]

Strain Gauge 1	Axial Stress [MPa]	Radial Stress [MPa]	Shear Stress (XY) [MPa]
At 40 Bar Pressure	214	47.5	-0.16
At 4 Bar Pressure	21.5	0	-0.8
Stress Range	193	47.5	0.66
Strain Gauge 2	Axial Stress [MPa]	Radial Stress [MPa]	Shear Stress (XY) [MPa]
At 40 Bar Pressure	243	143	157
At 4 Bar Pressure	23	4.7	21.5
Stress Range	220	138	135

Table 4.8: Shows stress obtained from strain-gauges mounted on a pipe containing a 45 degree dent, subject to cyclic internal pressure of 4.0-40 [Bar]

Strain Gauge 1	Axial Stress [MPa]	Radial Stress [MPa]	Shear Stress (XY) [MPa]
At 32 Bar Pressure	775	842	-280
At 3.2 Bar Pressure	86	79	-41
Stress Range	689	762	-238
Strain Gauge 2	Axial Stress [MPa]	Radial Stress	[MPa] Shear Stress (XY) [MPa]
At 32 Bar Pressure	552	289	21.5
At 3.2 Bar Pressure	32	7.1	7.6
Stress Range	520	282	13.9

Table 4.9: Shows stress obtained from strain-gauges mounted on a pipe containing a 45 degree dent, subject to cyclic internal pressure of 3.2-32 [Bar]

Strain Gauge 1	Axial Stress [MPa]	Radial Stress [MPa]	Shear Stress (XY) [MPa]
At 25 Bar Pressure	211.5	364	109
At 2.5 Bar Pressure	25	50	13
Stress Range	186	314	96
Strain Gauge 2	Axial Stress [MPa]	Radial Stress	[MPa] Shear Stress (XY) [MPa]
At 25 Bar Pressure	249	526	105
At 2.5 Bar Pressure	25	54	11.6
Stress Range	224	471	94

Table 4.10: Shows stress obtained from strain-gauges mounted on a pipe containing a 45 degree dent, subject to cyclic internal pressure of 2.5-25[Bar]

4.1.3 Result from residual stress measurement

Results from measured residual axial-stress and shear-stress along dent-center lines can be found in figure:4.12-4.15. A straight-line has been drawn in-between data-points for easier visualization. Each unique colour corresponds to a unique pipe. The measured residual shear-stress (figure:4.13+4.15) contains a large amount of scatter. This can traced back to the uncertainty of the measurements were often in the +-5-10MPa range, in addition the measured values are often small. On top of that there is the scatter in each specimen. Focusing on figure:4.12; a large gradient stress gradient is found in the area 3-3.5mm, where compressive residual-stresses shift to tensile as distance from dent-center increases. Remembering that cracks were observed in the area 1.7mm-3mm it is theorized that the combination small residual-stresses and whatever stress-range found at that location, provides the most favorable environment for crack-growth for this type of dent. Comparing figure4.14 4.12, one can see that the same shape is present. However, the compressive residual stress is slightly less, while the tensile residual stress is measured to be slightly larger. Despite this, cracks did initiate closer to the dent-shoulder, which suggests the following: The 45- and 90-degree dent has a similar stress-state near the edge of the dent, however the 45-degree dent has a more favorable crack-growth location around the dent-shoulder, causing the much shorter fatigue-life.

4.1.4 Result from pressure-test of imported geometry

Boundary-conditions was a hot-topic for the imported geometry. A large number of numerical pressure tests of the imported geometry, with different boundary conditions, were conducted to determine the boundary conditions that could best mimic the results from laboratory measurements. Consider then a pipe oriented such that its longitudinal direction is paralell to the x-axis.

The boundary-conditions the were found to be the fit for this problem are visualized in fig:4.16. The imported geometry was restrained against displacement in y- and z-direction along the longitudinal edges. While a real pipe is free expand outwards in both y- and z-directions, the imported geometry was only free to expand in the z-direction. Having the imported geometry expand in both y- and z-direction resulted in very, very large stresses that did not correlate well

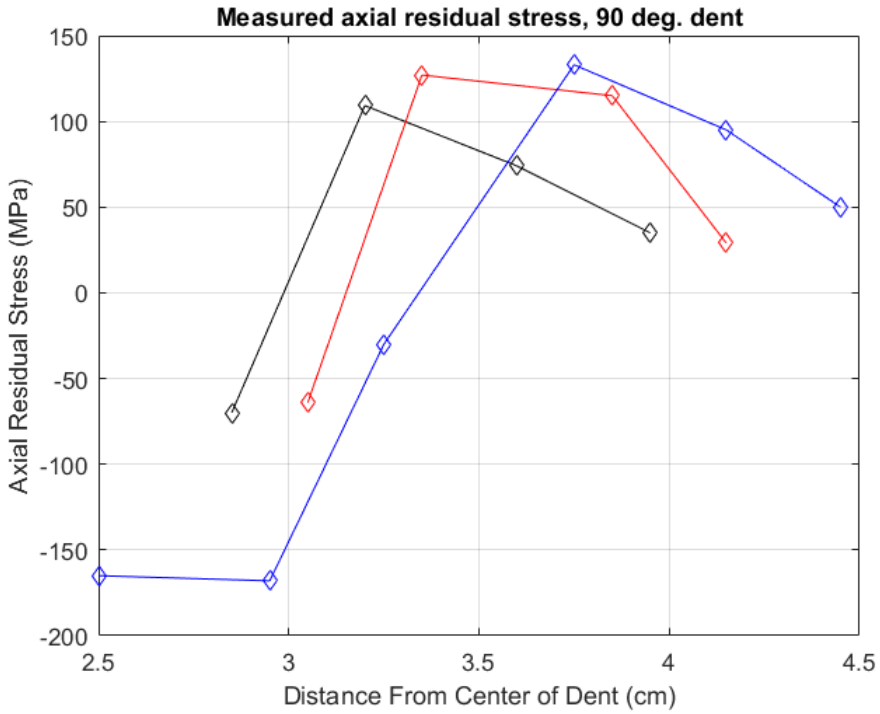

Figure 4.12: Shows measured axial residual stress along longitudinal direction of 90 deg. dent in 3 pipes after denting.

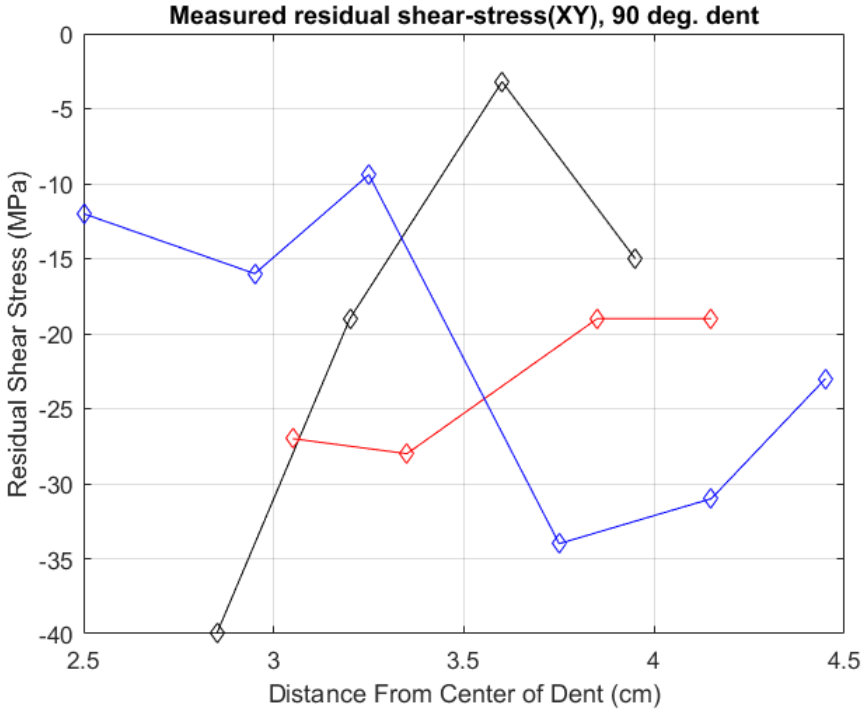

Figure 4.13: Shows measured residual shear stress along longitudinal direction of 90 deg. dent in 3 pipes after denting.

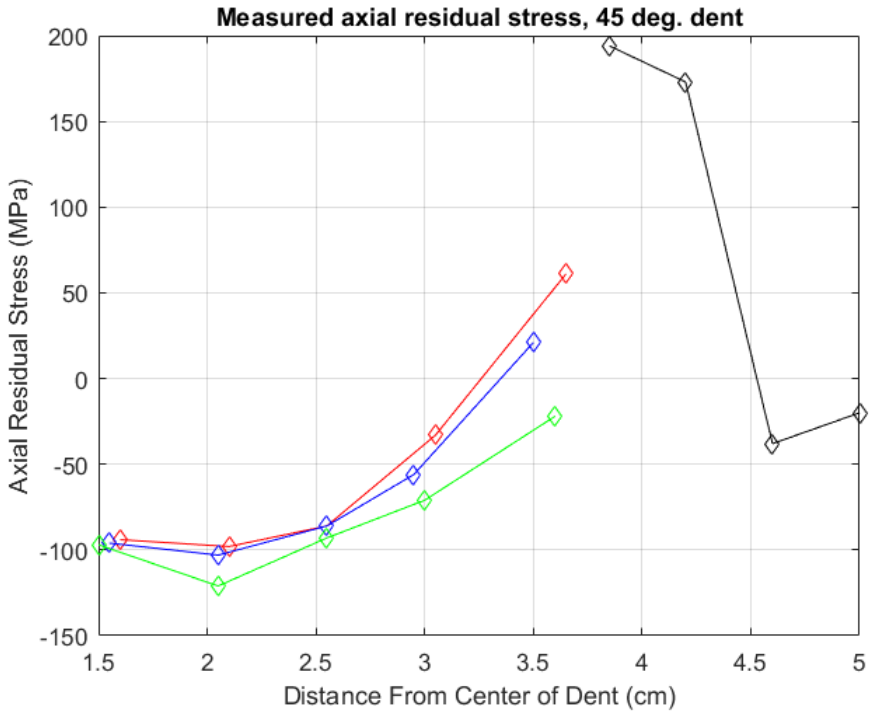

Figure 4.14: Shows measured axial residual stress along longitudinal direction dent direction if 45 degree-dent in 3 pipes.

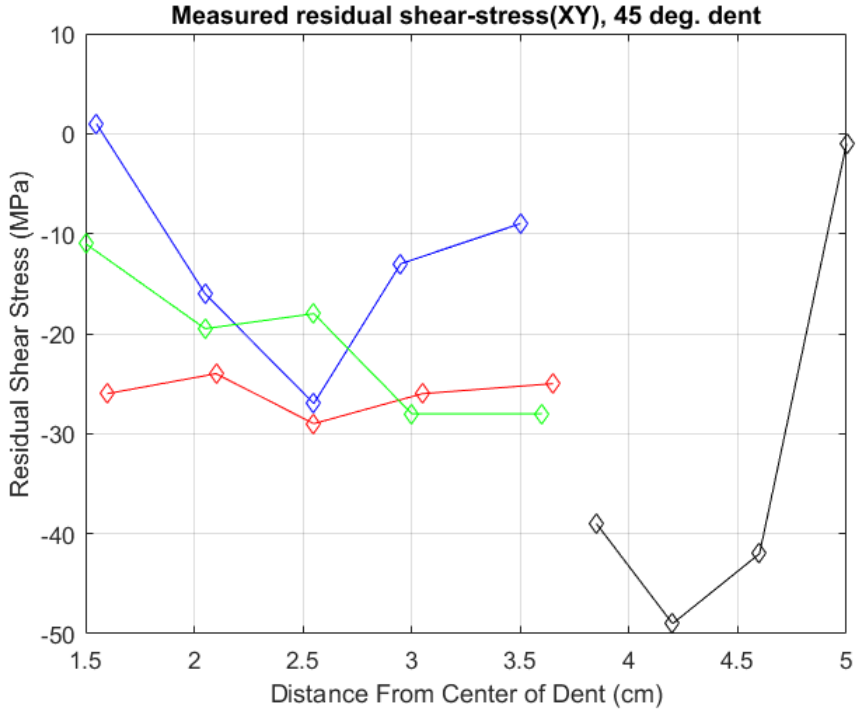

Figure 4.15: Shows measured residual shear-stress along longitudinal direction of 45 deg. dent in 4 pipes after denting.

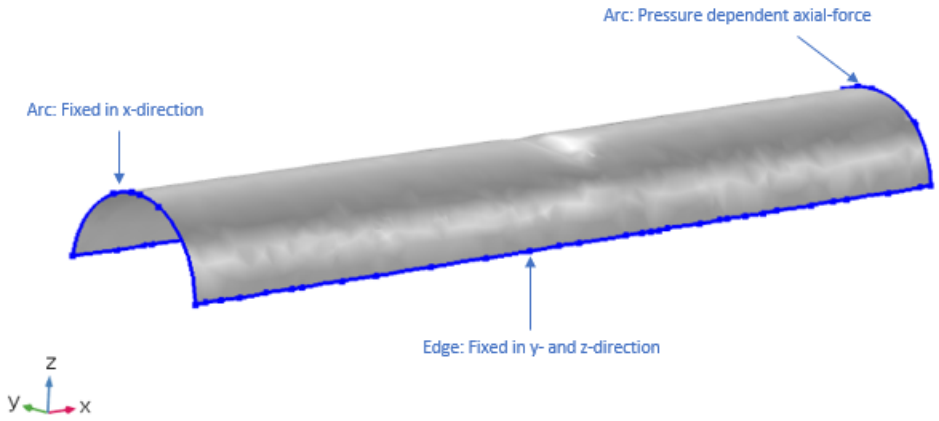

Figure 4.16: Illustrates boundary conditions applied to the imported geometries.

with the stresses obtained from the lab. One arc was fixed in the x-direction (longitudinal-direction) and a pressure-dependent edge-load was applied on the other, causing axial forces in the pipe as was also the case for laboratory tests. The magnitude of the axial edge-load was determined by:

$$F_x = \frac{P\pi(r_o^2 - r_i^2)r_o}{2t} \qquad [\mathrm{N}] \tag{4.1}$$

$$N_x = \frac{F_x}{c} \qquad [\mathrm{N\,m^{-1}}] \tag{4.2}$$

Where F_x is the axial-force, is the c is the circumferential length of the pipe, P is the varying internal pressure, r_o and r_i is the outer and inner radius of the pipe, t is the wall-thickness and N_x is the applied edge-load Roylance (2001).

4.2 Results from contact simulation

Note that the stress is obtained in terms of global coordinates. Cylindrical coordinates, which was used in lab-experiments and imported geometry simulation, was not available in Comsol due to asymmetry.

The force-displacements curves caused by simulated vertical 90- and 45-degree denting of pipes can be found in fig:4.17 and fig:4.18. A quick comparison between these figures shows that contact force is slightly less in the case of 90-degree denting as compared to 45-degree

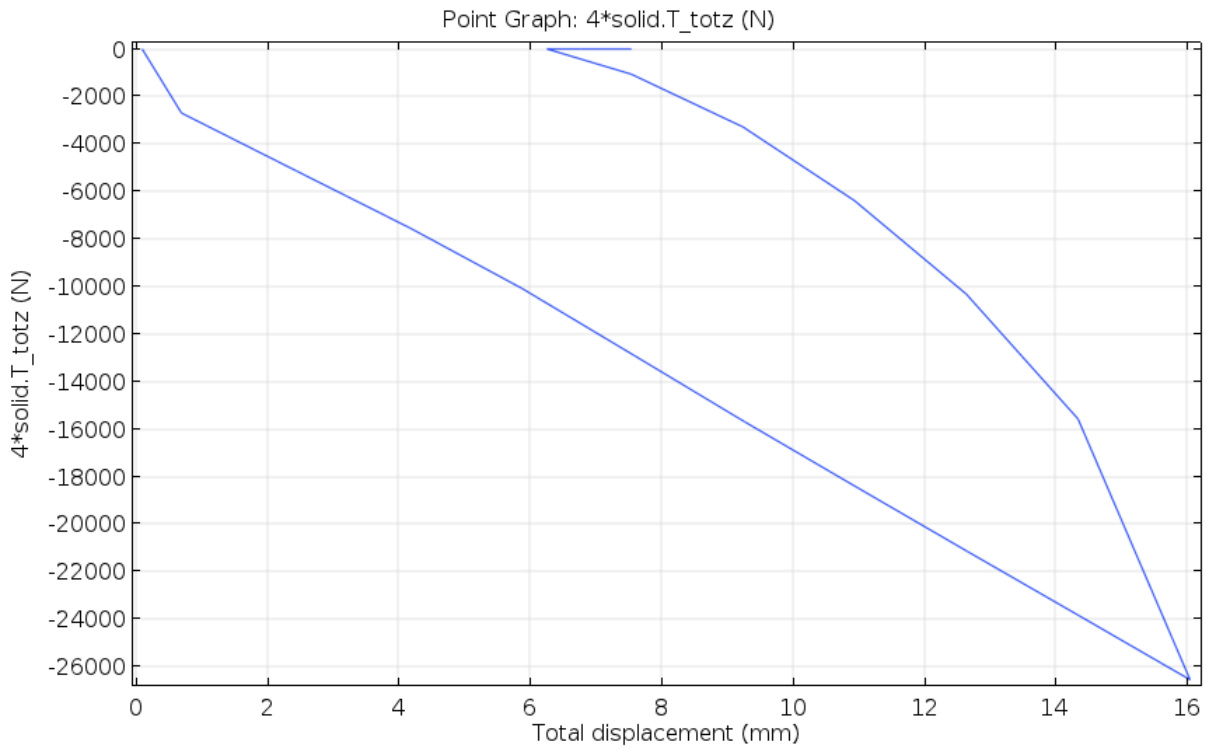

Figure 4.17: Shows force-displacement curve at the center of dent during simulated denting in Comsol. Dent angle is 90 deg.

denting(26kN vs 28 kN). When compared to 4.1 and 4.2 one can see the difference between simulated denting and denting conducted in lab is around 6kN in the case of both 90- and 45-degree denting. This suggests that simulated denting is 'softer' than the laboratory denting. The main reason may be due to differences in material properties between simulated and dented pipe. While Comsol uses only Young's modulus and not a flexural modulus which will cause deviations in the case where there is a notable difference between flexural modulus and Young's modulus. The simulated dents would re-round to a depth of 7.73mm (90-degree) and 6.37mm (45-degree), which is very similar to the re-rounded dent-depth measured in the laboratory dents table: 4.1.

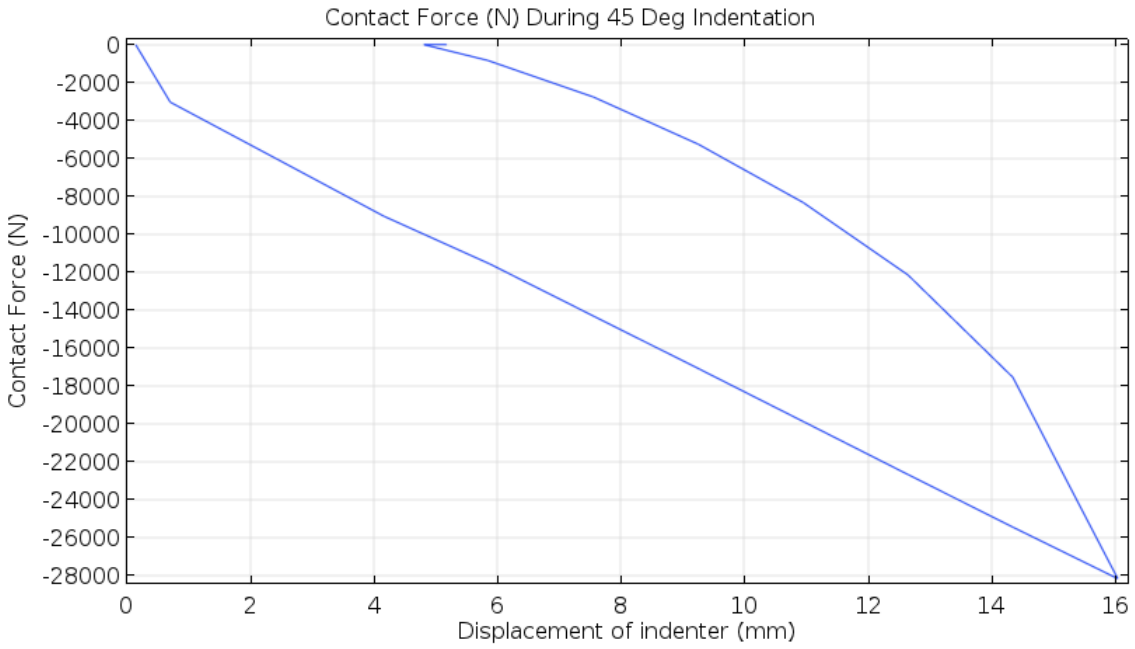

Figure 4.18: Shows force-displacement curve at the center of dent during simulated denting in Comsol. Dent angle is 45 deg.

4.2.1 Residual Stress

90-degree dents

Surface-plots of residual stress due to simulated 90-degree denting is found in figure:4.19-4.21. A proceeding trend is the large compressive residual-stresses contained in the dent due to contact. Most notable is the region of small tensile residual stress found at the edge of the dent in figure:4.19. This region corresponds to the spike found at x=0.035m in figure:4.22. From this graph, it can be observed that no other region has a higher total of residual stress. Comparing the axial-residual stress found in figure:4.22 with axial residual-stress (Sx) in figure:4.12, it is easy to see that the shape and location of both plots are both similar. However the magnitude of the residual stress is very different. The residual stress measured in the laboratory is tensile at its peak, while its corresponding, simulated value is still compressive in the -60MPa range. The most interesting finding is that the region at the end of the dent, containing small compressive and tensile residual stress, corresponds to the region where cracks were found to initiate/grow.

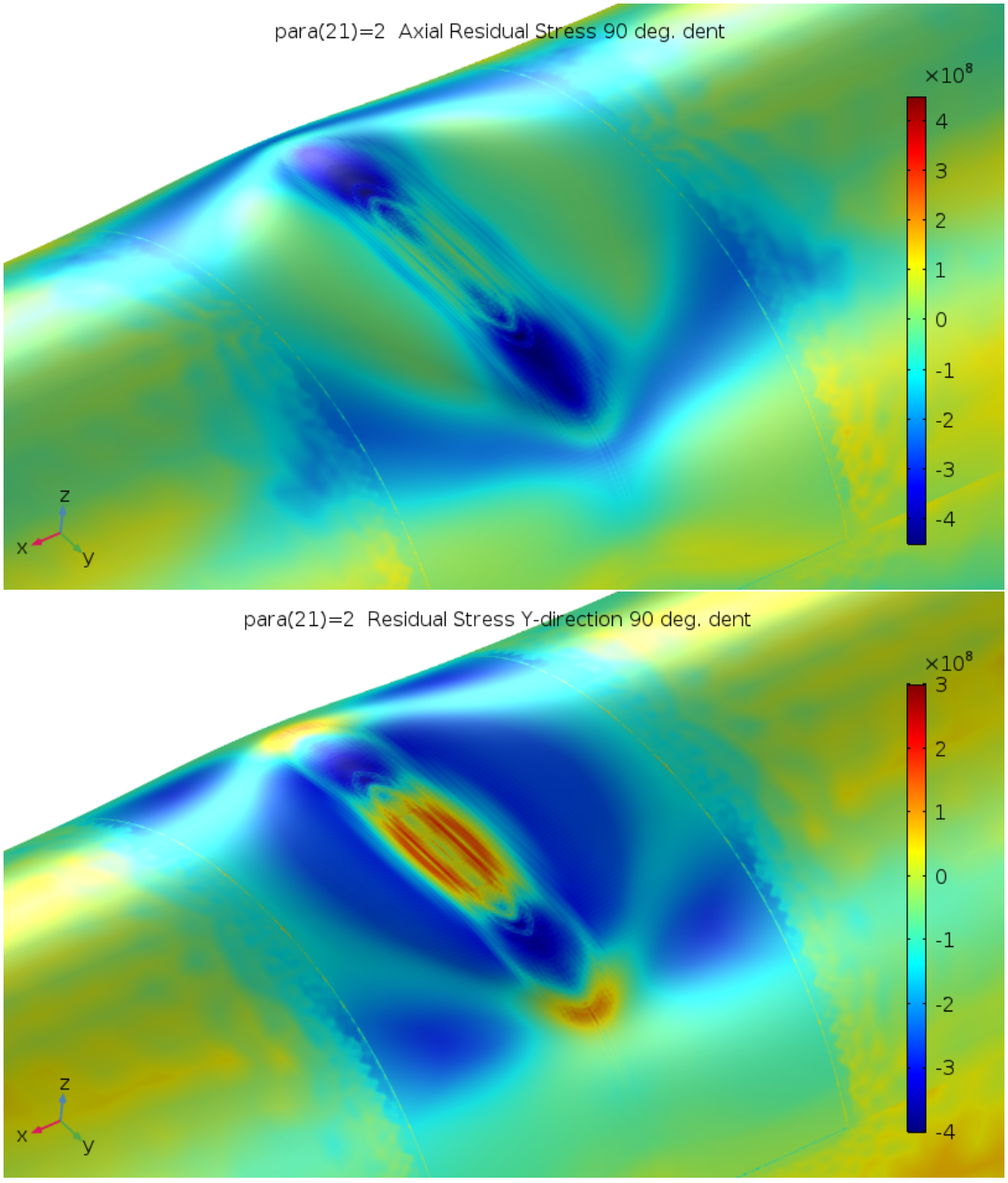

Figure 4.19: Shows residual stress in X and Y direction after 90 degree denting.

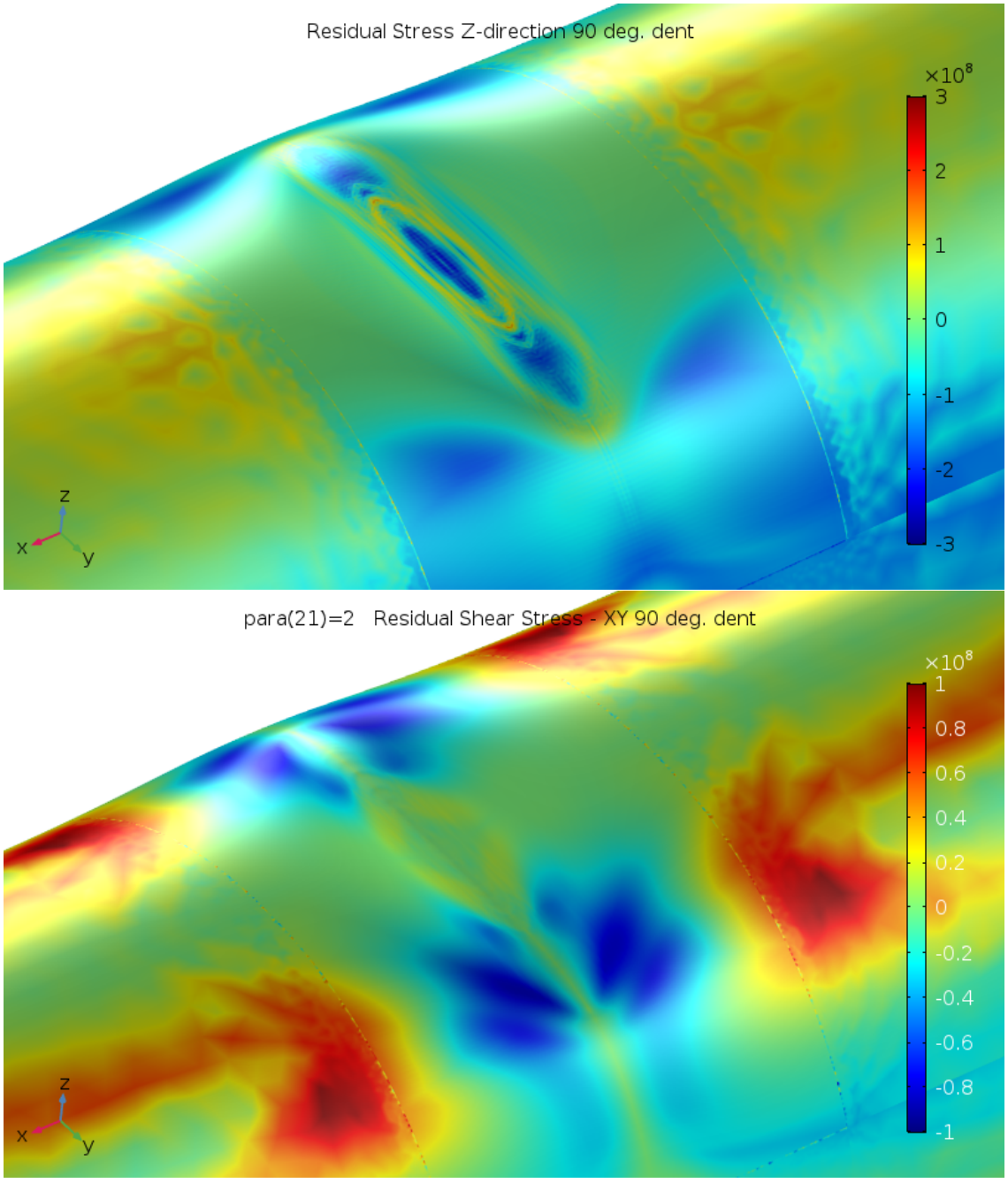

Figure 4.20: Shows residual stress in Z direction and residual shear stress (XY) distribution after 90 degree denting.

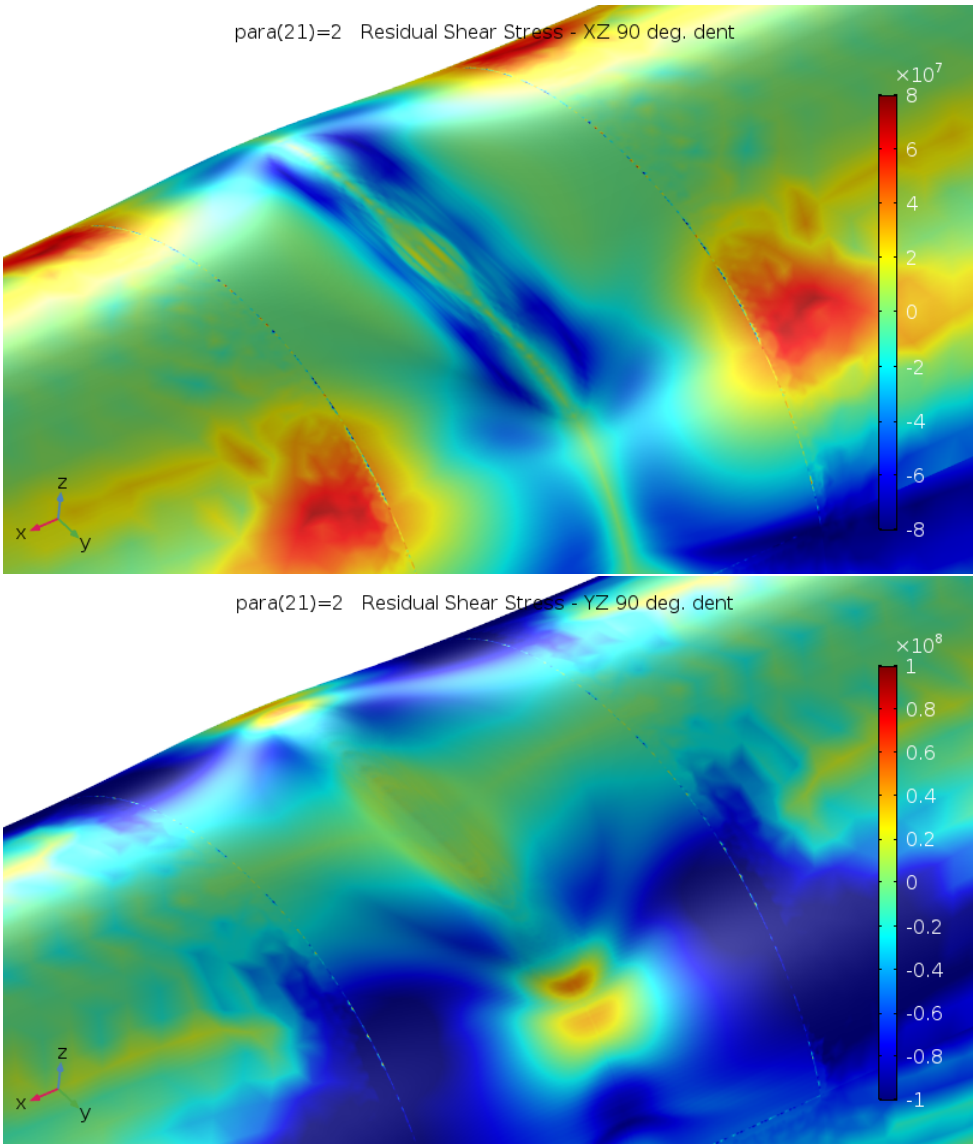

Figure 4.21: Shows residual shear stress (XZ and YZ) distribution after 90 degree denting.

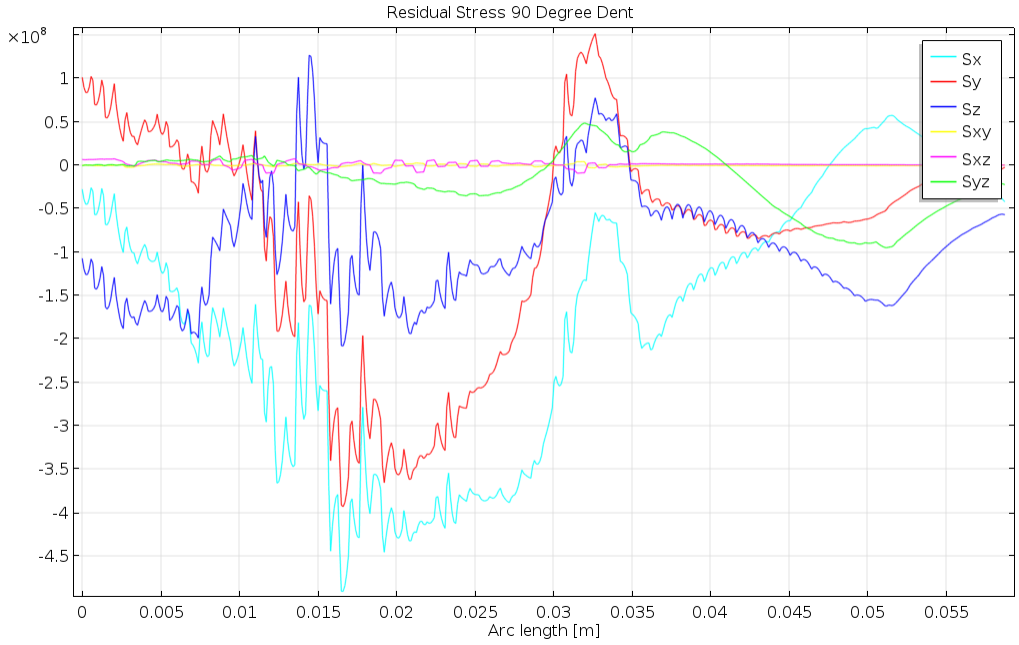

Figure 4.22: Shows residual stress distribution along longitudinal dent-direction after 90 degree denting. X=0 corresponds to dent-center.

45-degree dents

Graphs showing detailed overview of the residual stress along the dent longitudinal-direction is found in figure:4.26. As is the case for the simulated 90-degree denting, the residual stresses in the region are largely compressive, while they are subsiding the closer one gets to the dent-shoulder. Comparing the axial-residual stress found in figure:**??** with measured axial residual-stress (Sx) in figure:4.14, one can see that the magnitude of the residual stress and its distribution agrees rather well. However, the location of the tensile peak is shifted further towards the dent-exit, about 10mm, in the case of simulated denting. In addition, the measured axial-residual stress seems to flatten around -100MPa, while the simulated residual stress is decreasing to a much larger value, around 250-300MPa.

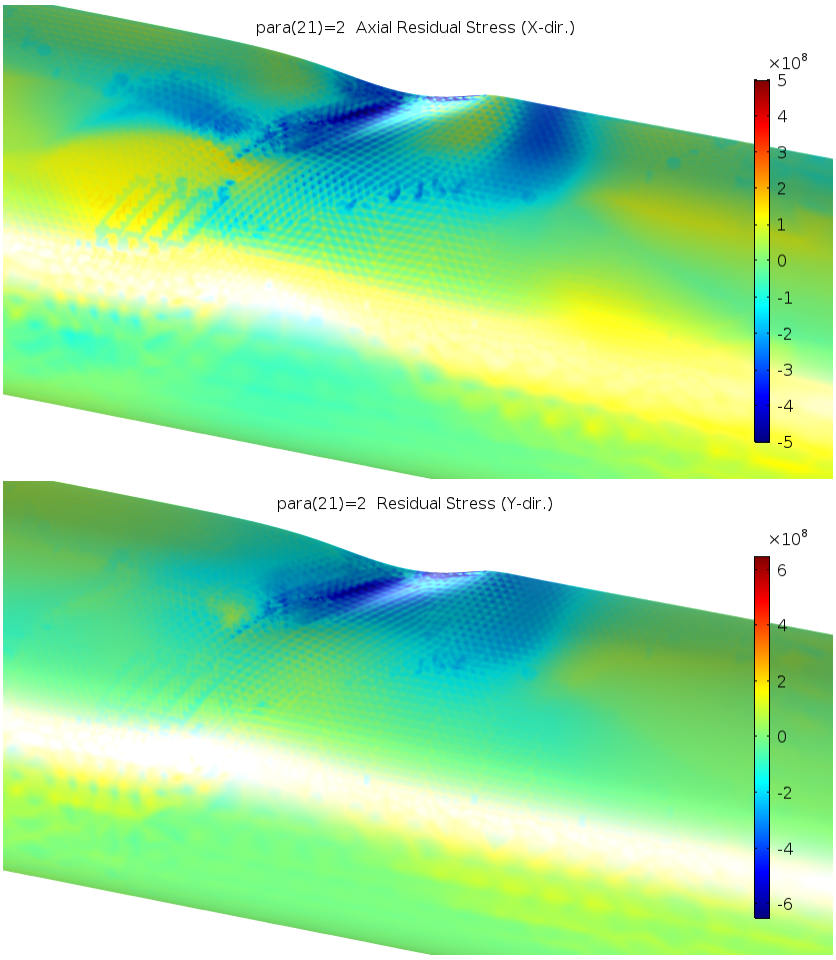

Figure 4.23: Shows residual stress in X and Y direction after 45 degree denting.

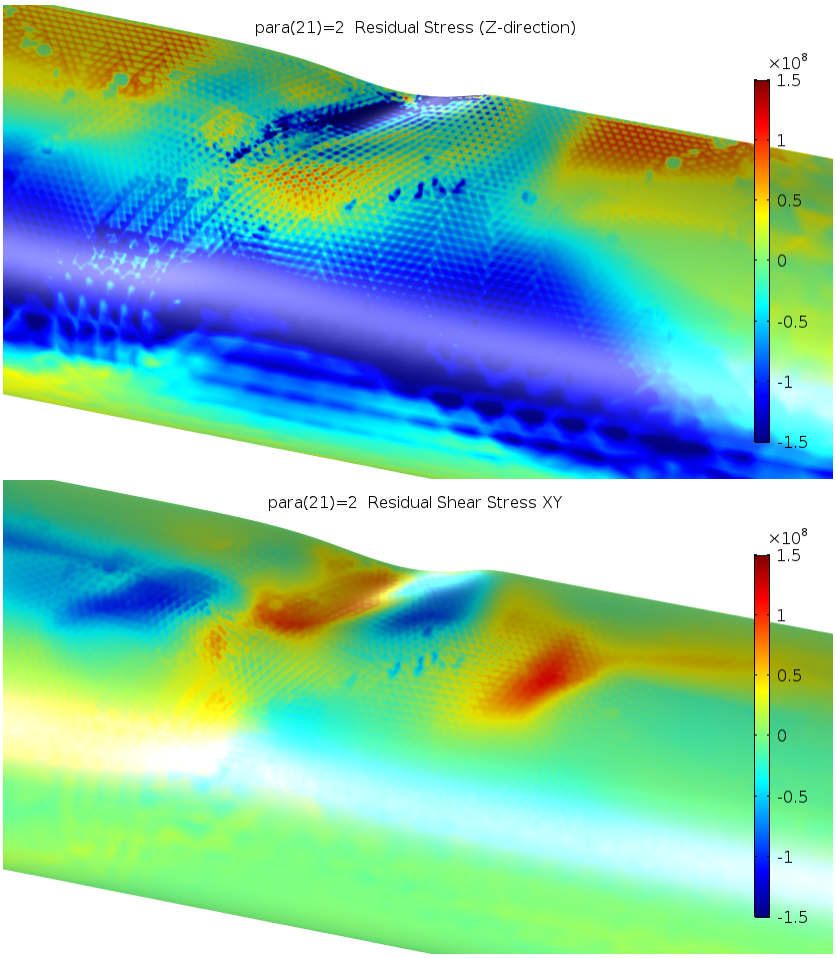

Figure 4.24: Shows residual stress in Z direction and residual shear stress (XY) distribution after 45 degree denting.

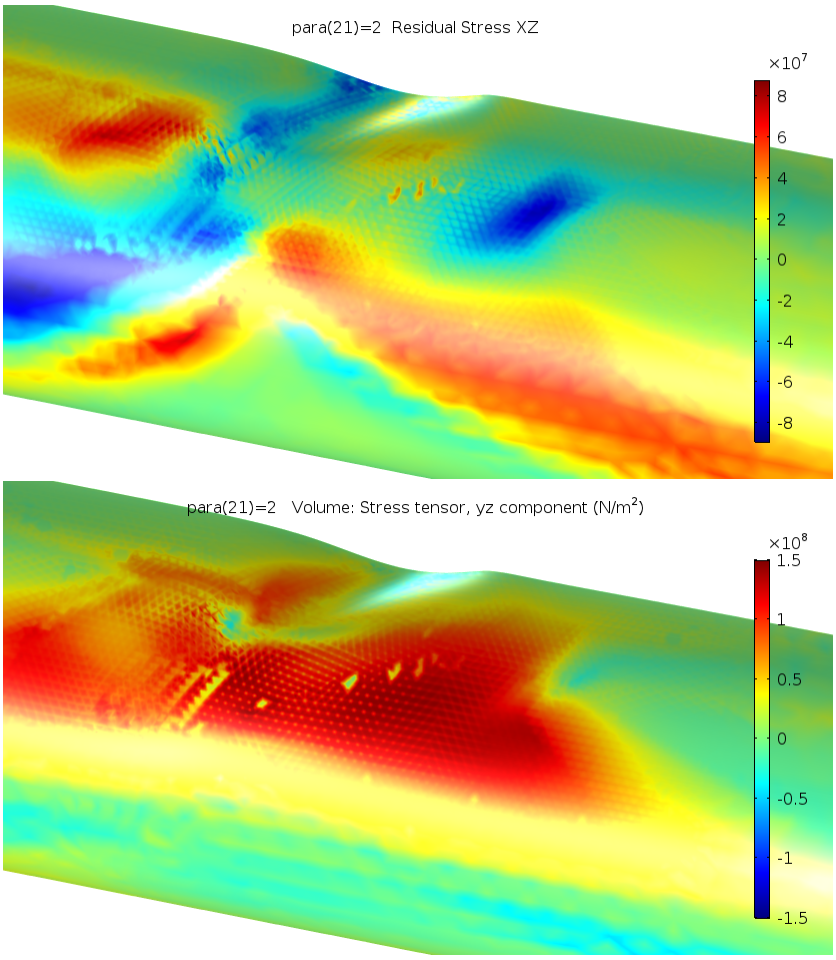

Figure 4.25: Shows residual shear stress (XY and YZ) distribution after 45 degree denting.

4.2.2 Result from fatigue/pressure test

Simulated 90 degree denting

From the stress-ranges shown in figure:4.28 and 4.29 it can be seen that the axial stress is dominating, as was the case for the stress obtained from strain-gauges. The region where cracks are observed to grow is also the region having the largest stress-range.

Simulated 45 degree denting

Surface-plots of residual stress due to simulated 45-degree denting is found in figure:4.23-4.24. The figures are angled such that it is possible to get a good overview of the region where cracks were observed (figure:4.8-4.10).
From the stress-ranges shown in figure:4.27,4.31, 4.30 and 4.32 it can be seen that the stress in the y-direction is the largest, while the stress-range in x-direction is slightly lower. This was also the case for the stress obtained from strain-gauges. The region where cracks are observed to grow is also the region having the largest stress-range.

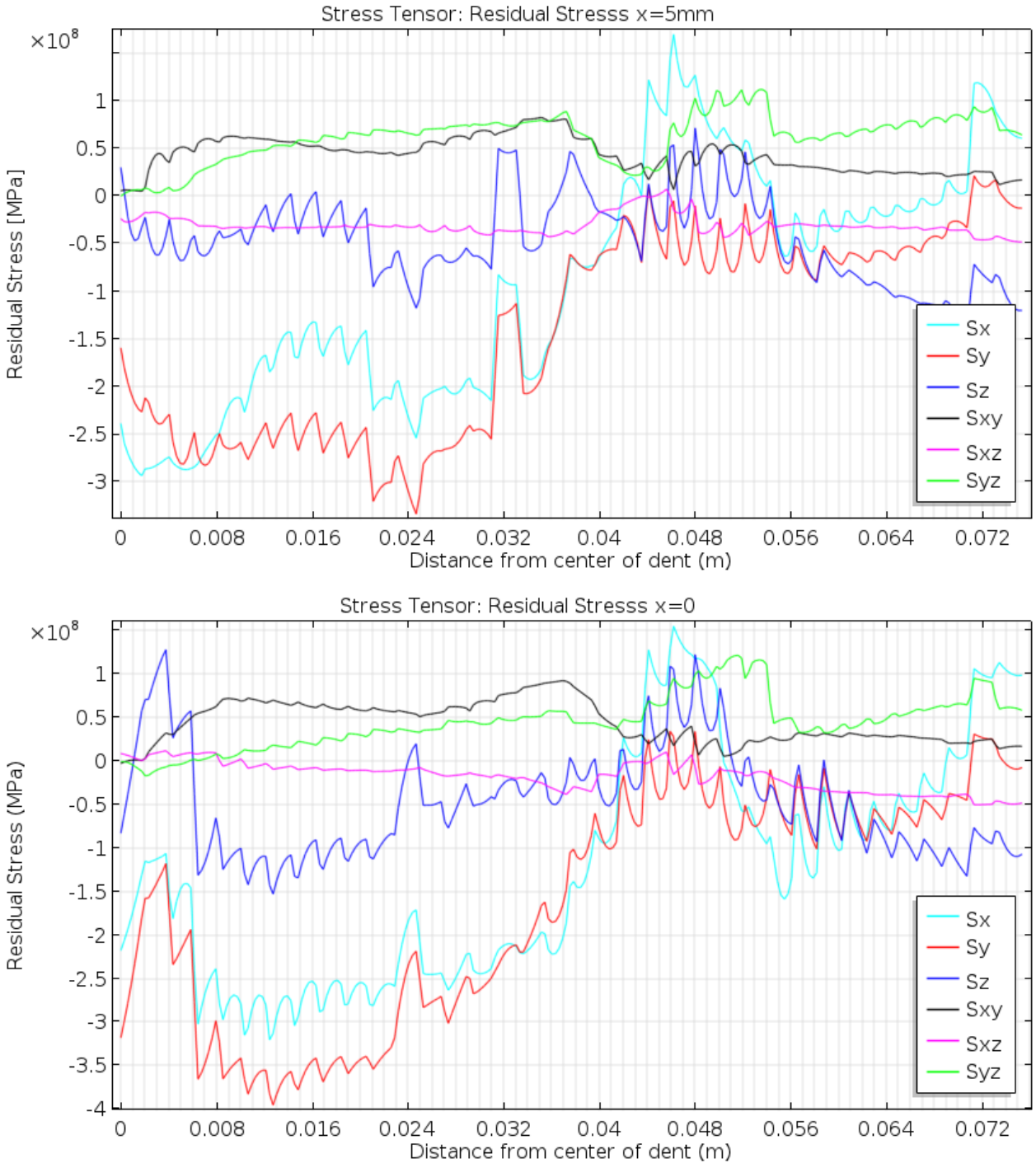

Figure 4.26: Shows residual stress distribution along longitudinal dent-direction after 45 degree denting. Graph on the top is extracted from x=-5mm, while graph on bottom side is extracted from dent-center.

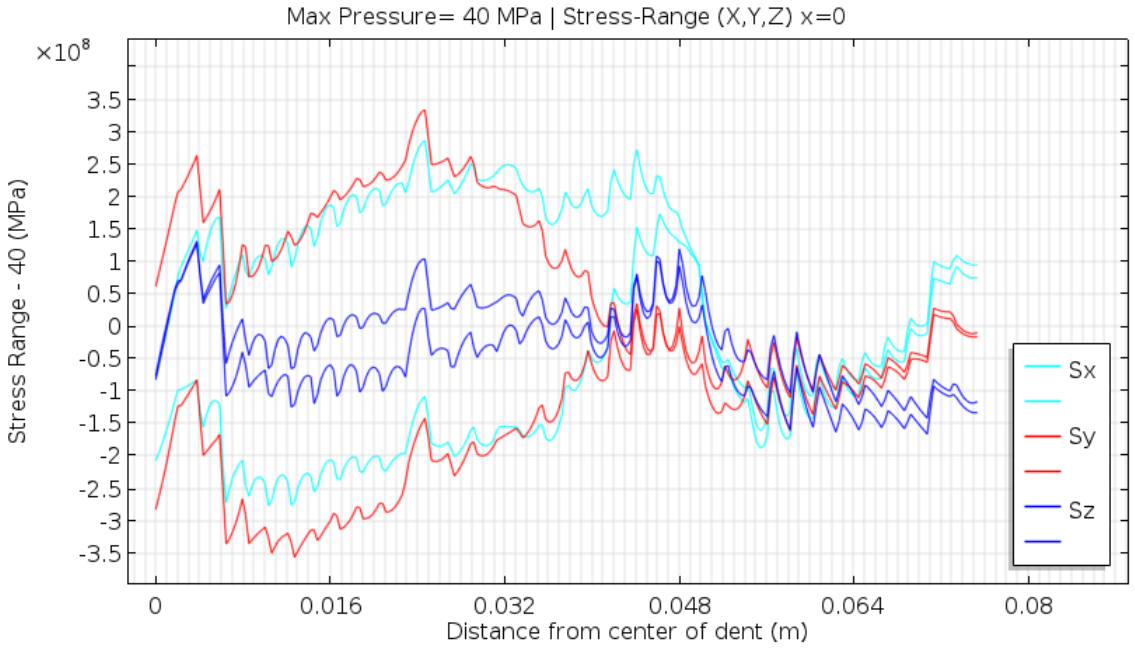

Figure 4.27: Shows stress range along dent-longitudinal axis when dent is subject to 4-40Bar internal pressure.

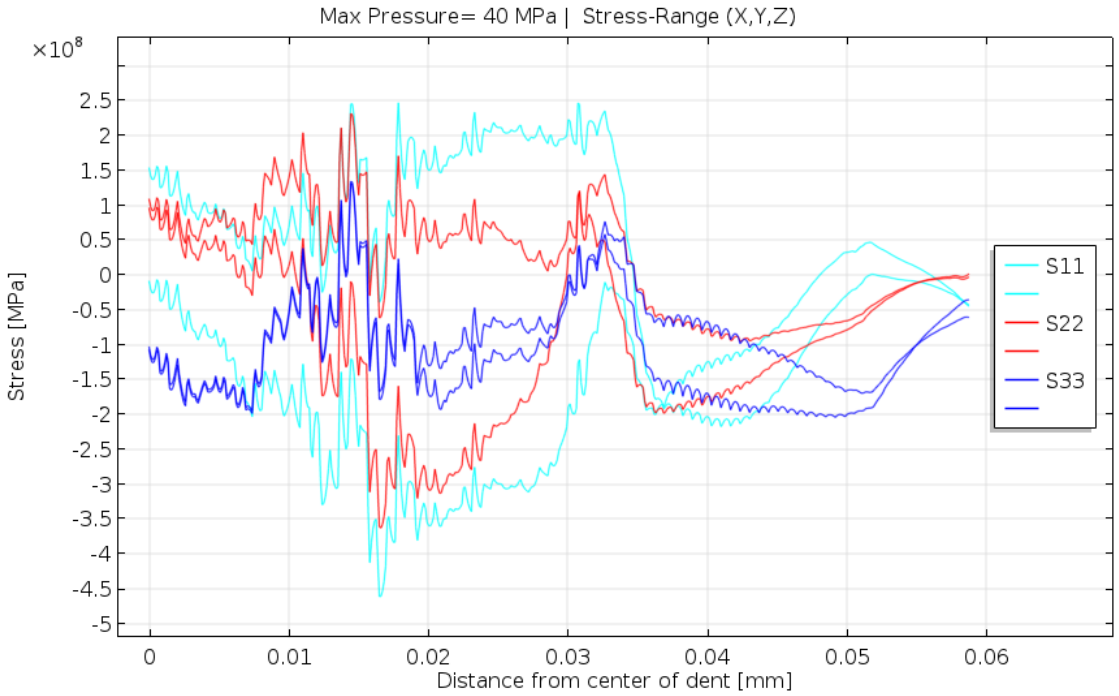

Figure 4.28: Shows shear-stress range along the 90 degree dent longitudinal axis when dent is subject to 4-40Bar internal pressure.

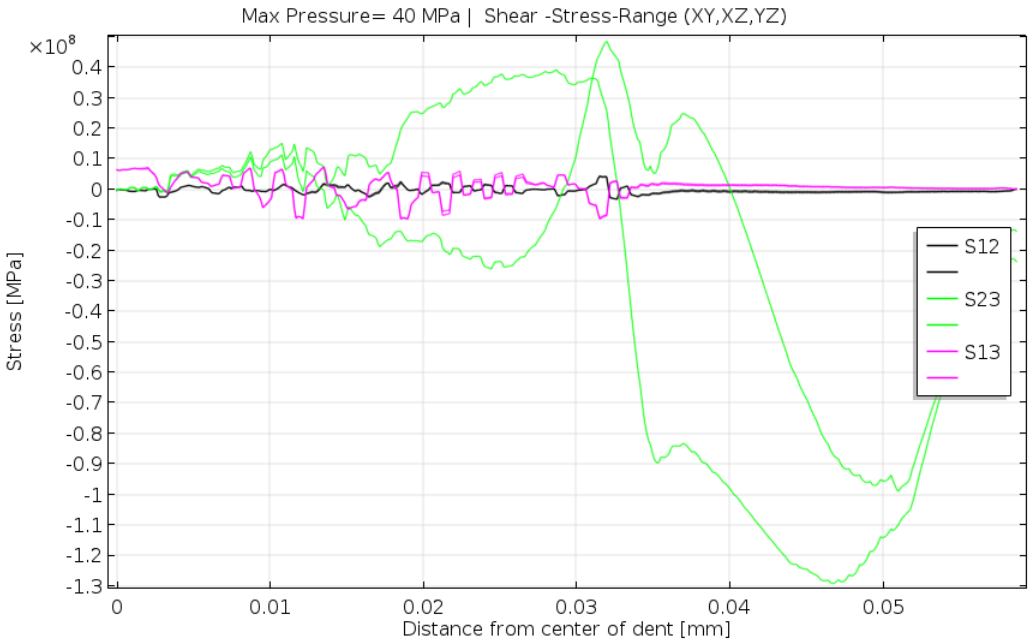

Figure 4.29: Shows shear-stress range along the 90 degree dent longitudinal axis when dent is subject to 4-40Bar internal pressure.

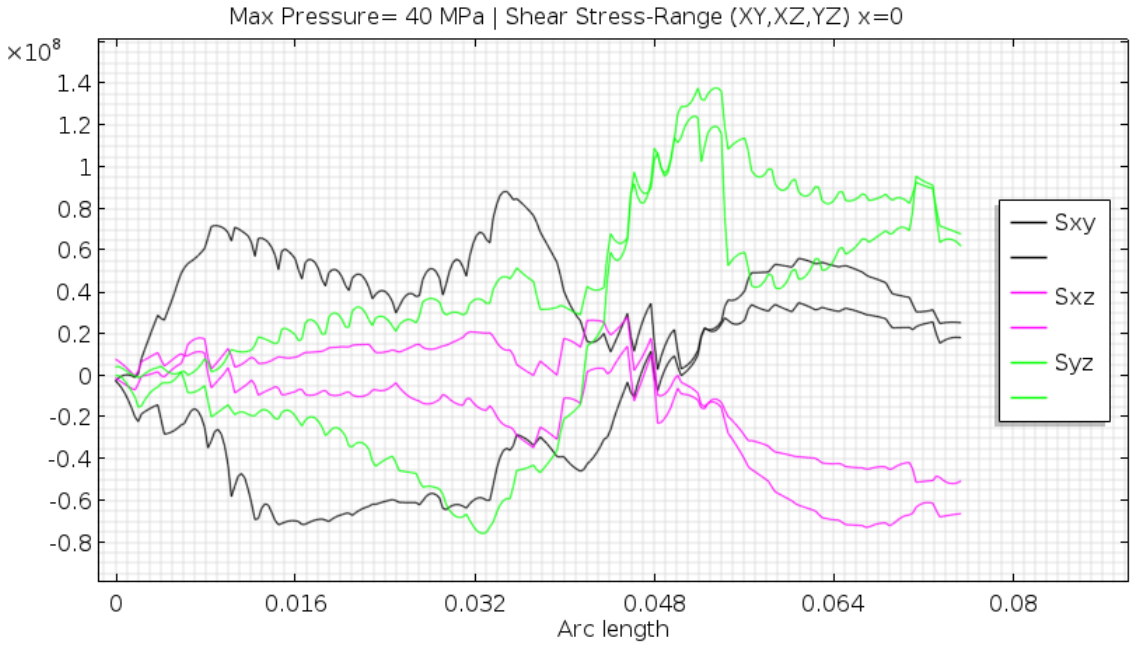

Figure 4.30: Shows stress range along the 45 degree dent longitudinal axis when dent is subject to 4-40Bar internal pressure.

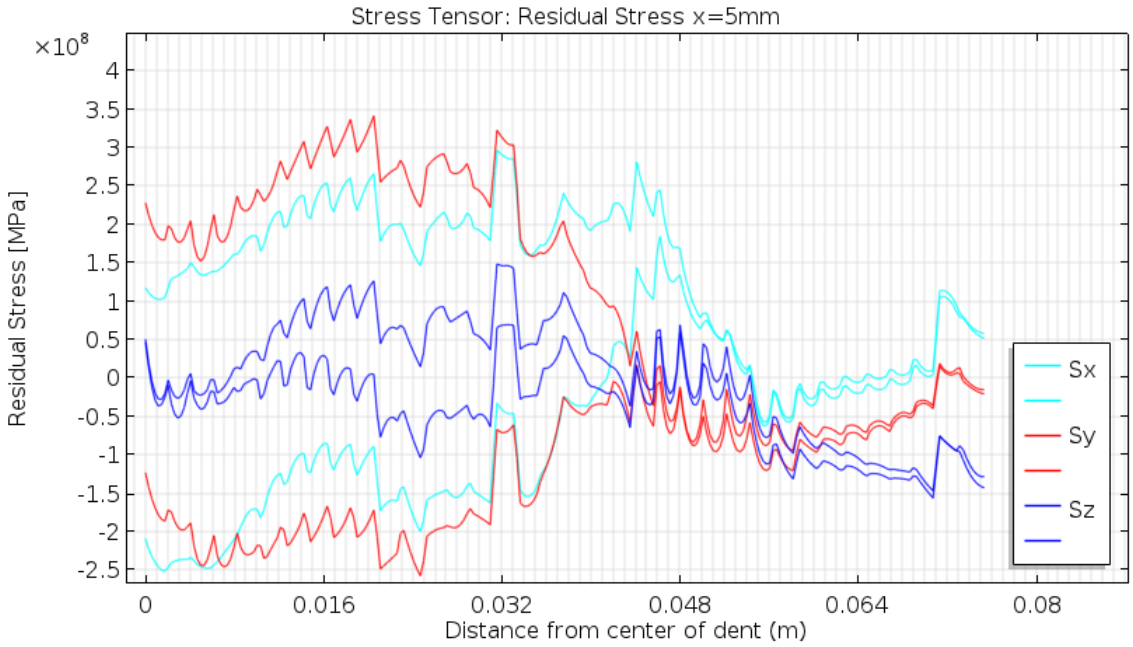

Figure 4.31: Shows stress range along dent-longitudinal axis when dent is subject to 4-40Bar internal pressure. X-axis offset is -5mm.

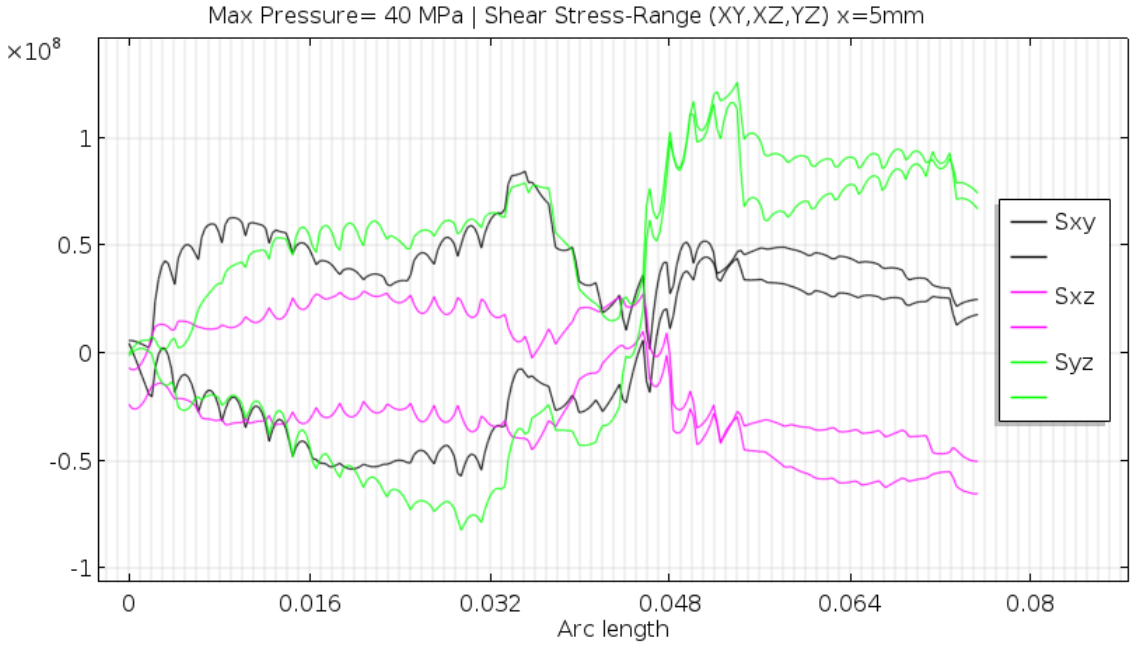

Figure 4.32: Shows stress range along the 45 degree dent longitudinal axis when dent is subject to 4-40Bar internal pressure. X-axis offset is -5mm.

4.2.3 Results from pressure test of imported geometry

The surface created from photogrammetry was pressured to the levels listed in table:4.2. Visualization of the stress-fields can be found in figure:4.33-4.39. Notable is the fact that the imported geometry does contain stress-concentrations at spots where cracks observed to nucleate and grow. The figures contain a certain amount of small stress-regions where the stresses are significantly higher or lower than the surrounding material. These locations appear to be nothing but numerical rubbish, and have consequently been ignored/evaded when extracting stresses for further analysis. Investigation of the stresses found on the imported geometry shows that the stresses are higher on the surface than on the inside.
The stress at maximum pressure during a pressure-test of the imported geometry can be found in table:4.11. The stress at minimum pressure was always very near 10% of the stress at maximum pressure. Stresses that are zero in the table were so found to be comparatively so small, that they were set to for readability. Stress-range and minimum values have therefor been left out of this table for the sake of simplicity. These stresses were used as input for the fatigue-analysis.
A quick comparison between the stresses obtained from strain-gauges in 90-degree dents (table:4.4 to 4.7) shows that the stresses from simulated pressure test of imported geometry is consistently smaller in axial direction, while the radial stress can be both larger and smaller. The shear stress is always around 0 while the shear stress from strain-gauges were usually small or compressive, except for in strain-gauge 1 in 4.6, where they are tensile.

4.3 Estimation of fatigue-life

In the case of fatigue-life estimation of dents based on data from lab-strain gauges and data from geometry imported to Comsol, only Findley's method at various levels of residual stress is included in the results. This is because none of the other methods included the effect of residual stress when it was specified as an in-plane stress. Specifying an in-plane residual stress was necessary because only stress-range could be obtained from named sources. Meanwhile the simulated denting had had residual-stress baked into the data provided to Quick Fatigue Tool.

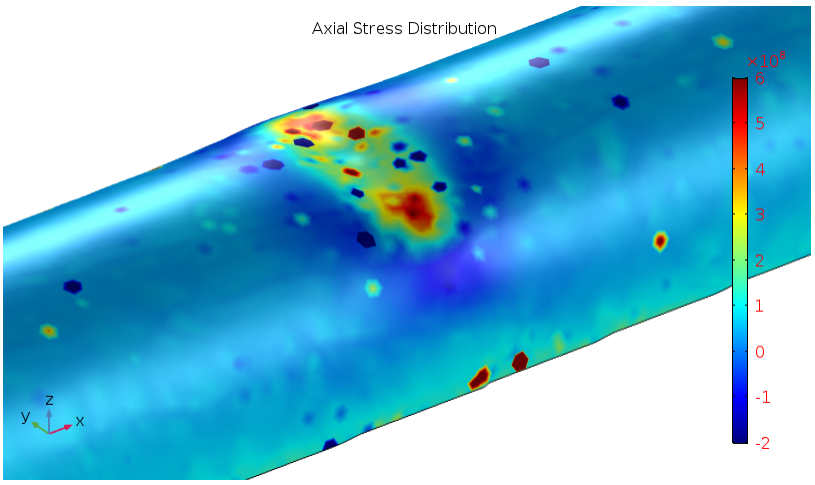

Figure 4.33: Axial stress-distribution in imported geometry containing 90-deg dent. Internal pressure is 37[Bar].

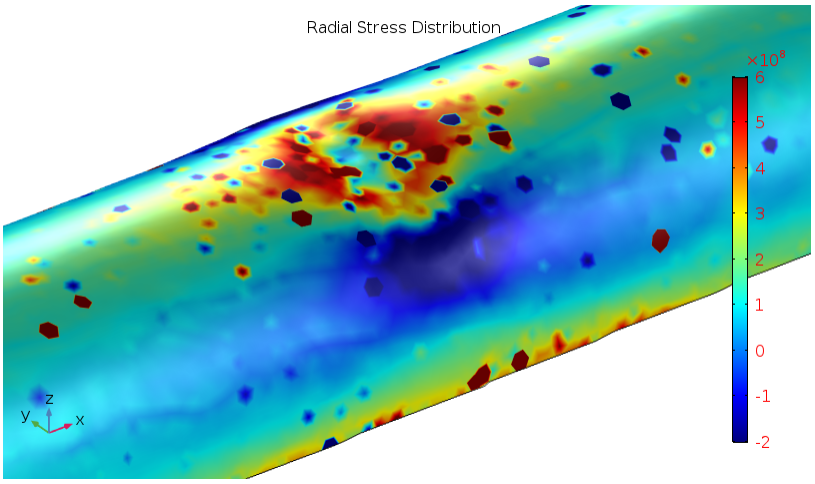

Figure 4.34: Radial stress-distribution in imported geometry containing 90-deg dent. Internal pressure is 37[Bar].

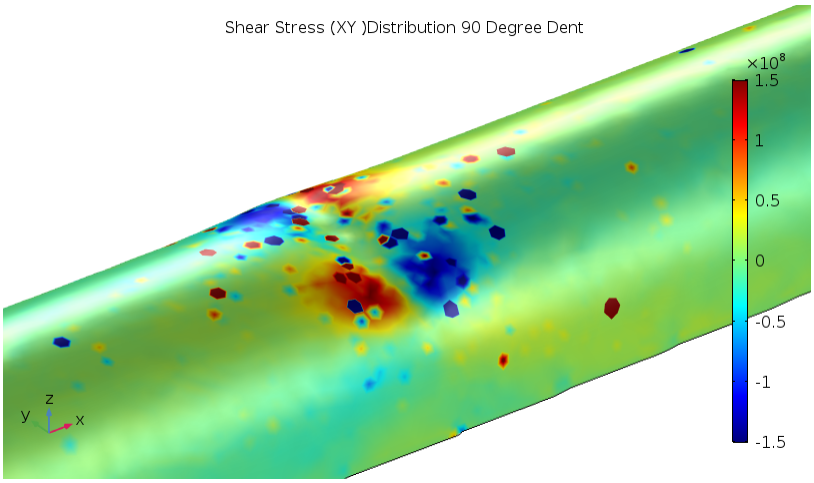

Figure 4.35: Shear stress-distribution (xy) in imported geometry containing 90-deg dent. Internal pressure is 37[Bar].

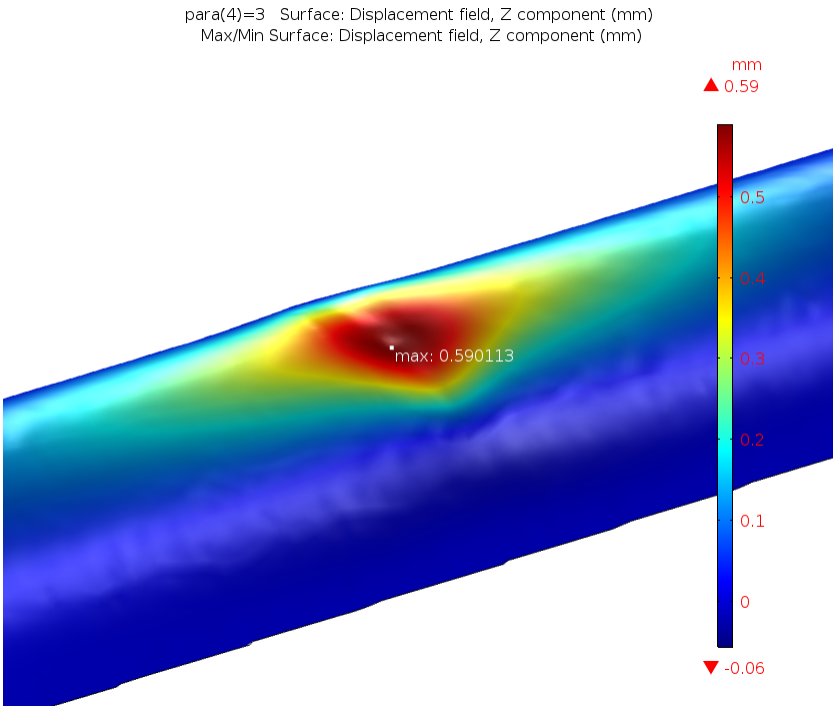

Figure 4.36: Displacement field in imported geometry containing 90-deg dent. Internal pressure is 37[Bar].

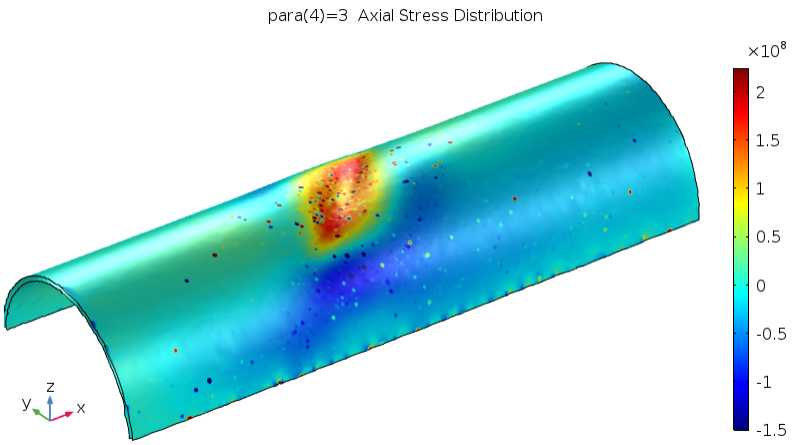

Figure 4.37: Axial stress-distribution in imported geometry containing 45-deg dent. Internal pressure is 32[Bar].

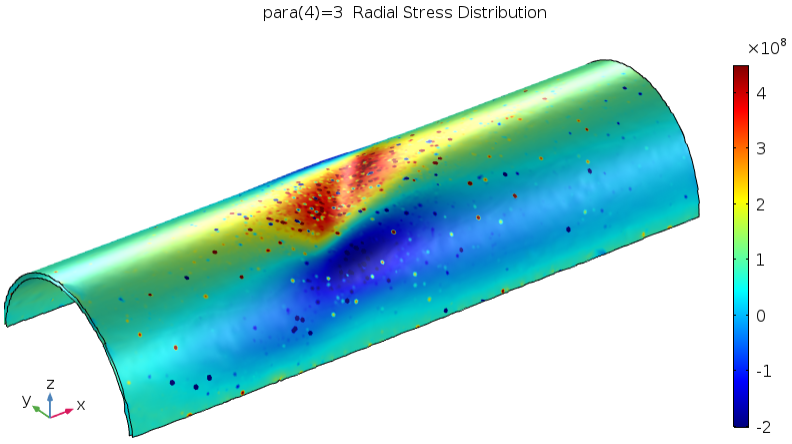

Figure 4.38: Radial stress-distribution in imported geometry containing 45-deg dent. Internal pressure is 32[Bar].

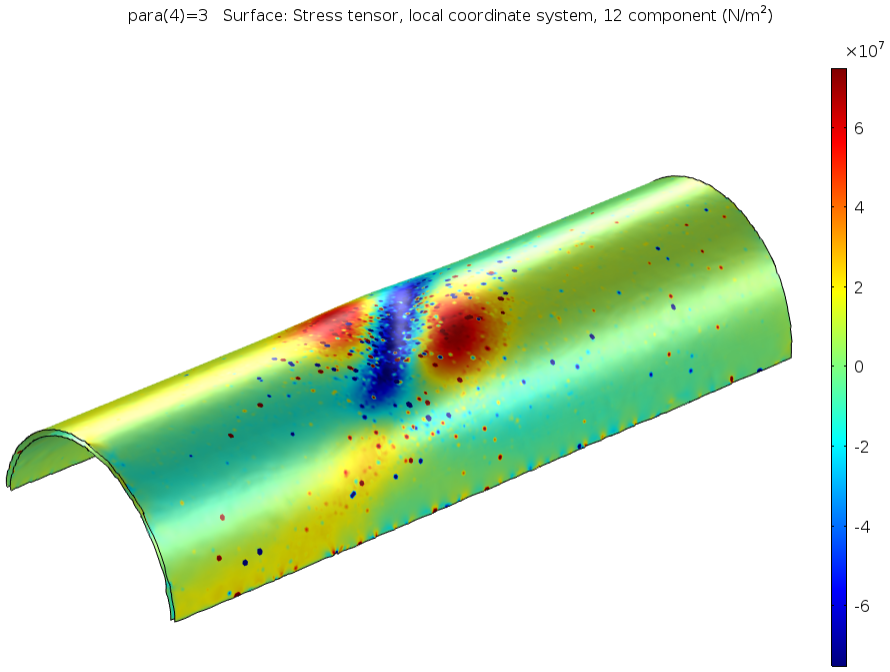

Figure 4.39: Shear stress-distribution (xy) in imported geometry containing 45-deg dent. Internal pressure is 32[Bar].

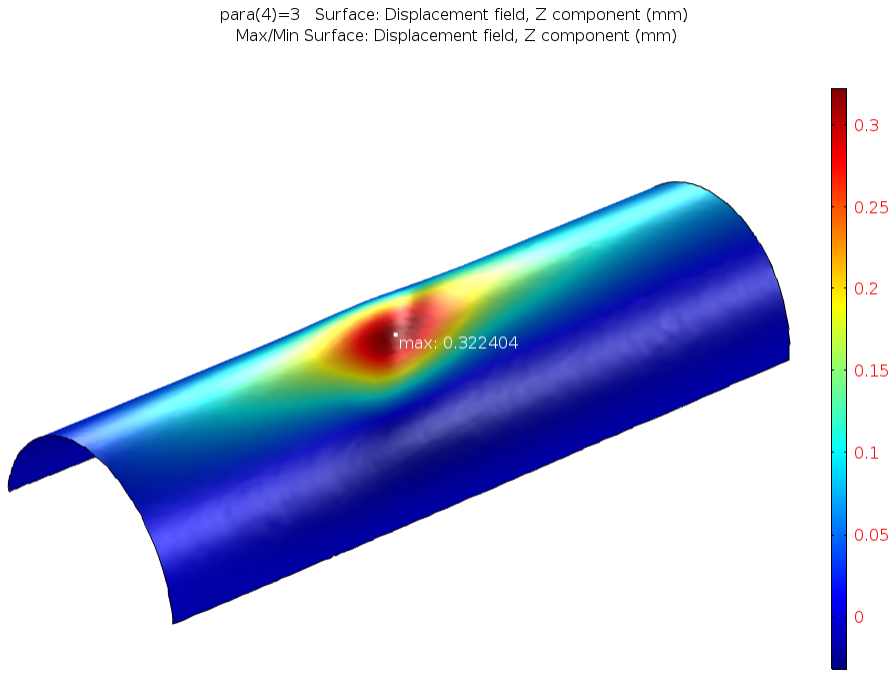

Figure 4.40: Displacement field in imported geometry containing 45-deg dent. Internal pressure is 32[Bar].

	90-degree dent		
Pressure [Bar]	σ_x[MPa]	σ_y[MPa]	$\tau_x y$[MPa]
5-50	500	385	0
4-40	430	300	0
3.7-37	400	250	0
3.2-32	350	240	0
	45-degree dent		
Pressure[Bar]	σ_x[MPa]	σ_y[MPa]	τ_{xy}[MPa]
4-40	350	240	0
3.2-32	160	400	30
2.5-25	120	320	20

Table 4.11: Shows the maximum stress extracted from the imported geometry at locations that had largest accumulation of stress.

Fatigue life of imported geometry has been predicted with the same level of accuracy as predicted by data from strain-gauges from laboratory experiments.
Out of the three available critical plane-criteria, only Finley's method proved to be able to predict fatigue life using stress-range from imported geometry and stress-range from strain-gauges.
Stress-based Brown-Miller, Findley's method and Normal stress criteria were all able to provide a fatigue-life estimate that is comparable to the fatigue-life observed from laboratory tests. However, the choice of mean-stress correction is important and Findley's method did still provide the best estimates.

4.3.1 Fatigue-Life Prediction

Fatigue-Life Estimates Based on Simulated Denting

Table:4.12 shows the predicted fatigue-life of a 90-degree dent based on stress from Comsol that corresponds to strain-gauge location 1 and 2. Because the crack did not initiate in this area, a good prediction should at least be in the vicinity of 345k cycles, which was the fatigue life of this specimen, or higher. Considering Strain-Gauge 2, since its found to have worst stress-state, Findleys's method shows to be be the best estimate in this case since its estimate is slightly larger than 345k.
Table:4.13 shows the predicted fatigue-life of a 45-degree dent based on stress from Comsol

Predicted fatigue life of 90 deg dent at 37 Bar. Based on stress-state from simulated pressure test							
Strain-gauge 1 location							
Mean Stress Correction	Morrow	Goodman	Soderberg	Walker	SWT	Gerber	None
Brown-Miller	No Dmg	305	No Dmg	-	-	2.32mill	-
Normal Stress	8.22mill	289	-	3.23mill	3.23mill	434k	-
Findley's metod	-	-	-	-	-	-	722k
Strain-gauge 2 location							
Mean Stress Correction	Morrow	Goodman	Soderberg	Walker	SWT	Gerber	None
Brown-Miller	275k	200k	820k	-	-	163k	-
Normal Stress	45k	32k	-	59k	275k	130k	-
Findley's metod	-	-	-	-	-	-	421k

Table 4.12: Overview of predicted Fatigue-life based on stress-state obtained from simulated pressure test of 90 deg dent, subjected to cyclic pressure of 37-3.7 MPa at the location of strain-gauge 1 and 2.

Predicted fatigue life of 45 deg dent at 32 Bar. Based on stress-state from simulated pressure test							
Strain-gauge 1 location							
Mean Stress Correction	Morrow	Goodman	Soderberg	Walker	SWT	Gerber	None
Brown-Miller	214k	186k	345k	-	-	180k	-
Normal Stress	37k	26k	-	34k	46k	25k	-
Findley's metod	-	-	-	-	-	-	380k
Strain-gauge 2 location							
Mean Stress Correction	Morrow	Goodman	Soderberg	Walker	SWT	Gerber	None
Brown-Miller	103k	60k	40k	-	-	118k	-
Normal Stress	14k	9.4k	-	7k	10k	16k	-
Findley's metod	-	-	-	-	-	-	140k

Table 4.13: Overview of predicted Fatigue-life based on stress-state obtained from simulated pressure test of 45 deg dent, subjected to cyclic pressure of 32-3.2 MPa at the location of strain-gauge 1 and 2.

Predicted fatigue life - 37 Bar laboratory test					
Strain-gauge 2					
Residual Stress	-100	-125	-150	-175	-200
Nr. of cycles	71k	161k	410k	1.26mill	5.05mill

Table 4.14: Predicted Fatigue-life of pipe with 90 deg dent, subjected to cyclic pressure of 37-3.7 MPa at various residual stress levels using Findley's method and stress obtained from strain-gauge 1 and 2.

that corresponds to strain-gauge location 1 and 2. The worst stress state is found at strain-gauge two. The fatigue life of this specimen was 185k cycles. The best estimate in this case is Findleys'method, which estimates 140k cycles to failure, which was expected to be higher because the cracks did initiate on the dent-shoulder not near the bottom.

Fatigue-Life Estimates Based on Data from Strain-Gauges

Table:4.14 shows the predicted fatigue-life of a 90-degree dent based on stress obtained from strain-gauge 2 in the laboratory. Strain-gauge 2 had the worst stress-state and therefor analysis of strain-gauge 1 was left out.
The specimen, from which the results in table table:4.15 is based upon, experienced 185k cycles before failure. One can see in this table that strain-gauge 1 represents the worst stress-state. In addition, Findley's method was not able to estimate a satisfactory number of cycles to failure without introducing a very large residual stress, much larger than any measured axial residual stress.
In the case of high-cycle fatigue, Quick-Fatigue Tool proved to be somewhat useful at predicting the fatigue life. Quick Fatigue Tool predicted that a pipe with 45 degree dent 2.5-25 Bar pressure would fail at a number of cycles that had the same order of magnitude as observed in the laboratory when introducing residual-stress that are of same magnitude as observed in lab.

Predicted fatigue life - 32 Bar laboratory test						
Strain-gauge 1						
Residual Stress	0	-200	-300	-325	-350	-400
Nr. of cycles	349	7k	75k	164k	400k	4mill
Strain-gauge 2						
Residual Stress	0	-100	-125	-150	-200	-
Nr. of cycles	13k	236k	605k	2.23mill	No Dmg	-

Table 4.15: Estimated fatigue-life of pipe with 45 deg dent, subjected to cyclic pressure of 32-3.2 MPa at various residual stress levels using Findley's method and stress obtained from strain-gauge 1 and 2.

	Residual Stress [MPa]				
Pressure [Bar]	0	-25	-50	-75	-100
5-50	26k	52k	112k	272k	778k
4-40	62k	140k	355k	1mill	4.23mill
3.7-37	95k	227k	633k	2.19mill	No Dmg
3.2-32	208k	571k	1.93mill	9.1mill	No Dmg

Table 4.16: Estimated fatigue-life of surface scan with 90 deg dent,subjected to cyclic pressure (3.7-37Bar) at various residual stress levels using Findley's method

Fatigue-life estimates based on imported geometry

Table:4.16 and 4.17 shows the estimated fatigue-life of a 90- and 45-degree dent that was observed to have a fatigue-life within the region of primary concern. Comparison of results from table:4.2 with 4.16 and 4.17. It was found that without introducing any in-plane residual-stress, the fatigue-life could not be estimated. However, introducing a slight amount of residual stress had a dramatic effect on the estimated fatigue-life. The best estimate for a 90-degree dent is found when introducing a residual stress in the range -25 to -50[MPa]. The best estimate for a 45-degree dent is found when introducing -25[MPa]. Obviously, the residual stress could have been tweaked to match the fatigue-life in the lab, but there is little to gain from that as the trend is already clear.

Effect of Surface Roughness

No measurements were conducted of the surface roughness of the pipe-material. Nevertheless, the user of Quick-Fatigue Tool is required to specify an Ra-curve, which specifies a corresponding stress-concentration, to be used for the analysis. This is because surface finish

Residual Stress [MPa]					
Pressure [Bar]	0	-25	-50	-75	-100
4-40	46k	99k	236k	658k	2.28mill
3.2-32	90k	215	591k	2.01mill	9.4mill
2.5-25	342k	1.06mill	4.09mill	No Dmg	No Dmg

Table 4.17: Calculated fatigue-life of surface scan with 45 deg dent, subjected to cyclic pressure (3.2-32Bar) of at various residual stress levels using Findley's method

'default.kt'	**Surface Finish**
1	Mirror Polished – Ra <= 0.25um
2	0.25 < Ra <= 0.6um
3	0.6 < Ra <= 1.6um
4	1.6 < Ra <= 4um
5	Fine Machined – 4 < Ra <= 16um
6	Machined – 16 < Ra <= 40um
7	Precision Forging – 40 < Ra <= 75um
8	75um < Ra

Figure 4.41: Shows overview over default surface finish available in Quick Fatigue Tool.

of the material has been found to have an effect on crack-initiation Pook (2007).

The surface of the pipe was guesstimated to correspond to a surface around row 4 or 5 in figure:4.41. The choice of surface roughness to be used was briefly investigated by running an analysis of a single stress-state with different values of surface roughness and comparing estimated fatigue-lives. The results are found in 4.18. The difference between the estimated fatigue-life in columns 4 and 5, which were the two values of main interest, was found to be 81k. Another surface roughness, Juvinall 2 in result-table, corresponding to a 'fine ground or commercially polished' surface (not included in figure 4.41), estimated a slightly higher fatigue-life, 211k. This option was selected for the analysis based on the assumption that 282k may be conservative, while 201k may be too conservative.

Surface Roughness	Juvinall 2	2	3	4	5	6
Cycles to Failure	211k	346k	282k	201k	175k	101k

Table 4.18: Shows estimated fatigue-life for different values of surface roughness. Surface roughness corresponding to number in row 1 can be found in 4.41.

Chapter 5

Discussion, Conclusion and Recommendations for Further Work

5.1 Discussion

5.1.1 Simulated Pressure Tests

The selected boundary conditions on the imported geometry are debatable. Trade-offs have been made to produce stresses that were close to what is observed in the lab, but behaviour from the real pipe is still different. Comparison between stresses obtained from strain-gauges and stresses found at the imported geometry is difficult because, as is shown by the contact simulation, measurements of residual stress, and differences in stress from the strain gauges at the same pipe the dented region contains large stress-gradients. In addition, there are uncertainties in the stresses imported from the dented geometry. Comsol had very few post-processing options available for the dented geometry. Because of this, stresses had to be obtained by attempting to click the same spot in the 3D-viewer, which inevitably resulted in some error. This error should, however, be small compared to errors introduced by material assumptions, SN-curves and so on. It seems better to use them as an indication for the magnitude one would like to obtain from the pressure-tests.

5.1.2 Estimated Fatigue Lives

Estimated fatigue life is based upon one stress-cycle. In appendix it is shown that the strain changes as the number of cycles increase, this is not accounted for in the analysis. The change is most severe in the shear-strains, which is not the dominating component during fatigue-tests but may still have an effect as the estimated fatigue-lives were found to be sensitive to the amount of residual stress present. Yet, due to the large uncertainties present in the calculation, its hard to gauge how much of an impact this has on the data.
A value of surface roughness has been assumed. Its value in the analysis has a been found to have a significant effect on the fatigue life. A conservative value has been selected, which did impact the amount of in-plane residual stress needed to calculate a fatigue-life which is in the vicinity of observed fatigue-life.
Only one critical-plane criteria have been found to be able to estimate fatigue-life. There are many critical plane criteria, therefor it cant be said for certain that the residual stress introduced in Findley's method will yield similar results from other criteria. Many assumptions have been introduced in estimation of the fatigue-life of dented pipes. Material hardening, SN-curve, surface roughness of the material, In-plane residual stress and so on. Naturally, this leads to a large amount of uncertainty, especially when only one criteria was found to be useful. Therefor the results should be treated as such. Nevertheless, the procedure used in this thesis has shown that the software can indeed come up with a number corresponding to a fatigue-life which is at the very least in the vicinity of the observed value without introducing what is considered to be drastic values of any kind.
The residual stress that had to be introduced in fatigue-life estimation when using stress from strain-gauges, were found to be of similar magnitude to the axial residual-stress measured in lab. The residual stress that had to be introduced to obtain a fatigue-life estimate that correlated with observed values, was much smaller. The reason for this seems to be mainly because the stresses obtained from the imported geometry was of a lower magnitude than the stress obtained from strain-gauges. And as such, lowering the stress-range slightly can have a significant effect on the fatigue-life as observed in the lab-fatigue tests.
The magnitude of the in-plane residual stress, specified during fatigue-life estimation, was applied to all directions. Whether this is a good assumption or not is uncertain. Measurements

of axial-residual stress in the lab were found to be of similar magnitude as the simulated values in some cases, while the magnitude was very different in others. The radial residual stress was not measured, it cant be concluded whether they are tensile, compressive or near 0 in the locations where cracks would form. Because of this, it is uncertain how well the specified in-plane residual stress resembles reality.

5.2 Conclusions

Pipes have been dented in laboratory to 16mm depth with two different angles, 45- and 90-degrees. The dents created by vertical displacement of indenter have been found to have a significantly higher impact on fatigue-life reduction of when compared to horizontal dents created in Aadal (2016). The dent geometry has been found to be more important than the dent depth. The 45-degree dents were more shallow than the 90-degree dents, yet it had a significantly shorter fatigue-life.
Residual stress in a dented area have been found to contain very large gradients, ranging from hundreds of tensile MPa to hundreds of compressive MPa over a distance of a few centimeters. The residual stress in areas where cracks would nucleate and propagate varied greatly between the two different dent geometries (90 and 45 deg dent), but it seems like crack-growth is favored in areas where the residual stress is comparatively low to the surrounding area.
If fatigue-life prediction by surface scan is going to be a reality, then these results suggest that accurate predictions of residual stress for various dent-geometries needs to be obtained. The imported geometry did provide the highest stress-range at locations which correlated well with the locations where cracks were found to initiate/grow. However, the stress-range was found to be lower than the stresses measured in reality. Consequently, the residual stress that had to be introduced was also smaller to obtain the same fatigue-life estimate. Also, the imported model is too stiff, doesn't displace as much as observed in tests/simulation. The imported geometry is inherently flawed, but there may be many tools out there that may improve it. While not entirely accurate, and with many assumptions, the method of predicting the fatigue life by the means of surface scan does indeed seem like it has potential.

5.3 Recommendations for Further Work

Investigate the effect of dent depth by denting several pipes with same angle, while varying dent depth for each dent.

Is it recommended that the imported geometry is improved. This can be done by acquiring a full-version of the the imported geometry, or possibly by acquiring another software with less restrictions. Investigate other tools that can be used to predict fatigue life

Investigate different types of dents and ways of colliding with pipe. Dent depth does not appear to be the most severe parameter in this thesis.

Residual stress has been found to be an important parameter for the fatigue-life of the dent. Detailed investigation of the residual surrounding the area where cracks initiate can be useful.

The dented region has been found to contain large stress-gradients, it would be interesting to have a larger amount of strain-gauges in the dented area to investigate the stress/strains in the area.

Only 1 fatigue criteria was found to produce adequate results in this thesis. There are many more multiaxial fatigue-criteria that can be programmed into Quick-Fatigue Tool and perform an extensive sweep to determine which criteria works the best and why.

Appendix A

Strains obtained from Strain-Gauges

A.1 Strains from 90-degree dents

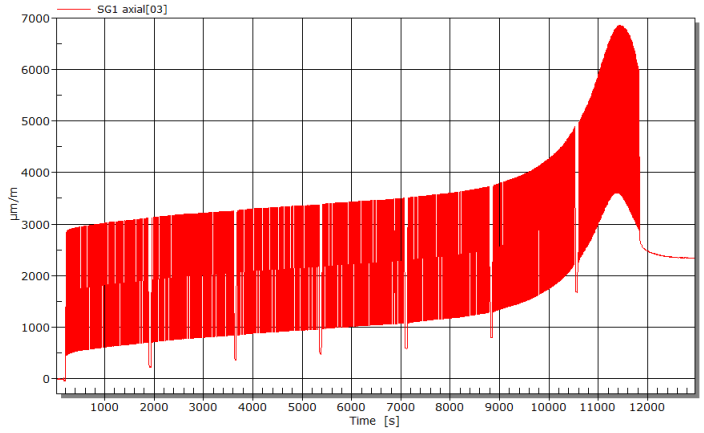
SG1 axial[03]
µm/m
7000
6000
5000
4000
3000
2000
1000
0
1000 2000 3000 4000 5000 6000 7000 8000 9000 10000 11000 12000
Time [s]

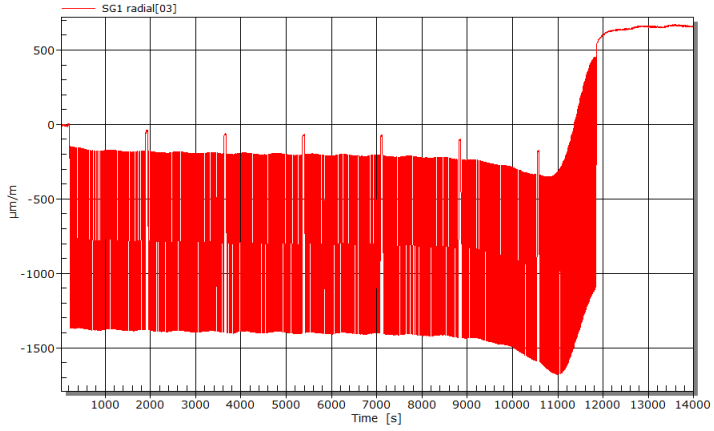
SG1 radial[03]
µm/m
500
0
-500
-1000
-1500
1000 2000 3000 4000 5000 6000 7000 8000 9000 10000 11000 12000 13000 14000
Time [s]

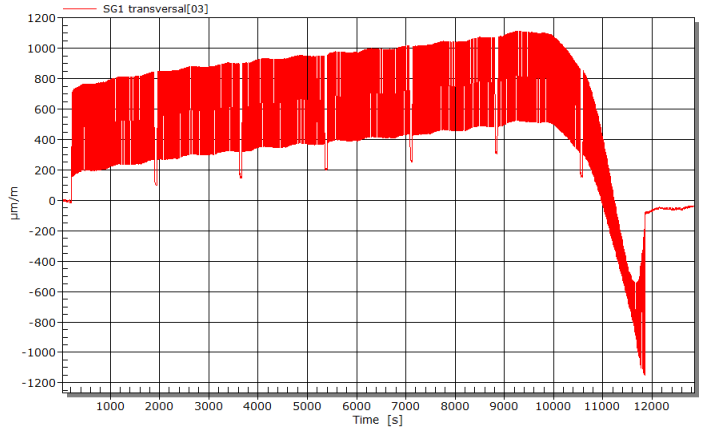
SG1 transversal[03]
µm/m
1200
1000
800
600
400
200
0
-200
-400
-600
-800
-1000
-1200
1000 2000 3000 4000 5000 6000 7000 8000 9000 10000 11000 12000
Time [s]

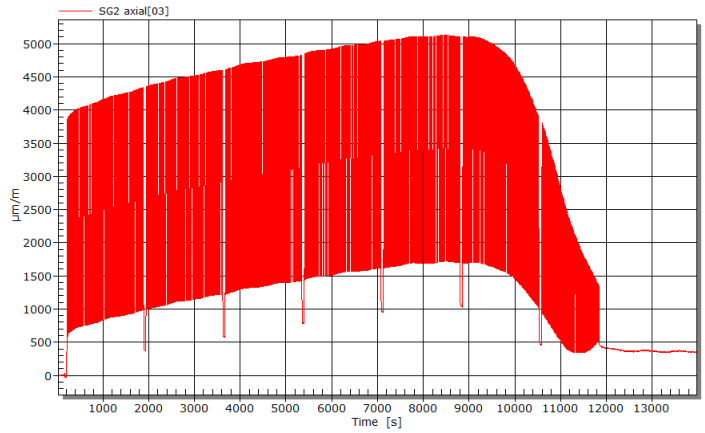
SG2 axial[03]
µm/m
Time [s]

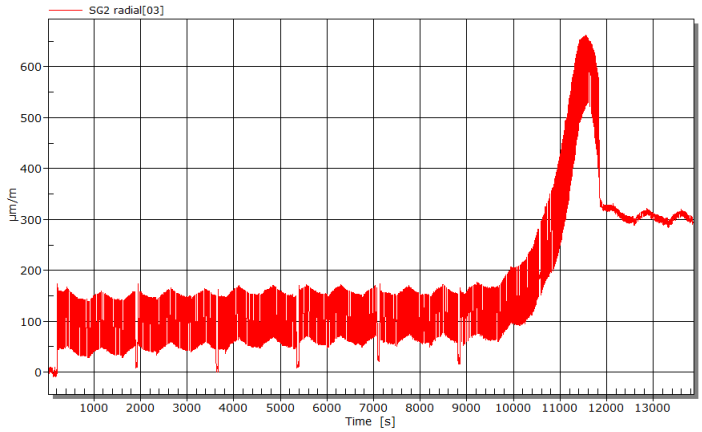
SG2 radial[03]
µm/m
Time [s]

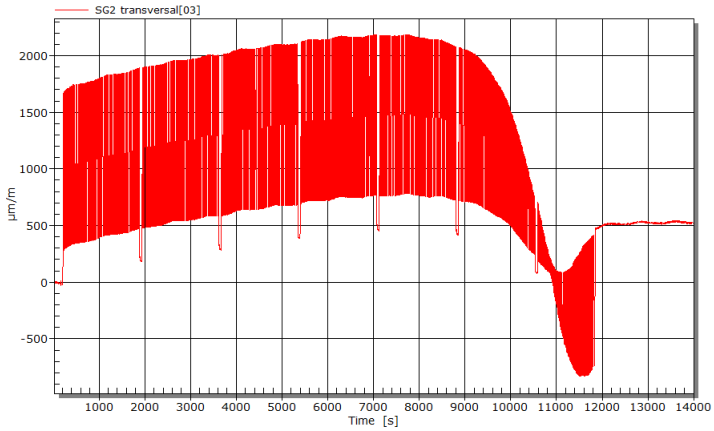
SG2 transversal[03]
µm/m
Time [s]

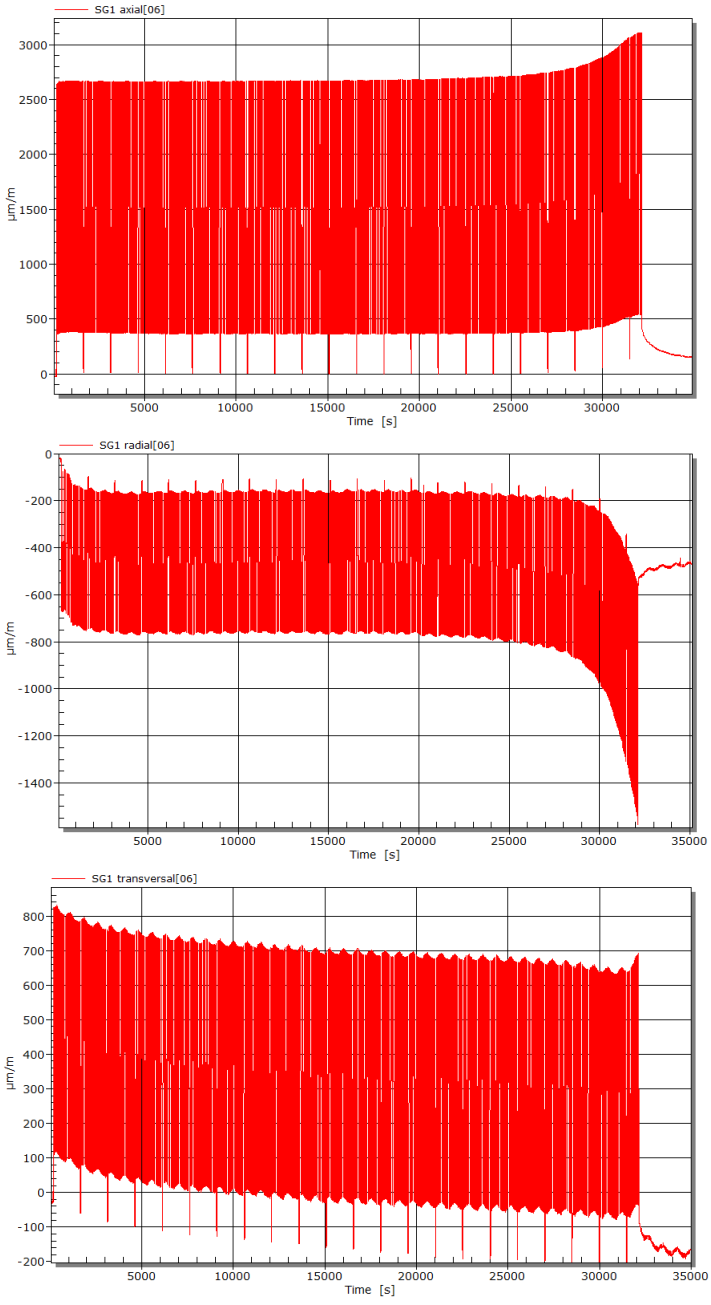
SG1 axial[06]
µm/m
Time [s]
SG1 radial[06]
µm/m
Time [s]
SG1 transversal[06]
µm/m
Time [s]

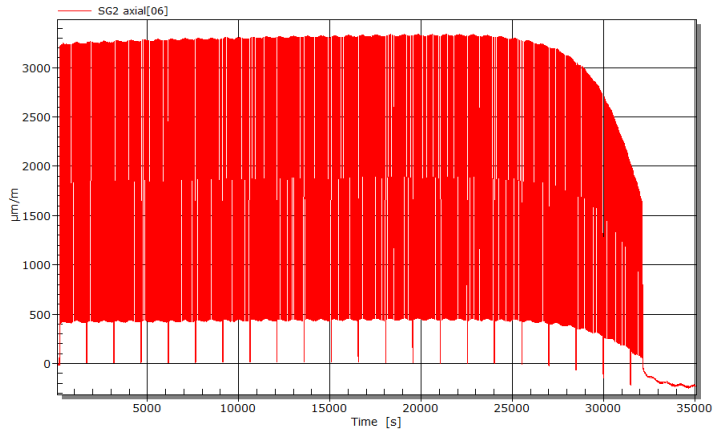
SG2 axial[06]
µm/m
3000
2500
2000
1500
1000
500
0
5000
10000
15000
20000
25000
30000
35000
Time [s]

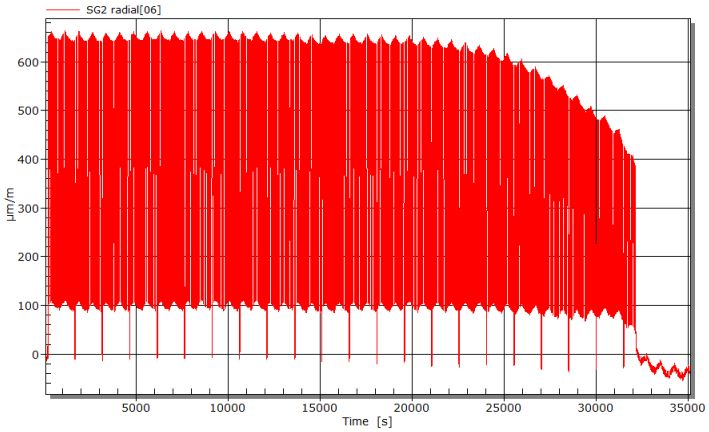
SG2 radial[06]
µm/m
600
500
400
300
200
100
0
5000
10000
15000
20000
25000
30000
35000
Time [s]

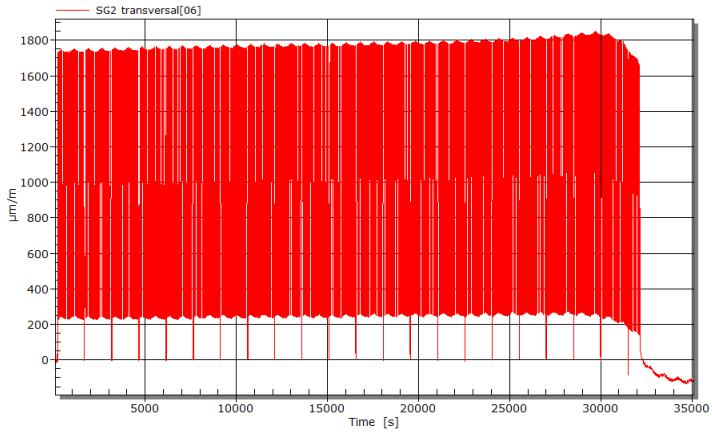
SG2 transversal[06]
µm/m
1800
1600
1400
1200
1000
800
600
400
200
0
5000
10000
15000
20000
25000
30000
35000
Time [s]

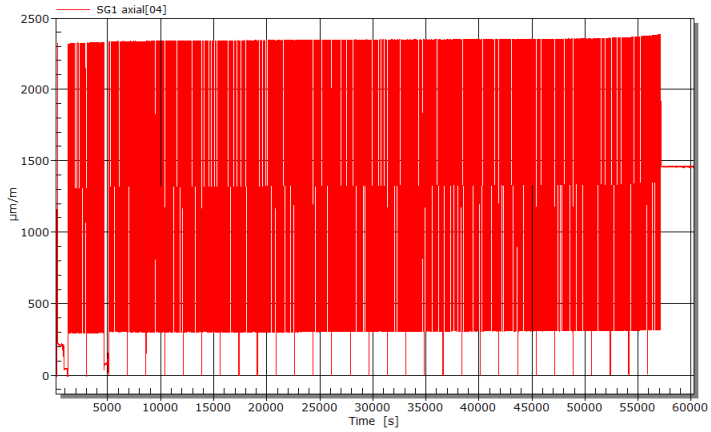
SG1 axial[04]
µm/m
2500
2000
1500
1000
500
0
5000 10000 15000 20000 25000 30000 35000 40000 45000 50000 55000 60000
Time [s]

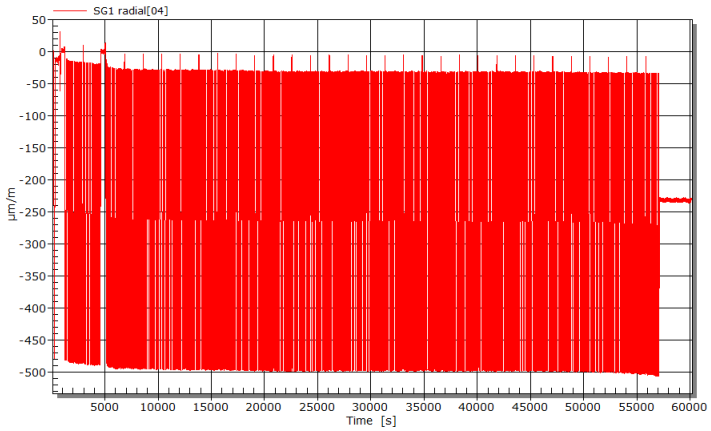
SG1 radial[04]
µm/m
50
0
-50
-100
-150
-200
-250
-300
-350
-400
-450
-500
5000 10000 15000 20000 25000 30000 35000 40000 45000 50000 55000 60000
Time [s]

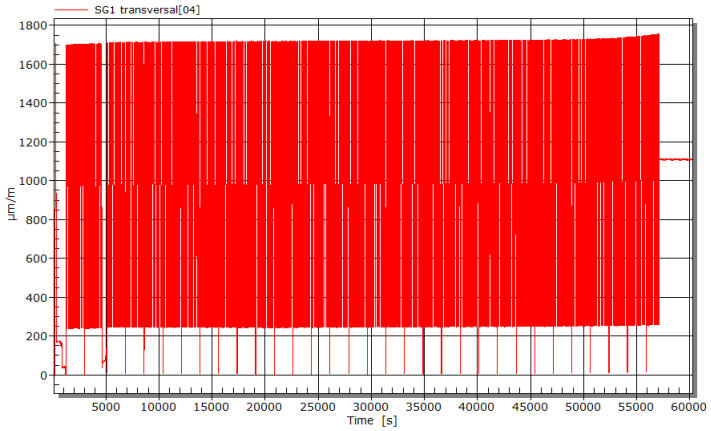
SG1 transversal[04]
µm/m
1800
1600
1400
1200
1000
800
600
400
200
0
5000 10000 15000 20000 25000 30000 35000 40000 45000 50000 55000 60000
Time [s]

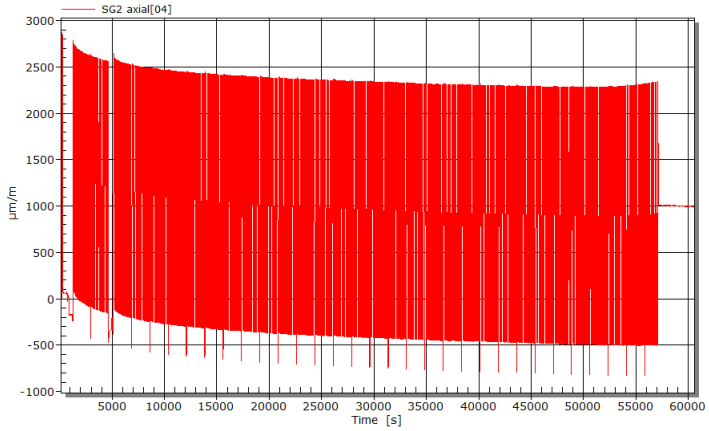
SG2 axial[04]
µm/m
Time [s]

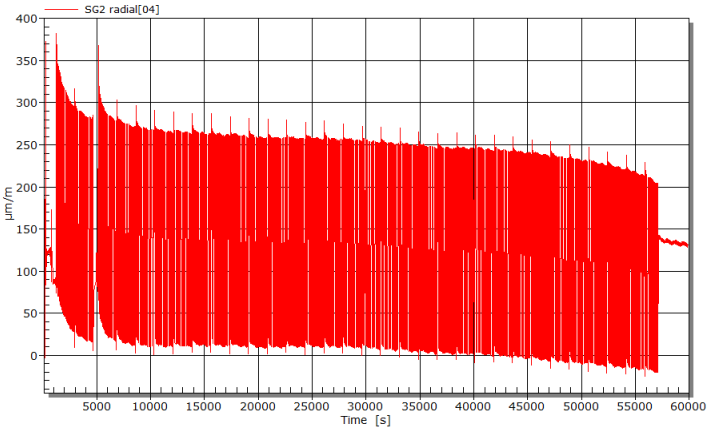
SG2 radial[04]
µm/m
Time [s]

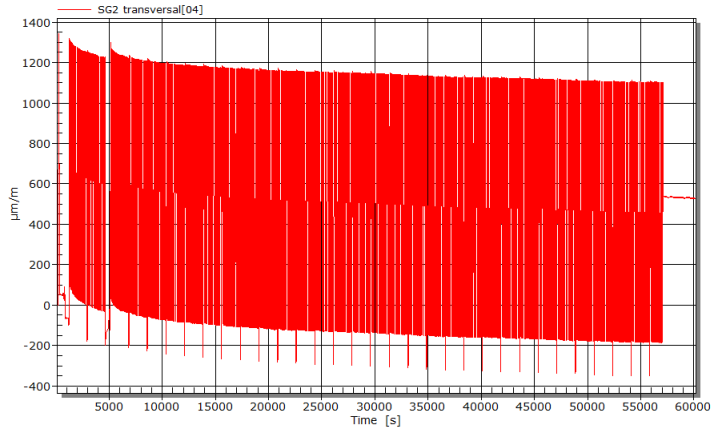
SG2 transversal[04]
µm/m
Time [s]

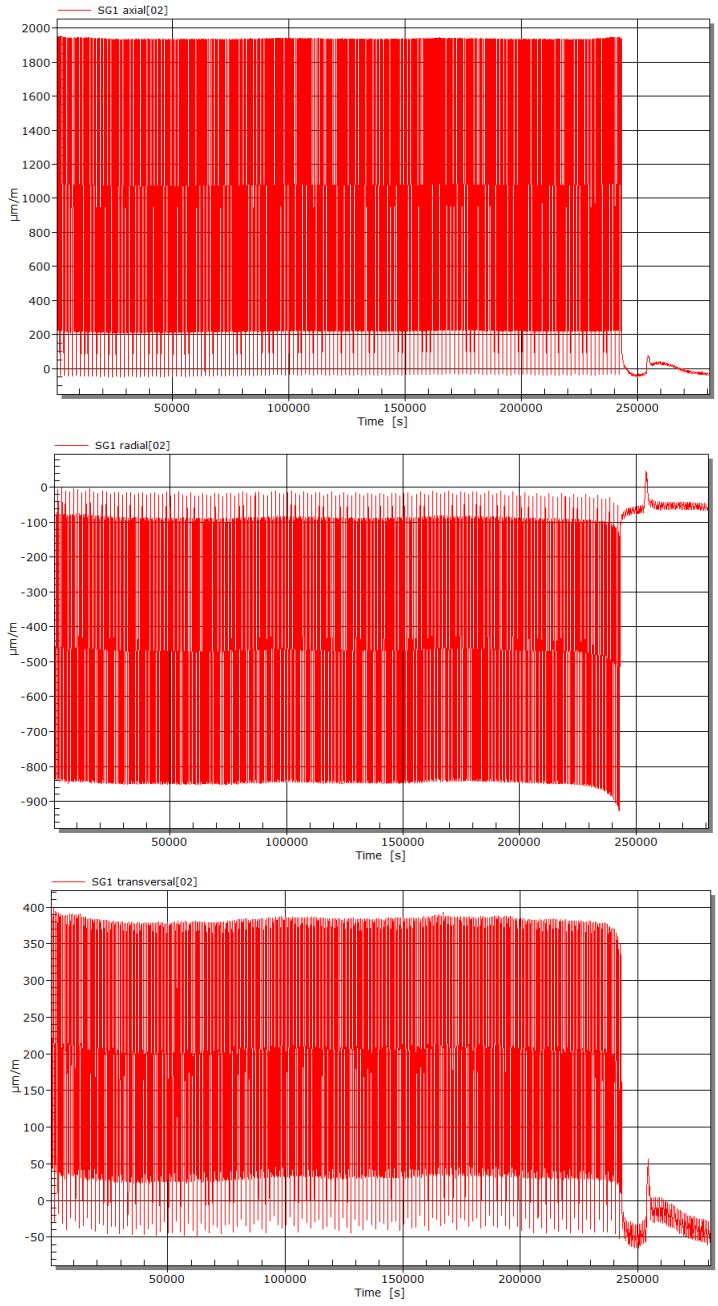
SG1 axial[02]
2000
1800
1600
1400
1200
1000
800
600
400
200
0
µm/m
50000
100000
150000
200000
250000
Time [s]
SG1 radial[02]
0
-100
-200
-300
-400
-500
-600
-700
-800
-900
µm/m
50000
100000
150000
200000
250000
Time [s]
SG1 transversal[02]
400
350
300
250
200
150
100
50
0
-50
µm/m
50000
100000
150000
200000
250000
Time [s]

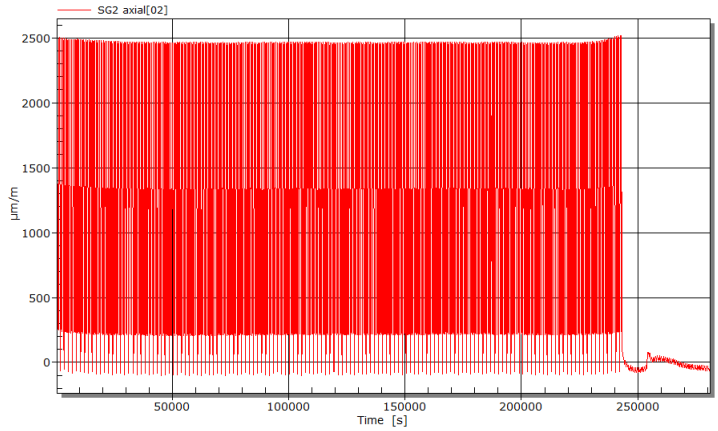
SG2 axial[02]
2500
2000
1500
1000
500
0
µm/m
50000
100000
150000
200000
250000
Time [s]

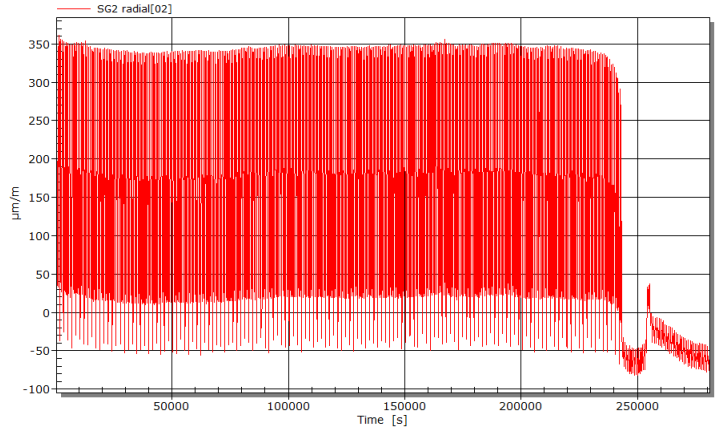
SG2 radial[02]
350
300
250
200
150
100
50
0
-50
-100
µm/m
50000
100000
150000
200000
250000
Time [s]

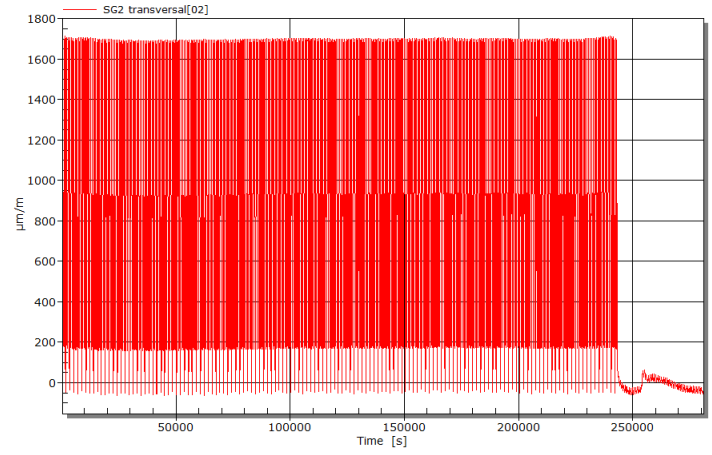
SG2 transversal[02]
1800
1600
1400
1200
1000
800
600
400
200
0
µm/m
50000
100000
150000
200000
250000
Time [s]

A.2 Strains from 45-degree dents

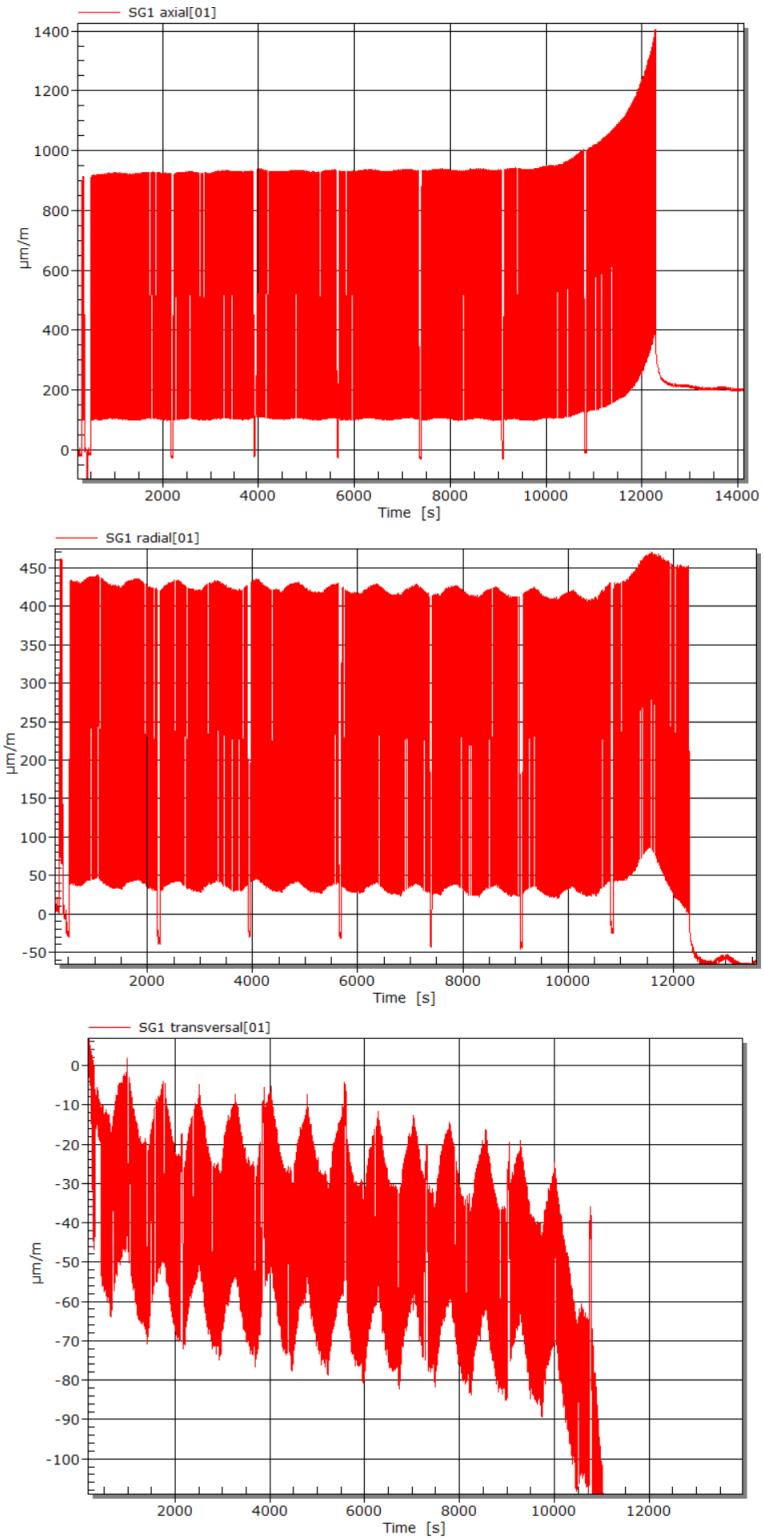

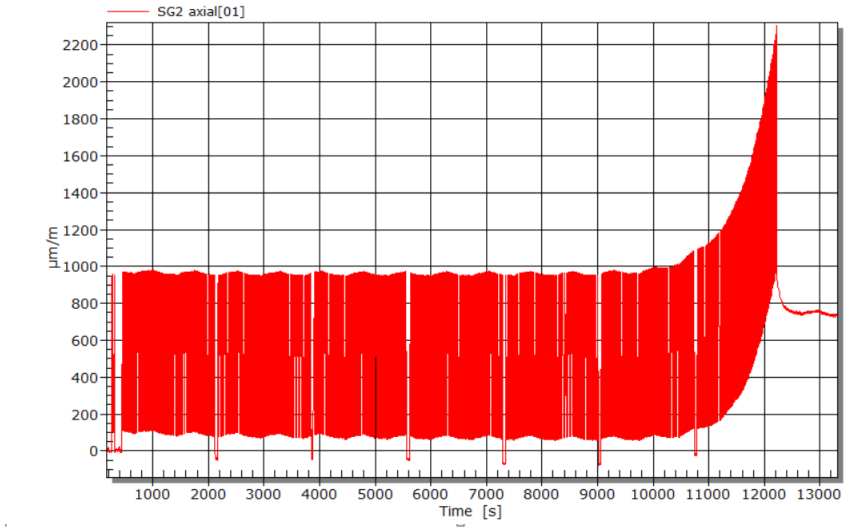
SG2 axial[01]
µm/m
Time [s]

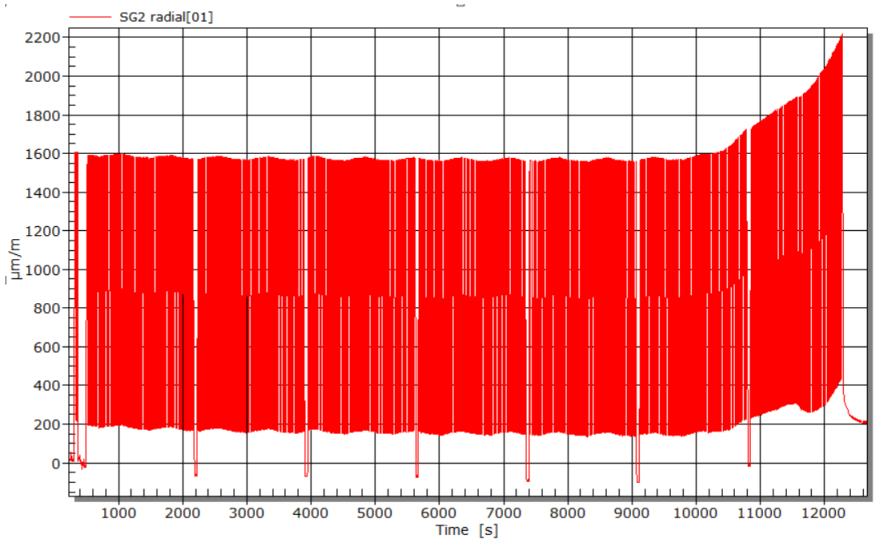
SG2 radial[01]
µm/m
Time [s]

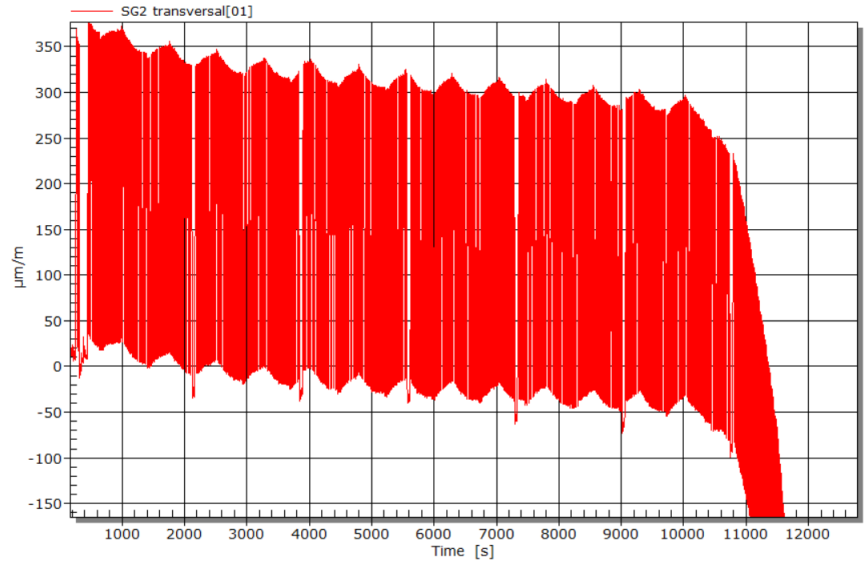
SG2 transversal[01]
µm/m
Time [s]

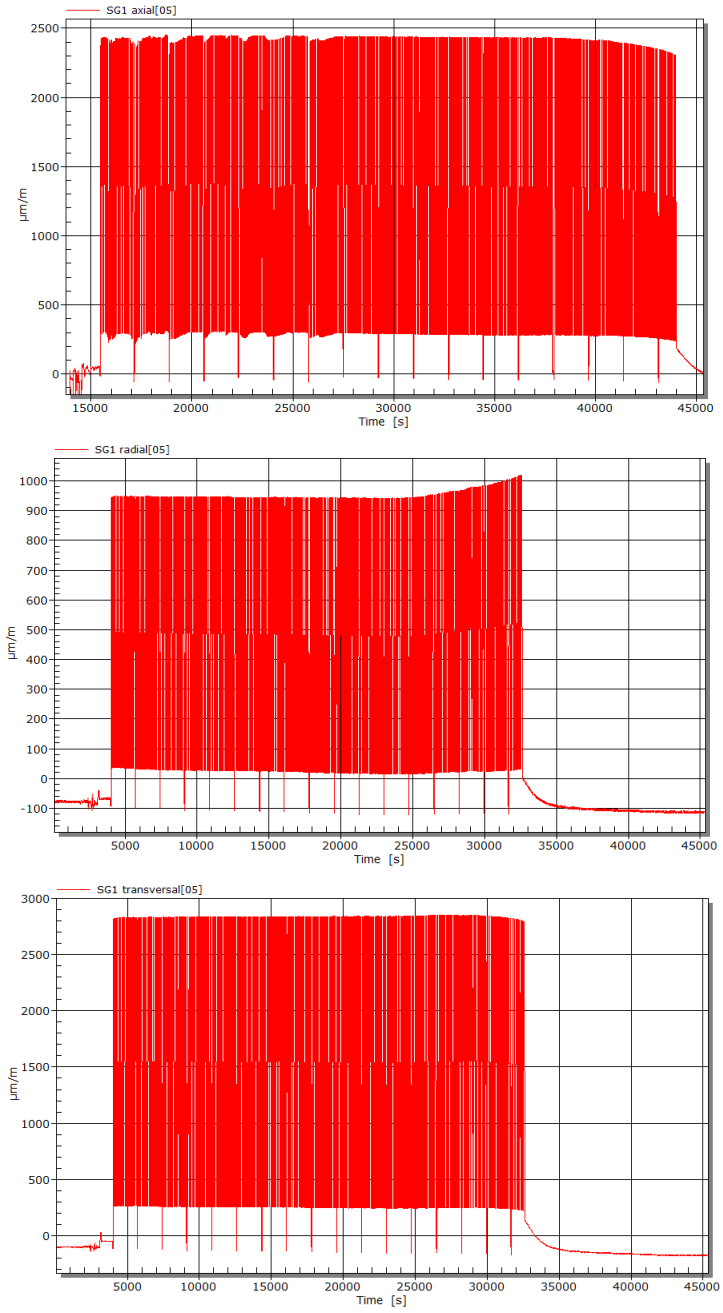
SG1 axial[05]
µm/m
Time [s]
SG1 radial[05]
µm/m
Time [s]
SG1 transversal[05]
µm/m
Time [s]

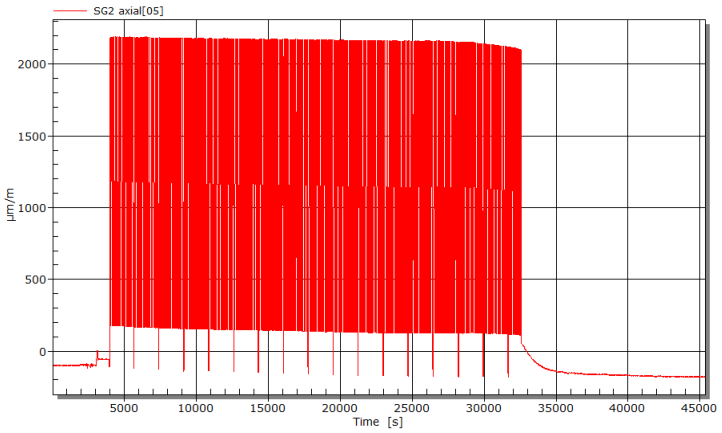
SG2 axial[05]
µm/m
2000
1500
1000
500
0
5000
10000
15000
20000
25000
30000
35000
40000
45000
Time [s]

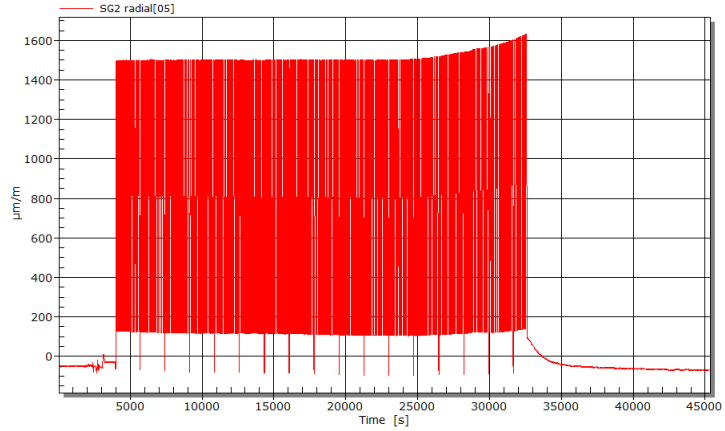
SG2 radial[05]
µm/m
1600
1400
1200
1000
800
600
400
200
0
5000
10000
15000
20000
25000
30000
35000
40000
45000
Time [s]

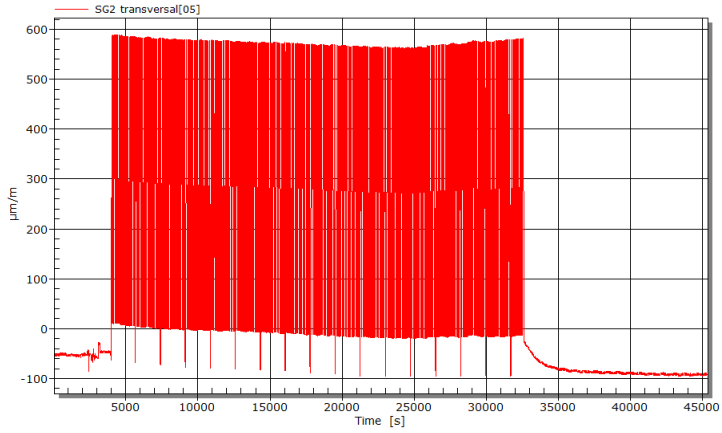
SG2 transversal[05]
µm/m
600
500
400
300
200
100
0
-100
5000
10000
15000
20000
25000
30000
35000
40000
45000
Time [s]

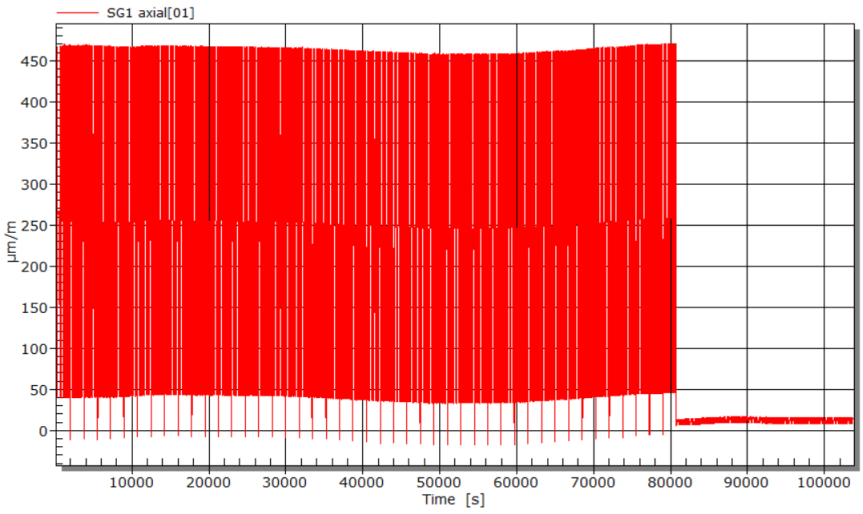
SG1 axial[01]
µm/m
Time [s]

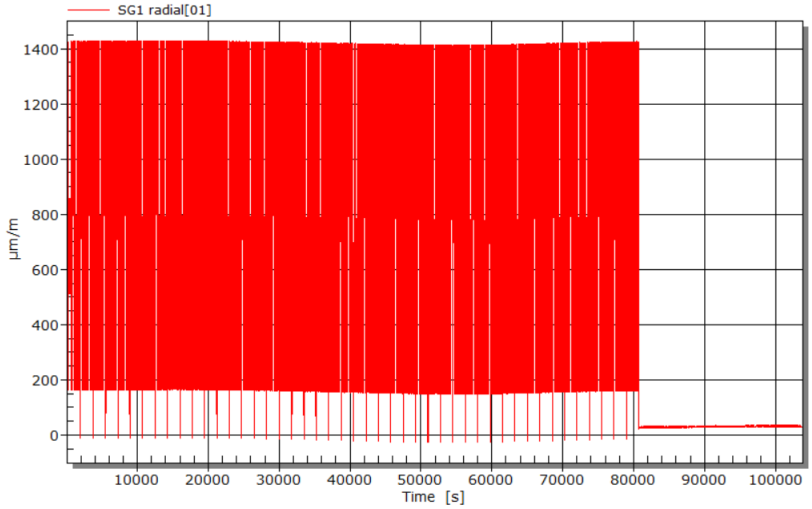
SG1 radial[01]
µm/m
Time [s]

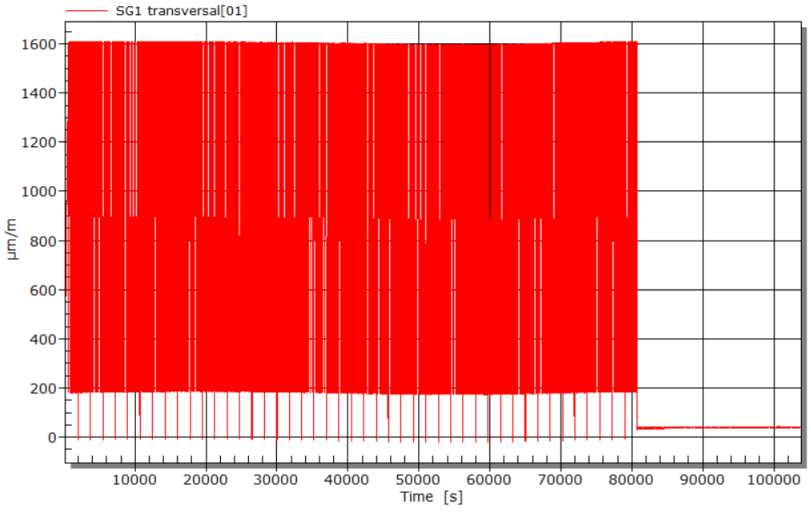
SG1 transversal[01]
µm/m
Time [s]

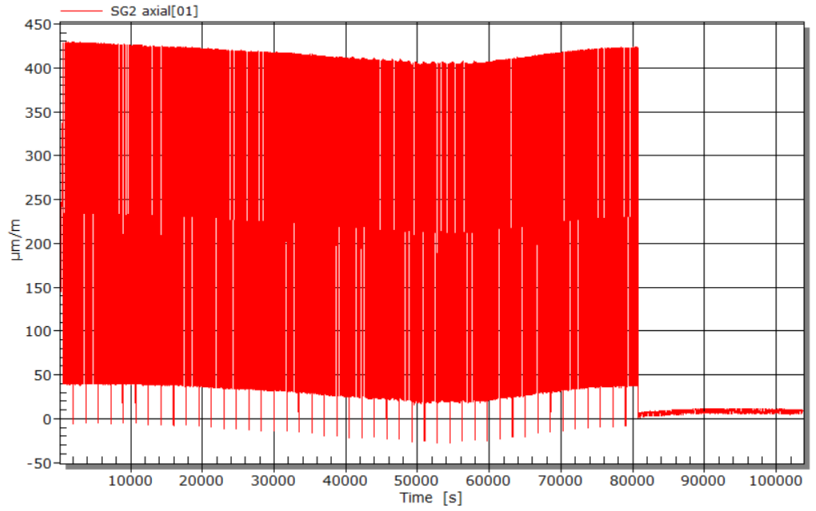
SG2 axial[01]
µm/m
Time [s]

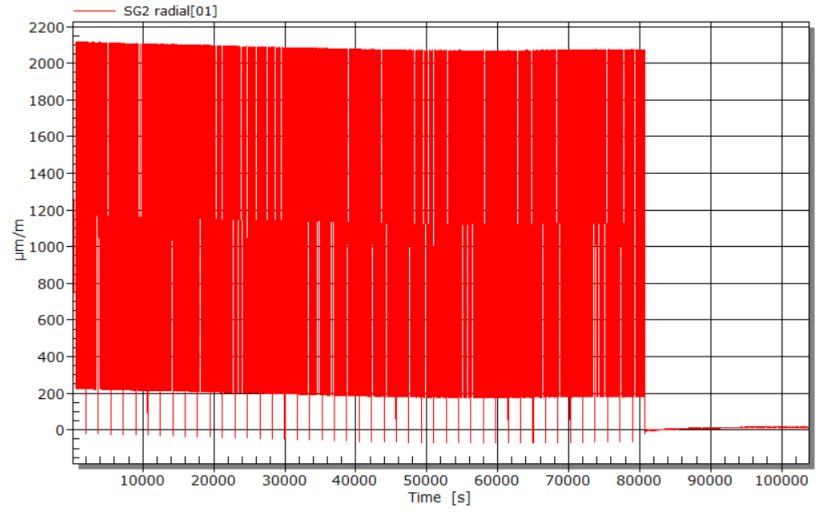
SG2 radial[01]
µm/m
Time [s]

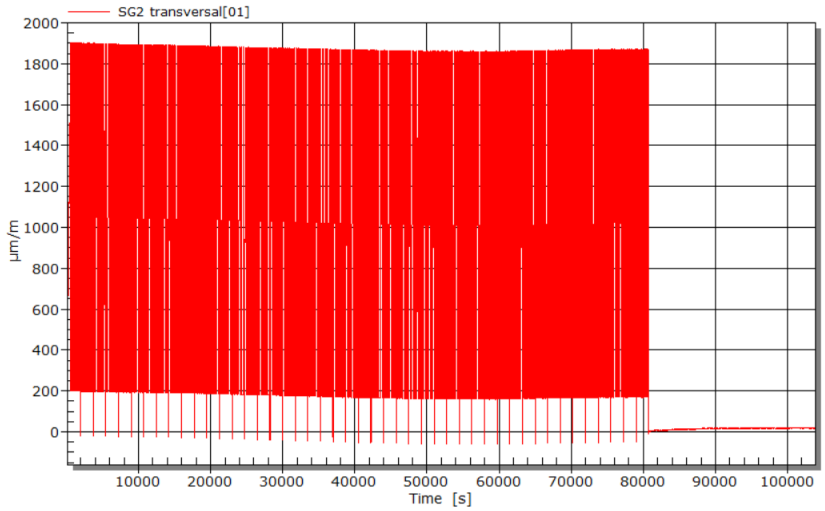
SG2 transversal[01]
µm/m
Time [s]

A.3 Displacements of 90-degree dents at dent center

A.3.1 Pressure-range: 4-40[Bar]

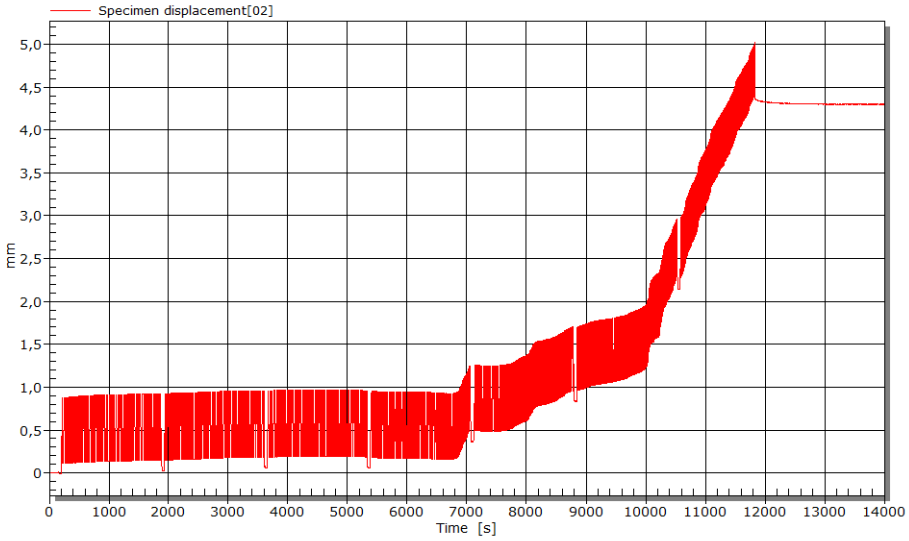

A.3.2 Pressure-range: 3.7-37[Bar]

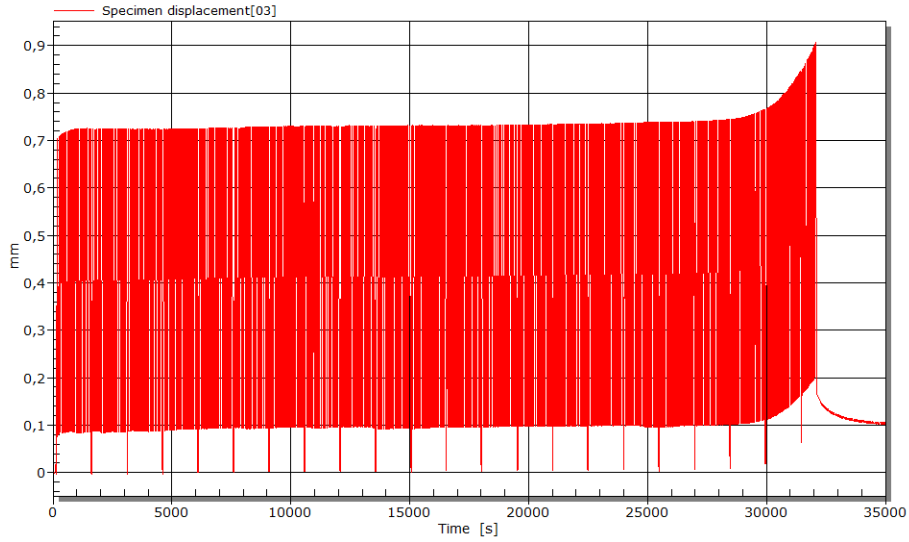

A.3.3 Pressure-range: 3.2-32[Bar]

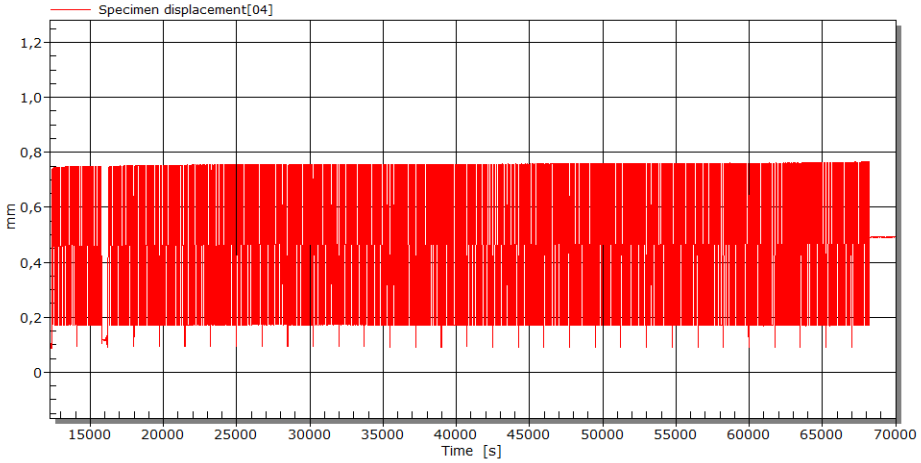

A.3.4 Pressure-range: 4-40[Bar]

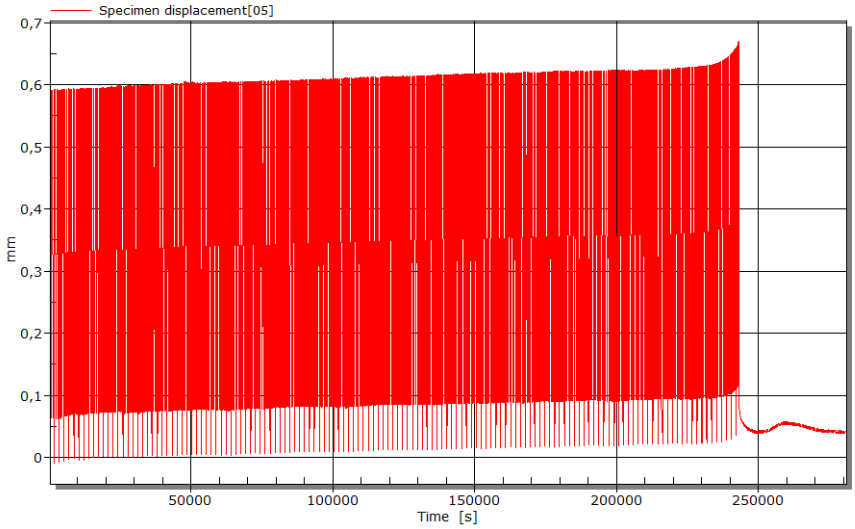

A.4 Displacements of 45-degree dents at dent center

A.4.1 Pressure-range: 4-40[Bar]

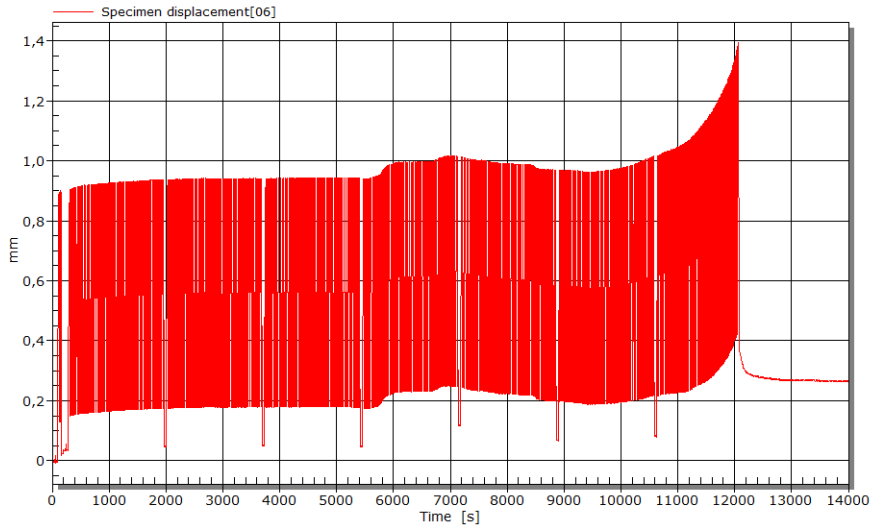

A.4.2 Pressure-range: 3.2-32[Bar]

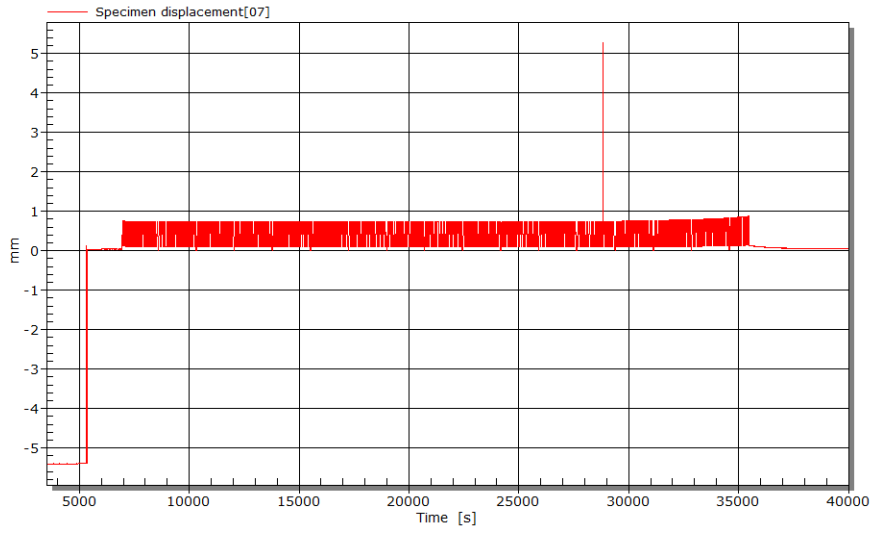

A.4.3 Pressure-range: 2.5-25[Bar]

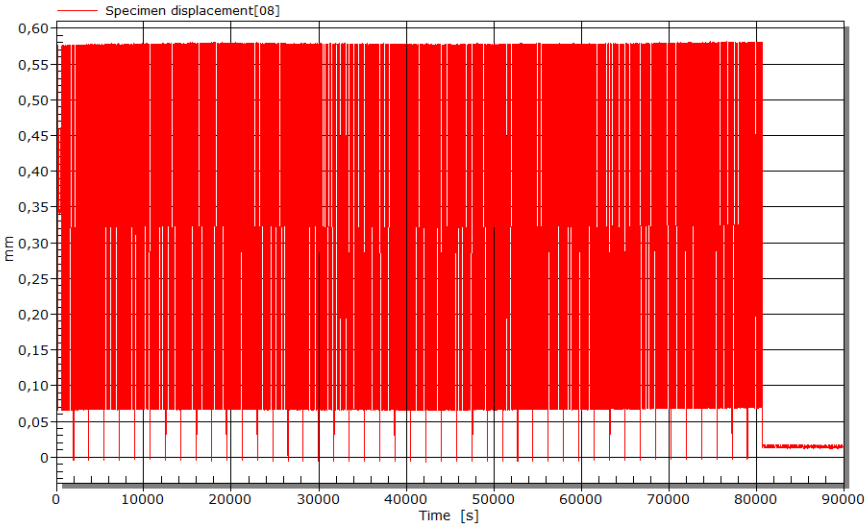

Bibliography

Aadal, A. H. (2016). Pipeline integrity assessment of dent with gouge after trawling impact.

Berge, S. (2016). *Compendium:Fatigue and Fracture Design of Marine Strutures*, volume 2. NTNU.

Cosham, A. and Hopkins, P. (2004). The effect of dents in pipelines—guidance in the pipeline defect assessment manual. *International Journal of Pressure Vessels and Piping*, 81(2):127–139.

eFatigue (2017a). Constant amplitdue. https://www.efatigue.com/constantamplitude/.

eFatigue (2017b). Variable amplitdue. https://www.efatigue.com/variable/.

Eliassen, K. E. (2016). Assessment of pipeline integrity after trawling impact by investigating dent with gouge.

Fitzpatrick, M., Fry, A., Holdway, P., Kandil, F., Shackleton, J., and Suominen, L. (2005). Determination of residual stresses by x-ray diffraction.

Huang, X. and Moan, T. (2007). Improved modeling of the effect of r-ratio on crack growth rate. *International Journal of fatigue*, 29(4):591–602.

of Technology, G. I. (2000). Strain gage rosettes: Selection, application and data reduction.

Pook, L. (2007). *Metal Fatigue: What It Is, Why It Matters. Solid Mechanics and Its Applications*. Springer.

Roylance, D. (2001). Pressure vessels. *Department of Material Science and Engineering, Massachusetts Institute of Technology, Cambridge, MA*, 2139.

Skibicki, D. (2014). The phenomena of non-proportionality in loading fatigue. In *Phenomena and Computational Models of Non-Proportional Fatigue of Materials*, pages 9–47. Springer.

Socie, D. and Marquis, G. (2000). *Multiaxial Fatigue*. Premiere Series Bks. Society of Automotive Engineers.

Socie, D. F. (2001). Multiaxial fatigue - presentation.

Socie, D. F. (2017). Multiaxial fatigue - presentation. https://www.researchgate.net/publication/221928011_Phenomenological_Modelling_of_Cyclic_Plasticity/figures?lo=1.

Vallace, L. (2018). Quick fatigue tool for matlab.